(12) INTERNATIONAL APPLICATION PUBLISHED UNDER THE PATENT COOPERATION TREATY (PCT)

(19) World Intellectual Property Organization
International Bureau

(43) International Publication Date
02 January 2025 (02.01.2025)

WIPO | PCT

(10) International Publication Number
WO 2025/006881 A1

(51) International Patent Classification:
B01D 61/38 (2006.01) *B01D 71/26* (2006.01)
B01D 69/14 (2006.01) *B01D 71/36* (2006.01)
B01D 69/10 (2006.01) *B01D 67/00* (2006.01)
B01D 69/12 (2006.01) *B01D 71/04* (2006.01)
B01D 71/02 (2006.01)

(21) International Application Number:
PCT/US2024/036011

(22) International Filing Date:
28 June 2024 (28.06.2024)

(25) Filing Language: English

(26) Publication Language: English

(30) Priority Data:
63/511,234 30 June 2023 (30.06.2023) US

(71) Applicant: **W. L. GORE & ASSOCIATES, INC.** [US/US]; 555 Paper Mill Road, Newark, DE 19711 (US).

(72) Inventors: **EDMUNDSON, Mark, D**; 551 Paper Mill Road, Newark, DE 19711 (US). **NATHAN, Rochitha**; 551 Paper Mill Road, Newark, DE 19711 (US). **SHARICK, Tsen-Shan**; 551 Paper Mill Road, Newark, DE 19711 (US). **GROVE, Corinne**; 551 Paper Mill Road, Newark, DE 19711 (US). **HOLLIDAY, Andrew**; 551 Paper Mill Road, Newark, DE 19711 (US). **KENALEY, Ryan**; 551 Paper Mill Road, Newark, DE 19711 (US).

(74) Agent: **JONAS, Victor P.**; Faegre Drinker Biddle & Reath, LLP, 2200 Wells Fargo Center, 90 South Seventh Street, Minneapolis, MN 55402-3901 (US).

(81) Designated States *(unless otherwise indicated, for every kind of national protection available)*: AE, AG, AL, AM, AO, AT, AU, AZ, BA, BB, BG, BH, BN, BR, BW, BY, BZ, CA, CH, CL, CN, CO, CR, CU, CV, CZ, DE, DJ, DK, DM, DO, DZ, EC, EE, EG, ES, FI, GB, GD, GE, GH, GM, GT, HN, HR, HU, ID, IL, IN, IQ, IR, IS, IT, JM, JO, JP, KE, KG, KH, KN, KP, KR, KW, KZ, LA, LC, LK, LR, LS, LU, LY, MA, MD, MG, MK, MN, MU, MW, MX, MY, MZ, NA, NG, NI, NO, NZ, OM, PA, PE, PG, PH, PL, PT, QA, RO, RS, RU, RW, SA, SC, SD, SE, SG, SK, SL, ST, SV, SY, TH, TJ, TM, TN, TR, TT, TZ, UA, UG, US, UZ, VC, VN, WS, ZA, ZM, ZW.

(84) Designated States *(unless otherwise indicated, for every kind of regional protection available)*: ARIPO (BW, CV, GH, GM, KE, LR, LS, MW, MZ, NA, RW, SC, SD, SL, ST, SZ, TZ, UG, ZM, ZW), Eurasian (AM, AZ, BY, KG, KZ, RU, TJ, TM), European (AL, AT, BE, BG, CH, CY, CZ, DE, DK, EE, ES, FI, FR, GB, GR, HR, HU, IE, IS, IT, LT, LU, LV, MC, ME, MK, MT, NL, NO, PL, PT, RO, RS, SE, SI, SK, SM, TR), OAPI (BF, BJ, CF, CG, CI, CM, GA, GN, GQ, GW, KM, ML, MR, NE, SN, TD, TG).

Published:
— *with international search report (Art. 21(3))*

(54) Title: COMPOSITE MEMBRANES, MEMBRANE-REINFORCED OPALOIDS, SUPPORTED LIQUID MEMBRANES, AND METHODS FOR MANUFACTURE THEREOF

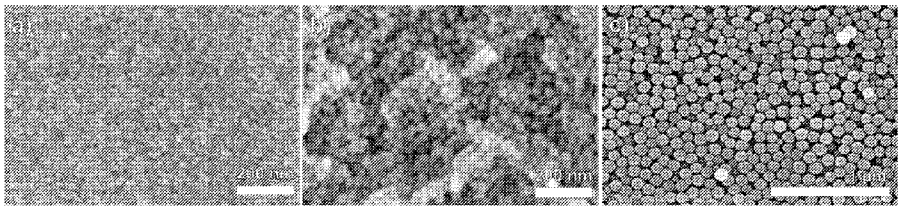


Figure 1

(57) Abstract: A composite membrane is described comprising a microporous polymer scaffold comprising a plurality of scaffold pores, each of said scaffold pores having a pore volume and the microporous polymer scaffold having a scaffold pore volume, wherein the microporous polymer scaffold has a bubble point pressure equal to or greater than 2 bar; and an opaloid within the plurality of scaffold pores, wherein the opaloid comprises sub-micron particles within the scaffold pore volume; and wherein the composite membrane comprises a plurality of composite membrane pores that are defined at least in part by the opaloid. The composite membrane can be used as a membrane support for a supported liquid membrane. Also described are methods of manufacturing the composite membranes.

WO 2025/006881 A1

COMPOSITE MEMBRANES, MEMBRANE-REINFORCED OPALOIDS, SUPPORTED LIQUID MEMBRANES, AND METHODS FOR MANUFACTURE THEREOF

FIELD OF THE INVENTION

[001] This disclosure relates to composite membranes comprising opaloids, particularly high-integrity membrane-reinforced opaloids, supported liquid membranes, and methods for manufacture thereof.

BACKGROUND

[002] Opaloids are solid materials comprising particles in tightly packed arrangements where the arrangements have a degree of order that may range from crystalline to nearly amorphous. Opaloids can have many interesting properties, such as a narrow distribution of pore sizes, relatively high porosity, crush resistance, stability at high temperatures, stability in many chemical environments, and wettability with various fluids (including water). However, the production of high-quality opaloids for practical applications can be very challenging, particularly for opaloids comprising ceramics because of the brittle nature of such materials. For example, significant challenges exist in: 1) fabricating large areas (e.g., areas larger in extent than about one millimeter to several centimeters in at least one dimension) with high integrity (for example, relatively free of through-plane defects such as cracks); 2) making highly flexible, free-standing structures that enable efficient roll-to-roll processing; 3) making mechanically robust structures that can withstand handling, installation, and use in industrial applications; and 4) enabling sufficiently rapid fabrication for economical, high-volume production.

[003] A supported liquid membrane (SLM) is a membrane system where a liquid is immobilized within the pores of a membrane support (e.g., a microporous polymer scaffold), typically via capillary forces. Supported liquid membranes have been extensively studied due to their excellent properties for various types of separations. However, challenges exist in their application because current SLMs can suffer from expulsion of the supported liquid due to trans-membrane pressure gradients; squeeze-out of the supported liquid due to mechanical compression; and the membrane supports can lack chemical, thermal, and/or mechanical stability.

[004] Accordingly, a need exists to develop products and methods that allow for the production of large-area, high-integrity opaloids and permit some or all of the advantageous properties of opaloids to be utilized more readily and economically in practical applications. Additionally, there is a need for improved membrane supports for supported liquid membranes that address some or all of the aforementioned issues with current supported liquid membranes.

SUMMARY

[005] According to a first aspect, there is provided a composite membrane comprising: a microporous polymer scaffold comprising a plurality of scaffold pores, each of said scaffold pores having a pore volume and the microporous polymer scaffold having a scaffold pore volume, wherein the microporous polymer scaffold has a bubble point pressure equal to or greater than 2 bar; and an opaloid within the plurality of scaffold pores, wherein the opaloid comprises sub-micron particles within the scaffold pore volume; and wherein the composite membrane comprises a plurality of composite membrane pores that are defined at least in part by the opaloid.

[006] The composite membranes of the present disclosure have been shown to have: a narrow distribution of small pore sizes, relatively high porosity, crush resistance, stability at high temperatures, stability in many chemical environments, wettability with various fluids (including water), high optical clarity, and/or high mechanical integrity under demanding conditions (for example, including tight wrap angles or high trans-membrane pressures). Accordingly, the inventors have realized the provision of composite membranes with highly tunable pore size, and properties that can embody the advantageous properties of opaloids whilst providing improved stability, integrity, and reproducibility. The composite membranes of the present disclosure may be effective in a wide range of applications. For example, the composite membranes may be effective as separators in electrochemical applications (i.e., as electrochemical separators) and as filter media in filtration applications. The composite membranes of the present disclsoure may also be referred to as membrane-reinforced opaloids or reinforced opaloid membranes. The composite membranes of the present disclosure may also be referred to as membrane-reinforced colloidal crystals or reinforced colloidal crystal membranes. The composite membranes of the present disclosure may also be referred to as membrane-reinforced colloidal semicrystals or reinforced colloidal semicrystal membranes.The composite membranes of the present disclosure may also be referred to as membrane-reinforced colloidal glasses or reinforced colloidal glass membranes.

[007] The composite membrane may comprise a bubble point pressure of equal to or greater than 10 bar. A composite membrane having a high bubble point pressure (for example, having a bubble point pressure that is equal to or greater than 10 bar) may be considered to have relatively few large defects that extend through the thickness. That is to say, if the composite membrane does comprise any defects (e.g., cracks), these are few in number and may be considered to be largely limited to localized defects (i.e., those that do not span the full thickness of the composite membrane). The composite membrane may comprise a bubble point pressure as further defined herein in the description of membrane-reinforced opaloid morphology.

[008] The opaloid may comprise sub-micron particles that may have passed through a colloidal glass transition point for a colloidal system comprising the sub-micron particles, for example a colloidal dispersion or colloidal suspension. The opaloid may therefore be considered to be a form of colloidal glass as further defined and discussed in the disclosure. The opaloid may comprise sub-micron particles having a three-dimensional packing arrangement of sub-micron particles that may be characterized by at least one of the following: a packing density of the sub-micron particles of from about 0.40 to about 0.85; a pore size (d) to inter-particle distance (ID) ratio (d/ID) from 0.2 to 2.0, and/or an inter-particle distance that is from 0.5 times to about 3 times the particle diameter of the sub-micron particle diameter or effective diameter. The opaloid may comprise a three-dimensional tight packing arrangement of sub-micron particles, wherein the tightness of the packing arrangement may be described by the inter-particle distance between the sub-micron particles of the opaloid. The composite membrane pores may be defined at least in part by an inter-particle distance within the three-dimensional packing arrangement. The inter-particle distance is further defined herein in the detailed description of membrane reinforced opaloid morphology. The inter-particle distance may be from about 0.5 times to about 3 times the particle diameter or effective diameter of the sub-micron particles.

[009] The three-dimensional packing arrangement of sub-micron particle is further defined herein, as described in the detailed description of membrane-reinforced opaloid morphology and the introduction to opaloids sections of the description. The three-dimensional packing arrangement may comprise a packing arrangement that comprises a packing arrangement selected from face-centered cubic packing, hexagonal close packing, body-centered cubic packing, simple cubic packing, random close packing, liquid-like packing, and combinations thereof. The three-dimensional packing arrangement of sub-micron particles can be determined by a primary structure factor peak in Lorenz-corrected small angle X-ray scattering spectra of the composite membrane (wherein the small angle X-ray scattering is performed according to the test methods described herein). The position of the primary structure factor peak maximum may correspond to an inter-particle distance that may be within about 0.6 times to about 3 times the sub-micron particle diameter or effective diameter. The inter-particle distance may also be determined via microscopy in combination with Quantitative Image Analysis as described further herein.

[0010] The sub-micron particles are described herein in the description of sub-micron particles section. The sub-micron particles may have a sub-micron particle diameter or effective diameter as defined herein. The sub-micron particles may have a particle diameter or effective diameter of from about 1 nm to about 1μm. The composite membrane pores have composite membrane pore size as defined herein in the the detailed description of membrane-

reinforced opaloid morphology, and the mode composite membrane pore size may be from about 0.15 times to about 2 times the sub-micron particle diameter or effective diameter.

[0011] The composite membrane may have a porosity as defined herein in the detailed description of membrane-reinforced opaloid morphology. The porosity of the composite membrane may be from about 10 % to about 75 %.

[0012] The opaloid may comprise an opaloid pore size as defined herein in the detailed description of membrane-reinforced opaloid morphology. The opaloid pore size may be about 0.15 times to about 1.5 times the sub-micron particle diameter or effective diameter.

[0013] The composite membranes of the present disclosure may have a contact thickness as defined herein in the detailed description of membrane-reinforced opaloid morphology. The composite membrane may have a contact thickness of less than or equal to 150 μm.

[0014] In some examples, the plurality of scaffold pores of the microporous polymer scaffold may be at least partially filled with the opaloid. In some examples, the plurality of scaffold pores may be filled with the opaloid. The term filled is defined herein in the detailed description of membrane-reinforced opaloid morphology. The opaloid may extend continuously within at least a portion of the scaffold pores in at least one direction, as defined herein in the detailed description of membrane-reinforced opaloid morphology. The opaloid may extend continuously within at least a portion of the scaffold pores in a least one direction by at least 1 mm.

[0015] The composite membranes of the present disclosure may have a Young's modulus that is from about 2 times to about 3 times larger than a Young's modulus of the microporous polymer scaffold. The composite membranes of the present disclosure may have a tensile strength that is substantially the same as a tensile strength of the microporous polymer scaffold when measured on an absolute basis (i.e., units of Newtons/mm, where the millimeter refers to the sample width). The composite membrane may comprise a composite opaloid yield strain and a composite membrane break strain, and wherein the composite membrane break strain is greater than the opaloid yield strain. The composite opaloid yield strain may correspond to a first tensile peak associated with the yielding of the opaloid during tensile testing. The composite membrane break strain may be the strain associated with breaking of the composite membrane during tensile testing. The composite membrane may have these properties along with other properties as described in the description of "additional properties of membrane-reinforced opaloids" section.

[0016] The microporous polymer scaffolds are defined herein in the detailed description of microporous polymer scaffolds of the present disclosure. The microporous polymer scaffold may be selected from one of a non-fluorinated polymer, a partially fluorinated polymer, a

perfluorinated polymer, and any combination thereof. The microporous polymer scaffold may comprise polyolefins, optionally polyethylene (PE) or polypropylene (PP). The microporous polymer scaffold may comprise any one selected from polytetrafluorethylene (PTFE), polyethylene (PE), or a copolymer of PTFE and PE, expanded polyethylene (ePE), expanded polytetrafluoroethylene (ePTFE), or combinations thereof.

[0017] The sub-micron particles within the scaffold pore volume may be sub-micron particles as described herein. The sub-micron particles may comprise at least one of ceramics or glasses, as described herein. The ceramic may be selected from silicon dioxide, aluminium oxide, titanium dioxide, cerium oxide, zirconium dioxide, yttria stabilized zirconium dioxide, other oxides, and other classes of ceramics including but not limited to carbides, nitrides, sulfides, borides, phosphides, selenides, titanates, carbonates, nitrates, sulfates, borates, and phosphates, or combinations thereof.

[0018] In some examples of the present disclosure, the sub-micron particles may comprise at least two different populations of sub-micron particles, wherein a first population of sub-micron particles has a first particle diameter (or effective particle diameter) and a second population of sub-micron particles has a second particle diameter (or effective diameter).

[0019] In some examples, the composite membrane may comprise a plurality of microporous polymer scaffolds. At least one of the plurality of microporous polymer scaffolds may have a bubble point pressure of equal to or greater than 2 bar, and the sub-micron particles within the scaffold pore volume as an opaloid.

[0020] The composite membranes having bubble point pressures of equal to or greater than 10 bar also may indicate that the composite membrane is capable of effective liquid retention within the composite membrane pores even when the composite membrane is subjected to compression or a pressure gradient. As such, composite membranes of the present disclosure may be advantageously suitable for use as membrane supports for supported liquid membranes.

[0021] The composite membranes disclosed herein may therefore by a membrane support for a supported liquid membrane as further defined herein in the “applications including supported liquid membranes” section of the present disclosure. In use as a supported liquid membrane, the composite membrane may comprise a liquid within the composite membrane pores.

[0022] The composite membranes of the present disclosure may have numerous applications and uses. In a non-limiting example, the composite membrane may be a filter

medium for organic solvent nanofiltration. In a non-limiting example, the composite membrane may be a separator for an electrochemical cell.

[0023] According to a second aspect, there is provided a membrane-reinforced opaloid comprising an opaloid; and a microporous polymer scaffold, wherein the microporous polymer scaffold comprises a plurality of scaffold pores and has a bubble point pressure of equal to or greater than 2 bar; and wherein the opaloid extends at least partially within the plurality of scaffold pores.

[0024] The opaloid comprises sub-micron particles and may comprise any of the opaloids as described and defined herein with respect to the first aspect and/or below. The microporous polymer scaffold may include any of the microporous polymer scaffolds as described and defined herein. The membrane-reinforced opaloid may otherwise be called a composite membrane as defined herein.

[0025] The membrane-reinforced opaloid may comprise opaloid pores defined at least in part by the opaloid extending within the plurality of scaffold pores. The opaloid may extend continuously within at least a portion of the scaffold pores in at least one direction by at least about 1 mm. The membrane-reinforced opaloid may comprise a bubble point pressure of equal to or greater than about 10 bar.

[0026] According to a third aspect, there is provided a composite membrane comprising a microporous polymer scaffold, wherein the microporous polymer scaffold comprises a plurality of scaffold pores, each of said scaffold pores having a pore volume and the microporous polymer scaffold having a scaffold pore volume. The microporous polymer scaffold may comprise a bubble point pressure of equal to or greater than 2 bar. The composite membrane further comprises sub-micron particles, wherein the sub-micron particles are incorporated within the plurality of scaffold pores and the sub-micron particles define a three-dimensional packing arrangement within the scaffold pore volume. The three dimensional packing arrangement may be characterized by at least one of the following: a packing density of the sub-micron particles of from about 0.40 to about 0.85; a pore size (d) to inter-particle distance (ID) ratio (d/ID) from about 0.2 to about 2.0, and/or an inter-particle distance that is from about 0.5 to about 3 times the particle diameter of the sub-micron particle diameter or effective diameter.

[0027] The microporous polymer scaffold may comprise any of the microporous polymer scaffolds as defined and as described herein. The sub-micron particles may comprise any of the sub-micron particles as defined and as described herein. The three-dimensional packing arrangement of this aspect may be considered to be an opaloid packing arrangement. Accordingly, the features of the opaloids that are described and defined herein are also

applicable to the three-dimensional packing arrangement of sub-micron particles of this aspect. Such features include but are not limited to for example, inter-particle pores, inter-particle distance (ID), inter-particle pore diameter (d) /particle diameter or effective diameter (D) ratio (d/D), integration distance (d_i), and composite membrane pore size as defined herein are also applicable with respect to the composite membrane of the third aspect.

[0028] According to a fourth aspect, there is provided a supported liquid membrane comprising any of the composite membranes described according to the present disclosure, and a liquid, wherein at least some of the composite membrane pores are filled with the liquid. The liquid may be retained within the composite membrane pores. The supported liquid membrane may be particularly useful for use in separations and/or electrochemical applications, for example as a separator for an electrochemical cell.

[0029] According to a fifth aspect of the present disclosure, there is provided a method of manufacturing a composite membrane. The method may comprise method step (a) obtaining a microporous polymer scaffold having a bubble point pressure of equal to or greater than 2 bar, wherein the microporous polymer scaffold comprises a plurality of scaffold pores, each of said scaffold pores having a pore volume and the microporous polymer scaffold having a scaffold pore volume; method step (b) incorporating sub-micron particles into the scaffold pore volume of the microporous polymer scaffold within the scaffold pores, and method step (c) forming an opaloid within the scaffold pore volume, wherein the opaloid comprises the sub-micron particles.

[0030] The method may comprise imbibing the microporous polymer scaffold with a colloidal system comprising the sub-micron particles. The colloidal system may comprise a colloidal precursor that is a colloidal suspension or colloidal dispersion. The colloidal precursor may comprise a continuous fluid phase and the sub-micron particles. The continuous fluid phase may be an aqueous phase. The colloidal system may therefore comprise an aqueous colloidal dispersion or colloidal suspension. The continuous fluid phase may be an organic phase. The colloidal system may therefore comprise an organic colloidal dispersion or colloidal suspension. The continuous fluid phase may also be termed a liquid carrier.

[0031] The method may comprise imbibing the microporous polymer scaffold with an aqueous colloidal dispersion or colloidal suspension of sub-micron particles at a concentration of about 5 wt% to 80 wt%. The method may comprise imbibing the microporous polymer scaffold with an aqueous colloidal dispersion or colloidal suspension of sub-micron particles at a concentration of about 10 wt% to 70 wt%. The method may comprise imbibing the microporous polymer scaffold with an aqueous colloidal dispersion or colloidal suspension of sub-micron particles at a concentration of about 20 wt% to 50 wt%.

[0032] The method may comprise imbibing the sub-micron particles into the microporous polymer scaffold from one side of the microporous polymer scaffold (e.g., by applying a thin film of the imbibing fluid on one side of the microporous polymer scaffold via Mayer bar coating), or from both sides (first and second surfaces) of the microporous polymer scaffold (e.g., by dip coating the microporous polymer scaffold in the imbibing fluid, or by applying a thin film of imbibing fluid to each side, simultaneously or consecutively). The sub-micron particles may be imbibed such that the opaloid is substantially contained within the pores of the microporous polymer scaffold (i.e., the thickness of opaloid deposited on the first or second surface of the microporous polymer scaffold, outside the pore volume of the microporous polymer scaffold, sometimes referred to as "buttercoat" layers, is minimal). The thickness of a minimal buttercoat layer may be less than about 2 microns, or less than about 1 micron, or less than about 0.5 microns, or less than about 0.2 microns, or less than about 0.1 microns. For example, the buttercoat layer may from about 0.05 μm to about 2 μm, or from about 0.05 μm to about 1 μm, or from about 0.01 μm to about 1 μm, or from about 0.01 μm to about 0.5 μm.

[0033] The imbibing process may comprise any of the imbibing process steps as set out in the present application. For example, the imbibing process may comprise a step in which the microporous polymer scaffold wetted with imbibing fluid is in contact with a backer as defined herein. The backer may be adhered to the composite membrane, and the force of adhesion may be such that the backer can be removed from (e.g., peeled off of) the composite membrane without substantially damaging the composite membrane.

[0034] The liquid carrier of the continuous fluid phase is not particularly limited, and any suitable liquid carriers known in the art may be used. If the continuous fluid phase of the colloidal system (i.e., the liquid carrier) does not spontaneously and readily wet the microporous polymer scaffold, then a variety of techniques may be employed to assist in achieving good wetting, such as by applying a differential pressure to force the liquid carrier into the microporous polymer scaffold, raising the temperature of the liquid carrier to lower its viscosity and surface tension, and/or pre-wetting the microporous polymer scaffold with another miscible liquid.

[0035] Liquid carriers that are aqueous or substantially aqueous may be preferred in some cases, for example because of the availability of stable and highly concentrated colloidal dispersions, or because of safety and environmental reasons. For example, when the sub-micron particles comprise a ceramic or glass then an aqueous or substantially aqueous colloidal system may be preferred. As defined herein, "substantially aqueous" may mean at least 50 wt% water, or at least 60 wt%, or at least 70 wt%, or at least 80 wt%, or at least 90 wt%, or at least 95 wt%. To enable an aqueous or substantially aqueous colloidal system to

wet a microporous polymer scaffold with minimal dilution, a suitable wetting agent may be emulsified in the aqueous or substantially aqueous colloidal system with the aid of a surfactant. Suitable wetting agents are further defined herein in the fabrication of membrane-reinforced opaloid description. The surfactant(s) can be a single surfactant or a combination of surfactants. Suitable surfactants are defined as those that are able to emulsify the desired wetting agent. Suitable surfactants are defined further herein in the fabrication of membrane-reinforced opaloid description. The colloidal system may contain additives such as dispersing agents to stabilize the colloidal dispersion or colloidal suspension, which are further defined herein in the fabrication of membrane-reinforced opaloid description.

[0036] The method may comprise further processing the composite membrane after method step (b), wherein the further processing comprises at least one of: heat treating, annealing or drying of the composite membrane. The further processing of the composite membrane may form the opaloid according to method step (c).

[0037] The further processing of the composite membrane may substantially remove any or all of the continuous fluid phase from the opaloid within the microporous polymer scaffold pores.

[0038] Forming the opaloid according to method step (c) may comprise passing the colloidal dispersion or colloidal suspension through the colloidal glass transition point for the colloidal dispersion or colloidal suspension.

[0039] The further processing may comprise heating the composite membrane to temperatures of about 250°C, or from about 100°C to about 300°C, or from about 130°C to about 300°C, or from about 150°C to about 300°C . The further processing may comprise heating the composite membrane to temperatures of about 250°C for a sufficient period of time, for example from about 10 seconds to about 120 minutes, or from about 30 seconds to about 120 minutes, or from about 1 minute to about 120 minutes. The sufficient period of time may be determined by visibly confirming that any or all of the continuous fluid phase has been removed from the opaloid within the microporous polymer scaffold. It will be appreciated by one of ordinary skill in the art that other conventional drying methods may be used, and that drying conditions, in particular time and temperature, may be modified depending on the needs of the process and on the limitations of the materials (e.g., including their melting points and/or glass transition temperatures and/or decomposition temperatures).

[0040] The method may further comprise a step of heat treating the dried composite membrane.

[0041] The method may further comprise filling the composite membrane pores with a liquid to be supported. The filling may comprise wetting the composite membrane with the

liquid to form a supported liquid membrane. The liquid may comprise a high-performance fluid as defined herein in the “applications, including supported liquid membranes” description. The composite membrane pores may be filled with the liquid by spontaneous wetting, or the wetting may be assisted by any of a variety of means that will be evident to one of ordinary skill in the art, such as by applying a differential pressure to force the liquid into the composite membrane, raising the temperature of the liquid to lower its viscosity and/or surface tension, pre-wetting the composite membrane with another miscible fluid, and any other appropriate methods as would be apparent to the person ordinarily skilled in the art.

[0042] The method may comprise layering a plurality of microporous polymer scaffolds. At least one of the plurality of microporous polymer scaffolds may have a bubble point pressure of equal to or greater than 2 bar, wherein the microporous polymer scaffold comprises a plurality of scaffold pores having a scaffold pore volume; and has sub-micron particles incorporated within the scaffold pore volume of the plurality of scaffold pores, and wherein the sub-micron particles are an opaloid within the scaffold pore volume.

[0043] The method may comprise layering a plurality of microporous polymer scaffolds prior to method step (b) incorporating the sub-micron particles into the scaffold pores.

[0044] The method may comprise forming a plurality of composite layers according to method steps (a) and (b), and then layering the composite layers prior to method step (c) forming the oplaloid within the scaffold pore volume, wherein method step (c) comprises forming the opaloid within the scaffold pores of each of the composite layers.

[0045] The method may comprise forming a plurality of composite layers according to method steps (a), (b) and (c) and then layering the plurality of composite layers to form the composite membrane.

[0046] The method may comprise forming a composite layer according to method steps (a), (b) and (c) and then layering with a further microporous polymer scaffold and performing method steps (a), (b) and (c) on the further microporous polymer scaffold to form the composite membrane.

[0047] The layering may comprise laminating the microporous polymer scaffolds, or composite layers together. The layering may comprise hot stacking, or dry pressing, or any other joining methods which would be apparent to the person skilled in the art.

[0048] The microporous polymer scaffold, or scaffolds may be any of the microporous polymer scaffolds described and defined herein. The sub-micron particles may be any of the sub-micron particles as described and defined herein.

[0049] According to a sixth aspect, there is provided a composite membrane comprising a plurality of composite layers, and wherein at least one of the composite layers comprises: a microporous polymer scaffold comprising a plurality of scaffold pores, and the microporous polymer scaffold having a scaffold pore volume, wherein the microporous polymer scaffold has a bubble point pressure equal to or greater than 2 bar; and an opaloid within the plurality of scaffold pores, wherein the opaloid comprises sub-micron particles within the scaffold pore volume.

[0050] The at least one of the composite layers that comprises the microporous polymer scaffold, and the opaloid of sub-micron particles may comprise the features of the composite membrane as described with respect to the first aspect.

[0051] Each of the plurality of composite layers may comprise a microporous polymer scaffold comprising a plurality of scaffold pores and a scaffold pore volume, wherein the microporous polymer scaffold has a bubble point pressure equal to or greater than 2 bar; and an opaloid within the plurality of scaffold pores, wherein the opaloid comprises sub-micron particles within the scaffold pore volume.

[0052] The composite membrane may comprise other composite layers having properties such that the composite membrane is suitable for its intended function. For example, one of the composite layers may comprise the microporous polymer scaffold.

[0053] The plurality of composite layers may be laminated together to form the composite membrane.

[0054] The microporous polymer scaffold or scaffolds may be any of the microporous polymer scaffolds described and defined herein. The sub-micron particles may be any of the sub-micron particles as described and defined herein.

[0055] According to a seventh aspect, there is provided a method of making a composite membrane according to the sixth aspect. The method may comprise forming at least one of the plurality of composite layers, wherein the forming of the at least one composite layer comprises method step (a) obtaining a microporous polymer scaffold having a bubble point pressure of equal to or greater than 2 bar, wherein the microporous polymer scaffold comprises a plurality of scaffold pores and having a scaffold pore volume; method step (b) incorporating sub-micron particles into the scaffold pore volume of the microporous polymer scaffold, and method step (c) forming an opaloid within the scaffold pore volume; and wherein the method further comprises method step (d) layering with a further composite layer or layers to form the composite membrane.

[0056] The method may comprise any of the method steps outlined with respect to the fifth aspect in order to make a selected composite membrane. The method may comprise imbibing the microporous polymer scaffold with a colloidal system comprising the sub-micron particles. The method may comprise further processing the composite layer after method step (b), wherein the further processing comprises at least one of: heat treating, annealing, or drying of the composite membrane.

[0057] The further processing of the composite layer may substantially remove any or all of the continuous fluid phase (for example, the dispersion or suspension phase) from the opaloid within the scaffold pores.

[0058] The method may comprise performing method step (d) prior to method step (b). For example, the method may comprise layering a plurality of microporous polymer scaffolds prior to method step (b) incorporating the sub-micron particles into the scaffold pores.

[0059] The method may comprise forming a plurality of composite layers according to method steps (a) and (b), and then layering the composite layers according to method step (d) prior to method step (c) forming the opaloid within the scaffold pore volume, wherein method step (c) comprises forming the opaloid within the scaffold pores of each of the composite layers.

[0060] The method may comprise forming a plurality of composite layers according to method steps (a), (b) and (c) and then method step (d) layering the plurality of composite layers to form the composite membrane.

[0061] The method may comprise forming a composite layer according to method steps (a), (b) and (c) and then method step (d) comprises layering with a further microporous polymer scaffold and performing method steps (a), (b) and (c) on the further microporous polymer scaffold to form the composite membrane.

[0062] The layering may comprise laminating the microporous polymer scaffolds or composite layers together. The layering may comprise hot stacking, or dry pressing, or any other joining methods which would be apparent to the person skilled in the art.

BRIEF DESCRIPTION OF FIGURES

[0063] The present disclosure will be better understood in view of the following figures. In the figures, identical reference numerals have been used for the same or equivalent features of the composite membrane, supported liquid membrane, and processes disclosed therein. The figures are not necessarily drawn to scale but may be exaggerated to illustrate various aspects of the present disclosure, and in that regard, the figures should not be construed as limiting.

[0064] **Figure 1** depicts representative scanning electron microscopy images (SEMs) of neat opaloids prepared from 3 different types of silica sub-micron particles with diameters of approximately a) 12 nanometers, b) 22 nanometers, and c) 100 nanometers, respectively;

[0065] **Figure 2** is a representative photograph of an opaloid prepared from silica sub-micron particles having a diameter of approximately 7 nanometers;

[0066] **Figure 3a** is a schematic depiction of a cross-section of a neat opaloid comprising monodisperse sub-micron particles in a three-dimensional arrangement;

[0067] **Figure 3b** is a schematic depiction of two adjacent particles, each having a diameter (D) that are elements of a particle packing arrangement within an opaloid as is shown in Figure 3a;

[0068] **Figure 4** is a schematic depiction of parameters associated with an opaloid overlaying an SEM of a neat opaloid;

[0069] **Figure 5a** depicts representative Small-Angle X-ray Scattering (SAXS) data sets for opaloids prepared from silica sub-micron particles having diameters of approximately 7 nanometers, 12 nanometers, 22 nanometers, 45 nanometers, and 100 nanometers;

[0070] **Figure 5b** is a graphical illustration of inter-particle distance (ID) determined from SAXS data as a function of nominal particle diameter (D) for opaloids prepared from silica sub-micron particles;

[0071] **Figure 6** is a graphical illustration of representative SAXS data for a material comprising aggregates of monodisperse spherical particles, showing the Guinier, fractal, and Porod scattering regimes and an absence of the structure factor peaks characteristic of opaloids. This figure was reproduced from Bushell et al. (”On techniques for the measurement of the mass fractal dimension of aggregates,” *Advances in Colloid and Interface Science*, **95**, 1-50 (2002))

[0072] **Figure 7** depicts a representative pore size distribution from BET/BJH analysis of an opaloid prepared from silica sub-micron particles having a diameter of approximately 12 nanometers;

[0073] **Figure 8** is a schematic depiction of expected values of the ratio of pore diameter to particle diameter (d/D) for different tightly packed arrangements of sub-micron particles where the coordination number, n, is 3, 4, 6, or 8;

[0074] **Figure 9a** depicts a comparison of specific surface area (SSA) measured by BET with expected particle size,

[0075] **Figure 9b** is a graphical illustration of a comparison of particle diameter calculated with SSA to the nominal sub-micron particle diameters reported by manufacturers;

[0076] **Figure 10a** is a schematic illustration of a cross-section of a representative microporous polymer scaffold used in the composite membranes of the present disclosure;

[0077] **Figure 10b** is a schematic illustration of an opaloid within the representative microporous polymer scaffold of Figure 9a;

[0078] **Figure 11** is a schematic illustration of a colloidal dispersion being concentrated to form an opaloid;

[0079] **Figure 12** depicts an SEM of a surface view of an opaloid comprising silica sub-micron particles having a diameter of approximately 22 nanometers in an expanded polytetrafluoroethylene (ePTFE) membrane where the ePTFE membrane had a bubble point of 1.9 bar overlaid with a schematic of parameters associated with a Membrane-Reinforced Opaloid (MRO);

[0080] **Figure 13** depicts an SEM of a surface view of a membrane-reinforced opaloid comprising a blend of two populations of sub-micron particles (silica sub-micron particles having a diameter of approximately 7 nanometers and perfluoroalkoxy alkane sub-micron particles having a diameter of approximately 90 nanometers) in an ePTFE microporous polymer scaffold, where the ePTFE had a bubble point of about 1.9 bar.

[0081] **Figure 14** depicts an SEM of a surface view of an MRO comprising silica sub-micron particles with a diameter of approximately 12 nanometers and an ePTFE microporous polymer scaffold where the ePTFE had a bubble point of about 1.9 bar.

[0082] **Figure 15** is a graphical illustration of SAXS data for a neat opaloid, and an MRO reinforced with an ePTFE microporous polymer scaffold where the ePTFE had a bubble point of 7.6 bar, where both the neat opaloid and the MRO were prepared from an aqueous colloidal dispersion of silica sub-micron particles with a diameter of approximately 12 nanometers;

[0083] **Figure 16** depicts BET/BJH data for four opaloids comprising sub-micron particles with a diameter of approximately 12 nm: neat (i.e., unreinforced), and MROs reinforced with ePTFE microporous polymer scaffolds that had bubble points of 1.9 bar, 4.8 bar, and 7.6 bar, respectively;

[0084] **Figure 17a** compares two of the data sets from **Figure 16** to define ϕ,

[0085] **Figure 17b** depicts ϕ plotted against the bubble point pressure for the microporous polymer scaffold for MROs with a sub-micron particle diameter of about 12 nanometers;

[0086] **Figure 17c** depicts ϕ plotted against particle diameter for MROs with a microporous polymer scaffold that had a bubble point of approximately 1.9 bar;

[0087] **Figure 18** depicts an SEM of a cross section of an MRO having an opaloid comprising silica sub-micron particles with a diameter of approximately 7 nanometers and an ePTFE microporous polymer scaffold where the ePTFE had a bubble point of about 7.6 bar;

[0088] **Figure 19a** depicts an SEM of a surface view of an MRO comprising yttria-stabilized zirconia (YSZ) sub-micron particles with particle diameter of about 32 nanometers and an ePTFE microporous polymer scaffold that had a bubble point of about 4.8 bar;

[0089] **Figure 19b** depicts an SEM of a cross-section of an MRO comprising yttria-stabilized zirconia sub-micron particles with particle diameter of about 32 nanometers and an ePTFE microporous polymer scaffold that had a bubble point of about 4.8 bar;

[0090] **Figure 20** depicts an SEM of a surface view of an MRO comprising yttria-stabilized zirconia sub-micron particles with particle size of 32 nanometers in a polyethylene microporous polymer scaffold where the scaffold had a bubble point of about 3.1 bar;

[0091] **Figure 21** depicts an SEM of a surface view of a membrane-reinforced opaloid comprising yttria-stabilized zirconia sub-micron particles having a diameter of approximately 32 nanometers in an ePTFE microporous polymer scaffold where the ePTFE had a bubble point of about 3.3 bar;

[0092] **Figure 22a** depicts representative Small-Angle X-ray Scattering (SAXS) data for a membrane-reinforced opaloid prepared with yttria-stabilized zirconia sub-micron particles having diameter of approximately 32 nanometers; **Figure 22b** depicts correlation distance – intensity data derived from SAXS for a membrane-reinforced opaloid prepared from yttria-stabilized zirconia sub-micron particles having diameter of approximately 32 nanometers. The triangle indicates a peak position at 19.2 nanometers;

[0093] **Figure 23a** depicts a sample of an MRO with a high level of transparency sitting on a black lab bench, **Figure 23b** shows a sample of the material of Figure 19a bent 180° back on itself to illustrate the flexibility of the material, and **Figure 23c** shows a sample of the same material lying flat on a business card with the words beneath the sample clearly legible with minimal distortion;

[0094] **Figure 24** shows optical haze measurements of three MROs, each comprising silica sub-micron with a diameter of approximately 12 nanometers, and each comprising a different ePTFE microporous polymer scaffold with one of three different bubble points: 1.9, 4.8, or 7.6 bar;

[0095] **Figure 25** is a graphical illustration of the capillary flow porometry measurements of three MROs, each comprising silica sub-micron particles with a diameter of approximately 12 nanometers, and each comprising a different ePTFE microporous polymer scaffold with one of three different bubble points: 1.9, 4.8, or 7.6 bar;

[0096] **Figure 26** is a schematic depiction of an experimental apparatus for performing Organic Solvent Nanofiltration (OSN);

[0097] **Figure 27** is a graphical illustration of the results of Organic Solvent Nanofiltration measurements on three MROs, each comprising silica sub-micron particles with a diameter of approximately 12 nanometers and each comprising a different ePTFE microporous polymer scaffold with one of three different bubble points: 1.9, 4.8, or 7.6 bar;

[0098] **Figure 28** is a graphical illustration comparing the measured liquid permeance data to the predicted permeance data for an MRO with a thickness of approximately 2.5 microns comprising silica sub-micron particles with a diameter of approximately 7 nanometers and an ePTFE scaffold that had a bubble point of 7.6 bar;

[0099] **Figure 29a** depicts a high-pressure flow cell that was used to measure liquid permeance at trans-membrane pressures up to 50 bar, and **Figure 29b** is a graphical illustration of the resulting liquid flux (in $L*m^{-2}*h$ or LMH), and permeance (in LMH/bar) through an MRO having a thickness of about 5 microns and comprising silica sub-micron particles with a diameter of about 7 nanometers and an ePTFE microporous polymer scaffold that had a bubble point of approximately 7.6 bar;

[00100] **Figure 30a** is a graphical illustration of a tensile measurementin the MD direction of a microporous polymer scaffold and an MRO comprising the microporous polymer scaffold. The MRO had a thickness of approximately 18 microns comprising yttria-stabilized zirconia sub-micron particles with a diameter of approximately 32 nanometers and an ePTFE scaffold that had a bubble point of 3.3 bar and a mass-per-area of 11.6 g/m^2. Gauge length was 9.525 mm, Gauge width was 3.175 mm;

[00101] **Figure 30b** and **Figure 30c** are a graphical illustrations of tensile measurements in the TD and MD directions, respectively, of a microporous polymer scaffold and an MRO comprising the microporous polymer scaffold. The MRO had a thickness of approximately 2.5 microns comprising silica sub-micron particles with a diameter of approximately 7 nanometers and an ePTFE scaffold that had a bubble point of 7.6 bar and a mass-per-area of 2 g/m^2. Gauge length was 19.5 mm, Gauge width was 2.5 mm;

[00102] **Figure 31** is a graphical illustration depicting the relationship between volume-specific pore volume and porosity; and

[00103] **Figure 32** is a graphical illustration of the calculated relationship between capillary pressure (ΔP) and pore diameter (d) for cylindrical pores assuming the Young-Laplace equation with a surface tension of 19.75 mN/m and a contact angle of zero degrees.

DETAILED DESCRIPTION

Definitions

[00104] Throughout the description and claims, the terms take the meanings explicitly defined herein, unless the context clearly dictates otherwise.

[00105] The phrases "in one embodiment", "in an embodiment" and "in some embodiments" etc. as used herein do not necessarily refer to the same embodiment(s), though they may. Furthermore, the phrases "in another embodiment" and "in some other embodiments" as used herein do not necessarily refer to a different embodiment, though they may. All embodiments of the disclosure are intended to be combinable.

[00106] The terms "comprises" and "comprising" mean to include, but are not limited to, such that further features may be present.

[00107] It is to be noted that all ranges described herein are exemplary in nature and include any and all values in between. Measurements that are reasonably close to the stated measurement deviate from the stated measurement by a reasonably small amount as understood and readily ascertained by individuals having ordinary skill in the relevant arts. In the event it is determined that individuals having ordinary skill in the relevant arts would not readily ascertain values for such reasonably small differences, the terms "substantially," "approximately," and "about" can be understood to mean plus or minus 10% of the stated value.

Introduction to Opaloids including Colloidal Crystals

[00108] Particles, including sub-micron particles and nanoparticles, may be assembled into three-dimensional arrangements with varying packing densities and degrees of order. Examples of such materials may include opaloids and sol-gel solids. Opaloids are solid materials comprising sub-micron particles in tightly packed arrangements where said arrangements have a degree of order that may range from crystalline to nearly amorphous. For illustration, **Figure 1** shows representative scanning electron microscopy images of opaloids prepared from 3 different types of silica sub-micron particles with diameters of approximately 12 nm, 22 nm, and 100 nm (in **Figures 1a**, **1b**, and **1c**, respectively). **Figure 2** shows a representative photograph of an opaloid prepared from silica sub-micron particles with a diameter of approximately 7 nanometers. These opaloids were hard, brittle solids as evidenced by the large cracks and chunks evident in **Figure 2**. The individual chunks could be readily picked up with tweezers and were qualitatively hard like window glass.

[00109] Opaloids may be produced, for example, by producing a stable colloidal dispersion or colloidal suspension (e.g., one in which the colloidal particles are stabilized against aggregation by e.g., surface charge on the colloidal particles resulting in DLVO-type repulsion,

by polymeric or oligomeric dispersing agents adsorbed on the surfaces of the colloidal particles resulting in steric stabilization, by some combination of these two approaches, or by other colloidal stabilization techniques as will be readily understood by one of ordinary skill in the art) concentrating the stable colloidal dispersion or colloidal suspension through the colloidal glass transition, and substantially drying the material to produce a consolidated solid structure. In contrast, sol-gel solids are solid materials characterized by poorly ordered fractal and aggregate structures. These poorly ordered structures are an inherent result of the gelation dynamics characteristic of sol-gel processes. Such gelation produces aggregates at concentrations below the colloidal glass transition, which prevents the solids from consolidating into the tight, ordered packing arrangements characteristic of opaloids. Therefore, the structure of opaloids is inherently more ordered than that of sol-gel solids. Furthermore, opaloids may have characteristic repeating length scales comparable to the size of the particles, whereas sol-gel solids, if they exhibit any repeating structure at all, may have characteristic repeating length scales comparable to the size of the aggregates. Opaloids and sol-gel solids therefore represent distinct classes of materials. The focus of the present invention is opaloids.

[00110] Opaloids include the widely studied class of materials called “colloidal crystals.” The fabrication and applications of colloidal crystals are discussed extensively in H. Cong et al., “Current status and future developments in preparation and application of colloidal crystals,” Chem. Soc. Rev., 42, 7774 (2013). Cong et al. describe a colloidal crystal as an ordered array or packing of monodisperse colloidal particles. A familiar example of a colloidal crystal is an opal, a naturally occurring gemstone comprising tightly packed arrangements of sub-micron particles of silica that may be highly ordered (e.g., comprising face-centered cubic (fcc), and/or hexagonal close packed (hcp) structures). For clarity, the term opaloid is inclusive of opals and other colloidal crystals, but is broader. Opaloids may be naturally-occurring or synthetic. Opaloids may comprise packing arrangements of sub-micron particles where the packing arrangements are crystalline, semi-crystalline, and/or nearly amorphous. Non-limiting examples of particle packing arrangements of opaloids include face -centered cubic packing (fcc), hexagonal close packing (hcp), body-centered cubic (bcc), simple cubic, liquid-like packing, as well as arrangements that are substantially similar to the foregoing examples but that may differ, for example, due to structural imperfections or packing defects. Opaloids may be polycrystalline (e.g., they may comprise multiple crystalline or semi-crystalline domains that border each other, and/or that may be separated by nearly amorphous or amorphous domains). Packing arrangements that are polycrystalline or that comprise an intermediate degree of order may optionally be referred to as colloidal semicrystals. The composition of opaloids is not particularly limited (e.g., they may comprise materials other than silica and/or may not comprise silica). However, it is noted that sub-micron particles comprising ceramics

and/or glasses may be particularly useful in the present disclosure, e.g., for high thermal stability, high chemical stability, high mechanical stability (e.g., crush resistance), and excellent wettability with various fluids including those with high surface tension. The sub-micron particles that comprise an opaloid may be essentially monodisperse (e.g., as in the case of a colloidal crystal as described above), but may also be polydisperse because, for example, the high degree of uniformity that may be required to enable highly crystalline order is not required in the case of semi-crystalline or nearly amorphous opaloids. In addition, multiple populations of essentially monodisperse colloidal particles (e.g., 2, 3, or more populations) may by design coexist in the same opaloid. For example, specific size ratios and volume fractions of different monodisperse particles may be combined to enable tight packing in specific crystalline or semi-crystalline arrangements. Examples of such size ratios and volume fractions were described, along with an algorithmic method of predicting them, in "Prediction of binary hard-sphere crystal structures" (L. Filion & M. Dijkstra, Physical Review E, 79, 046714, 2009). As another non-limiting example, mixed populations of sub-micron particles may comprise cases where each population of particles comprises different materials (e.g., a population of sub-micron particles of one ceramic blended with a population sub-micron particles of another ceramic, or a population of ceramic sub-micron particles blended with a population of polymer sub-micron particles). In such cases, each population may be substantially monodisperse or polydisperse and the particle sizes of the populations of particles may or may not differ from each other. Such mixed populations of colloidal particles can be prepared, for example, by mixing or blending two or more colloidal dispersions (for example, each corresponding to a substantially monodisperse population of particles) prior to consolidating the mixed or blended particles into an opaloid. Such colloids and opaloids with mixed or blended particle size distributions may be distinguished from typical polydisperse particle size distributions by the presence of multiple peaks in the particle size distribution (e.g., they may exhibit a multi-modal distribution), and/or they may be present in specific size ratios and volume fractions to enable tight packing in crystalline or semi-crystalline arrangements. The shapes of the sub-micron particles are also not particularly limited, and may include spheres, spheroids, cylinders, and other shapes of both low and high aspect ratio as would be understood by one of ordinary skill in the art.

[00111] For clarity, the term "opaloid" as used herein was derived from the word "opal" and the suffix "-oid," the latter being chiefly used in science to form nouns with the meaning, "something having the form or appearance of, something related or allied in structure, but not identical'" as described in the Oxford English Dictionary, (updated OED Third Edition, March 2004; most recently modified version published online December 2021, from www.oed.com/view/Entry/130874#eid33383147, retrieved June 7, 2023). This noun form of opaloid is readily distinguishable from the rarely used English adjective meaning "resembling

an opal in color or appearance" as described in the Oxford English Dictionary, (updated OED Third Edition, March 2004; most recently modified version published online March 2022, from www.oed.com/view/Entry/131683?redirectedFrom=opaloid#eid, retrieved June 7, 2023). www.oed.com/view/Entry/131683?redirectedFrom=opaloid#eid, retrieved June 7, 2023).

[00112] Opaloids can have many desirable properties, such as a narrow distribution of small pore sizes, relatively high porosity, crush resistance, stability at high temperatures, stability in many chemical environments, wettability with various fluids (including water), high optical clarity.. However, the production of high-quality opaloids for practical applications can be very challenging, particularly for opaloids comprising sub-micron particles comprising ceramics or glass, because of the brittle nature of such materials. For example, significant challenges exist in: 1) fabricating large areas (e.g., areas larger in extent than about one millimeter to several centimeters) with high integrity (i.e., relatively free of through-plane defects such as cracks); 2) making highly flexible, free-standing structures that enable efficient roll-to-roll processing; 3) making mechanically robust structures that can withstand handling, installation, and use in industrial or other applications; and 4) enabling sufficiently rapid fabrication for economical, high-volume production. Accordingly, an object of the present invention is to overcome these challenges to enable economical production of high-quality opaloids and permit some or all of the advantageous properties of opaloids to be utilized more readily in practical applications.

Contrasting the Colloidal Glass Transition and Gelation

[00113] Without wishing to be bound by theory, the characteristic structures and properties of opaloids, as well as the manner in which they differ from other materials such as sol-gel solids, may be clarified through a better understanding of the colloidal glass transition and gelation dynamics for the cases of opaloids and sol-gel solids, respectively.

[00114] Glass transition dynamics enable ordered tight packing of colloidal particles, characteristic of opaloids. Unlike molecular glasses, which may undergo a transition from a liquid to a glass upon cooling, colloidal dispersions or colloidal suspensions may undergo a glass transition upon concentrating (i.e., when the packing density of the dispersed phase within the continuous phase increases to the point that it exceeds a critical threshold). This is the so-called colloidal glass transition, which was described as follows by E. Weeks in "Introduction to the Colloidal Glass Transition," ACS Macro Lett., 6, 27-34 (2017), "Their glass transition is not as a function of temperature, but rather of concentration. At low concentration, particles undergo Brownian motion and diffuse through the sample freely. At higher concentrations, the particles pack together randomly (with a liquid-like structure), and macroscopically the sample viscosity grows dramatically as a function of concentration. Below the glass transition concentration, Brownian motion enables the sample to equilibrate, and the

sample is still considered a liquid. Above the glass transition concentration, equilibration is no longer possible on experimental time scales, and macroscopically the sample has a yield stress like a regular elastic material." More detailed dynamics of this process were described in "Dynamics of Colloidal Glasses and Gels" (Y. Joshi, Annu. Rev. Chem. Biomol. Eng. 2014. 5:181–202), using monodisperse, spherical particles as a case study, "…at low volume fractions (φ_v), the suspension is in a fluid state. Upon increasing φ_v slowly beyond 0.494, crystals with $\varphi_v = 0.545$ start nucleating and coexist with the fluid phase. Beyond $\varphi_v = 0.545$, only the crystalline state exists. With further increases in φ_v, the crystals become compact up to $\varphi_v \approx 0.74$, which is the maximum packing fraction associated with the face-centered cubic or hexagonal close packing. If φ_v is increased quickly from the fluid state, thereby preventing nucleation of crystals, the suspension enters the so-called supercooled regime. In this regime, individual particles can be considered to be arrested in cages formed by their neighbors. Owing to thermal motion, the particle rattles inside the cage before escaping (diffusing). This cage-diffusion timescale, also known as α relaxation time (τ_α), increases with φ_v and diverges as $\varphi_v \rightarrow 0.58$, the concentration associated with the colloidal glass transition. Monodispersed spherical particles can exist in the random disordered configuration up to only $\varphi_v = \varphi_{rcp} \approx 0.64$, the random close-packing fraction. φ_{rcp} increases with polydispersity. The elasticity of particulate glasses originates in caging…" The Joshi reference further states, "For spherical particles with hard-sphere interactions, MCT [mode coupling theory] predicts an ideal glass transition at the volume fraction of 0.525." Note that the volume fractions of particles stated in the quote from the Joshi reference were specific to the case study being examined, and these particle volume fractions may differ for other colloidal systems due to, for example, particles with different shapes or degrees of stabilization. For example, the volume fraction associated with the colloidal glass transition may be about 0.4, or about 0.45, or about 0.49, or about 0.5, or about 0.55, or about 0.58, or about 0.60, or about 0.65, or about 0.7, or about 0.75, or about 0.8, or about 0.85. The importance of the colloidal glass transition as the dividing line between low and high solids concentrations, the former of which requires long-range structures (e.g., gels) for rigidity, and the latter of which does not, was further clarified in "Colloidal Gelation" (Del Gado et al., Chapter 14 of Fluids, Colloids and Soft Materials: An Introduction to Soft Matter Physics, First Edition. Edited by Alberto Fernandez Nieves and Antonio Manuel Puertas.© 2016 John Wiley & Sons, Inc. Published 2016 by John Wiley & Sons, Inc.), where the authors note that, "At larger concentrations, the formation of space-spanning networks is no longer a requirement for rigidity" and that above the colloidal glass transition, "the constituent of the system is permanently trapped in cages of nearest neighbors." In summary, the foregoing passages describe the colloidal glass transition in detail and illustrate how it enables colloidal particles to consolidate into tightly packed

structures (e.g., those in which the volume fractions of the constituent particles are greater than about 0.4) with high degrees of order, characteristic of opaloids.

[00115] In contrast, sol-gel processes are characterized by gelation dynamics. As described in “Colloidal Sol-Gel: A powerful, low-temperature aqueous synthesis route of nano-sized powders and suspensions" (Open Ceramics 8, 100200 (2021)), a “sol” is a colloidal system comprising a discontinuous solid phase dispersed in a continuous liquid phase. Sols are typically produced through the hydrolysis of a precursor comprising a metal atom surrounded by ligands that do not contain metal. Depending on the hydrolysis conditions, the solid phase of the resulting sols may be categorized as either fine particles or polymerized molecules (e.g., oligomers), resulting in either a colloidal sol or polymeric sol, respectively, with the latter being significantly more common in the art. Upon gelation (i.e., the “gel” transition step in the sol-gel process) the solid phase forms a network with long-range structure leading to a gel that typically has high viscosity and may be described as comprising a solid phase and a liquid phase that are co-continuous. Gelation occurs at low concentrations (i.e., below the colloidal glass transition, most typically far below it, e.g., as illustrated by the extremely high porosity characteristic of silica aerogels) and is usually induced through chemical means (e.g., through neutralization of surface charges in the sol), resulting in particle gelation and aggregation, as well as poorly-ordered fractal and aggregate structures. As described by Schmidt (Journal of Non-Crystalline Solids 100 (1998) 51-64.), "For stable colloids (which in general remain stable due to the surface charge of their colloidal particles) the neutralization of surface charges (isoelectric point) leads to gelation, including the following basic reactions: neutralisation of surface charges, aggregation, further condensation by reactive surface groups, gelation (accompanied by a strong viscosity increase) to a solid gel." The poor degree of order of fractal gel structures and methods of characterizing the structure are well-established in the literature, for example, by Sinkó et al. (Journal of Non-Crystalline Solids 354 (2008) 5466–5474), “The structure of ill-ordered materials, such as amorphous glasses, fractal systems, or aggregate structures is difficult to describe in direct pictures, these structures can well be characterized by scattering experiments.” The authors further describe how “The aggregate structure defines a random packing of colloidal particles.” In summary, the foregoing passages describe the gelation dynamics of the sol-gel process in detail and illustrate how they result in poorly ordered fractal and aggregate structures characteristic of sol-gel solids.

[00116] Well-ordered opaloids (e.g., those comprising sub-micron particles that have gone through a colloidal glass transition), and sol-gel materials with a fractal structure can be further distinguished by their characteristic length scale. Opaloids exhibit repeating order on the length scale of individual particles and may show a narrow distribution of inter-particle distances, whereas sol-gel structures may exhibit repeating order on the aggregate length

scale. This distinction is described in the following passage from “Dynamics of Colloidal Glasses and Gels” (Y. Joshi, Annu. Rev. Chem. Biomol. Eng. 2014. 5:181–202), "... the colloidal glassy and gel state can be distinguished based on the length scale beyond which the density becomes homogeneous. In particulate colloidal glasses [including e.g., opaloid], this length scale is close to the inter-particle distance, whereas in gels it is approximately the aggregate length scale."

[00117] Due substantially to the gelation dynamics described above, sol-gel processes and the resulting sol-gel solids have several drawbacks that limit their utility. Secondary structure formed during the gelation process can limit the dynamics of packing, producing irregular and polydisperse void structures. Bonding or sintering between particles can result in brittle or inflexible materials, limiting the toughness or durability of produced articles. Porosity may become limited as additional precursor converts to solid during the gelation phase. Furthermore, sol-gel solids, being based primarily on hydrolizable precursors as described above, represent a narrower set of materials than opaloids, which encompass but are not limited to the full gamut of ceramics and glasses. Sol-gel chemistry can also impose significant complexity as well as onerous time constraints on industrial manufacturing processes such as roll-to-roll manufacturing processes. It is an object of the present invention to overcome these deficiencies by developing improved materials and processes based on opaloids.

[00118] Although concentrating a colloidal dispersion or colloidal suspension through the colloidal glass transition may be a preferred element of a process for fabricating opaloids, opaloids are not particularly restricted in their method of manufacture. If the appropriate arrangement of sub-micron particles (e.g., as described above in the Introduction to Opaloids Including Colloidal Crystals) can be made without the use of a colloidal dispersion or colloidal suspension, it may nevertheless be considered an opaloid as defined herein.

[00119] For clarity, the use of the term “colloidal” may be interpreted depending on the context according to both meanings described in Slomkowski et al., “Terminology of polymers and polymerization processes in dispersed systems (IUPAC Recommendations 2011)*” Pure Appl. Chem., Vol. 83, No. 12, pp. 2229–2259 (2011): a “state of subdivision such that the molecules or polymolecular particles dispersed in a medium have at least one dimension between approximately 1 nm and 1 μm, or that in a system discontinuities are found at distances of that order.” Consistent with the first part of this definition (the two parts of the definition being separated by a comma), the term “colloidal” in “colloidal dispersion” or “colloidal suspension” may be interpreted as comprising particles dispersed in a medium in which the particles are within the characteristic length scale from approximately 1 nm to approximately 1 μm in size. Consistent with the second part of this definition, the term “colloidal” as used in “colloidal crystal” or “colloidal semi-crystal” may be interpreted as comprising sub-micron particles (e.g., nanoparticles) that are approximately 1 nm to

approximately 1 μm in size, and/or as indicating that the inter-particle distances (ID) and/or pore sizes (d) of opaloids are also typically in this size range.

[00120] The term "colloidal glass" can be interpreted according to both parts of Slomkowski's definition of "colloidal" quoted above. Consistent with the first part of Slomkowski's definition, the term "colloidal glass" in the scientific literature typically refers to a colloidal dispersion or colloidal suspension that has undergone a colloidal glass transition and exhibits highly viscous, glass-like behavior as described by Weeks as quoted above, "macroscopically the sample viscosity grows dramatically as a function of concentration. Below the glass transition concentration, Brownian motion enables the sample to equilibrate, and the sample is still considered a liquid. Above the glass transition concentration, equilibration is no longer possible on experimental time scales, and macroscopically the sample has a yield stress like a regular elastic material." However, the term colloidal glass can also be interpreted according to the second part of Slomkowski's definition, meaning the sub-micron particles (including nanoparticles) of colloidal glasses are typically 1 nm to 1 μm in size, and the inter-particle distances (ID) and/or pore sizes (d) of colloidal glasses are also typically in this size range. Thus, the term "colloidal glass" does not necessarily imply that the particles are dispersed or suspended in a fluid. Instead, it can refer more broadly to tightly packed arrangements of sub-micron particles that retain features or discontinuities on the colloidal length scale. It may also be interpreted as an acknowledgement that such arrangements of sub-micron particles are usually produced from a precursor that was itself a colloidal dispersion or colloidal suspension. The opaloids described in the present disclosure may therefore be considered a form of colloidal glass. However, for clarity, the inventors prefer the term "opaloid" to "colloidal glass" as a term to describe the broad class of materials that is the focus of the present disclosure.

Detailed Description of Neat Opaloid Morphology and Properties

[00121] This section will establish basic nomenclature for describing opaloid structures without mechanical reinforcement. Such opaloids without mechanical reinforcement (e.g., without an integrated microporous polymer scaffold) may also be called "neat" opaloids. Material properties of neat opaloids will also be discussed.

[00122] **Figure 3a** shows a schematic of a cross-section of a neat opaloid 9 comprising monodisperse sub-micron particles 10 in a three-dimensional arrangement. The sub-micron particles in **Figure 3a** are depicted as having a high degree of order (e.g., a substantially face-centered cubic arrangement), but as described above other packing arrangements are possible, for example more amorphous arrangements such as liquid-like packing. The neat opaloid may comprise large defects (e.g., cracks) 11 that extend through the entire thickness

of the opaloid, and may comprise other defects (e.g., cracks) 12 that do not extend through the entire thickness.

[00123] As described above, opaloids comprise tightly packed three-dimensional arrangements of sub-micron particles. **Figure 3b** shows two adjacent particles of diameter D that are elements of a particle packing arrangement within an opaloid. The tightness of the packing arrangement may be described by the inter-particle distance (ID, typically expressed in units of nanometers), which is the distance between the centers of adjacent sub-micron particles (or if the particles are non-spherical, then between the centroids of adjacent particles). Inter-particle distance may be considered a population property that is inherently polydisperse and may be described by an ID distribution. In an opaloid, the ID may be of colloidal size. Further, the ID of two adjacent particles may be approximately the particle diameter D (note that for polydisperse particles the effective D is the sum of the radii of the two adjacent particles, and if a particle is irregularly shaped then its effective radius is the radius of a sphere that occupies the same volume, and analogously its effective diameter is the diameter of a sphere that occupies the same volume). However, even in a tightly packed arrangement the distance between two adjacent particles may be smaller or larger than the sum of their radii. The distance may be smaller, for example, because particles with irregular shapes may enable tighter packing. The distance may be larger, for example, because sub-micron particles in the opaloid may not pack in perfect crystalline arrangements or because they may be coated in a material such as a polymeric material (e.g., a dispersing agent). The ID may be, for example, greater than about 0.5 times the effective particle diameter D and less than about 3 times the effective particle diameter D. The ID may be, for example, greater than about 0.5 times the effective particle diameter D and less than about 2.5 times the effective particle diameter D. The ID may be, for example, greater than about 0.5 times the effective particle diameter D and less than about 2 times the effective particle diameter D. In some examples, the amount of material (e.g., polymeric material) between adjacent particles may be minimized or eliminated. In the latter case, for example, the sub-micron particles may have direct contact with each other. The opaloid may substantially lack an organic binding agent (e.g., a polymeric binder). The opaloid may comprise sub-micron particles that are bonded together substantially by van der Waals forces, by inorganic bonds, or by a combination of the two.

[00124] The inter-particle distance may be determined via microscopy in combination with Quantitative Image Analysis, for example using the method depicted on the scanning electron micrograph in **Figure 4**. As indicated by the subscripts in the figure (i.e., D_n and ID_n), a sufficient number of particles (to measure D) and pairs of adjacent particles (to measure ID) may be analyzed to generate representative statistics for the opaloid. To obtain a high-quality microscopy image, the conditions must be appropriately tailored to the specific sample being

examined (e.g., appropriate magnification, working distance, accelerating voltage, etc.). The practice of tailoring such observing conditions is well-known to those of ordinary skill in the art. Quantitative Image Analysis may be used for determining ID when the inter-particle distance is larger than about 80 nm or larger than about 100 nm. If the inter-particle distances are less than about 100 nm or less than about 80 nm, then Small Angle X-ray Scattering (SAXS) may be used to determine the inter-particle distance. **Figure 5a** shows representative SAXS data sets for neat opaloids prepared with 5 different types of silica sub-micron particles with diameters of approximately 7 nm, 12 nm, 22 nm, 45 nm, and 100 nm. The peaks in the SAXS data are identified with triangles and correspond to structures of a given length scale, typically from 0.5 nm to 80 nm. For these data, peaks indicate nanoscale organization of particles (spherical in this case) and are observable due to the contrast between SiO_2 and pores (vacuum). The peaks can be referred to as structure factor peaks. Peak positions are given by the scattering vector, q, and the average center-to-center inter-particle distance, ID, is obtained from the position of the primary peak, q_1, or lowest q-value peak: ID = $2\pi/q_1$. As shown in **Figure 5b**, there is reasonable agreement between nominal particle diameters (D) and the inter-particle distance (ID) values determined by SAXS for neat (i.e. non-reinforced) packing arrangements of SiO_2 sub-micron particles. The dashed line in **Figure 5b** is the 45° line passing through the origin and is included as a guide to the eye. For 7 nm and 45 nm silica sub-micron particle opaloids, weak, broad peaks indicate a more disordered structure and broader distribution of center-to-center IDs compared to the other data in the chart. A weak higher order feature was observed, but it is difficult to determine the peak position or assign the scattering profile to cubic or close-packed morphology. In contrast, opaloids with 12, 22, and 100 nm silica sub-micron particles exhibited narrow peaks, corresponding to a narrow distribution of IDs. Narrow peaks also indicate greater long-range order, where particles exhibit more uniform symmetry over length scales greater than the nearest neighbors. Multiple higher order peaks may also signify long-range order. Higher order peaks may also result from larger particles and inter-particle distances, which shift the scattering pattern to lower q and allow higher order peaks to be detected within the instrument's range. Higher-order scattering peaks are characterized by peak positions q_2, q_3, … q_n. The packing arrangement can be deduced by comparing SAXS peak position ratios, $q_1/q_1 : q_2/q_1 : q_3/q_1 : \ldots q_n/q_1$, to characteristic values for specific arrangements, where q_n corresponds to the positions of the higher order peaks. Peak position ratios for common spherical packing geometries may include 1 : 1.41 : 1.73 : 2.00 : 2.24 : 2.45 : 2.83 (simple cubic packing), 1 : 1.41 : 1.73 : 2.00 : 2.24 : 2.45 : 2.65 (body-centered cubic packing), 1 : 1.15 : 1.63 : 1.91 : 2.00 : 2.31 : 2.52 : 2.58 : 2.83 : 3.00 (face-centered cubic packing), or 1 : 1.06 : 1.13 : 1.46 : 1.73 : 1.87: 1.92 (hexagonal close packing). In **Figure 5a**, peaks are observed at peak position ratios $q_1/q_1 : q_2/q_1 : q_3/q_1 : \ldots q_n/q_1$ of 1 : 1.64 : 2.34, 1 : 1.67 : 2.43, and 1 : 1.70 : 2.50 : 3.28 :

4.04 : 4.81, for neat opaloids with 12, 22, and 100 nm silica sub-micron particles, respectively. The SAXS peak position ratios are consistent with having substantially close-packed arrangements; however, deviations from reported peak position ratios indicate that these neat opaloids do not exhibit perfect crystalline order. Deviations from expected values may be due to, for example, packing defects or polydispersity. A given observed peak position ratio may be within about 1% , or within about 2 %, or within about 3 %, or within about 4 %, or within about 5% of the nearest characteristic peak position ratio and certain peak position ratios may not be observed, for example depending on the form factor scattering of the sub-micron particles.

[00125] Structure factor peaks may be identified in the Lorenz-corrected data (intensity*q^2) as will be understood by one of ordinary skill in the art. Opaloids may be characterized by the presence of 1 or more structure factor peaks in the SAXS data, or by the presence of 2 or more structure factor peaks in the SAXS data, or by the presence of 3 or more structure factor peaks in the SAXS data, or by the presence of 4 or more structure factor peaks in the SAXS data, or by the presence of 5 or more structure factor peaks in the SAXS data, or by the presence of from 1 to 5 structure factor peaks in the SAXS data, or by the presence of from 1 to 10 structure factor peaks in the SAXS data, or by the presence of from 2 to 5 structure factor peaks in the SAXS data, or by the presence of from 2 to 10 structure factor peaks in the SAXS data. For a material to be considered an opaloid, it is not required that the peak position ratios for the structure factor peaks correspond to the theoretical peak position ratios for known arrangements of particles.In contrast, the SAXS data depicted in **Figure 6,** which was reproduced from Bushell et al. ("On techniques for the measurement of the mass fractal dimension of aggregates," *Advances in Colloid and Interface Science*, **95**, 1-50 (2002)), shows an absence of the structure factor peaks characteristic of opaloids. Instead, it shows representative SAXS data for a material comprising aggregates of monodisperse spherical particles, illustrating the Guinier, Fractal, and Porod scattering regimes. These data are characteristic of the poorly ordered fractal and aggregate structures characteristic of sol-gel solids. When analyzing SAXS data, care must be taken not to misinterpret the features shown in **Figure 6**, such as the "knee" at the transition between the Guinier regime and the Fractal regime, or the q^{-4} dependence of the scattering intensity in the Porod regime, as structure factor peaks. As described above, structure factor peaks may be preferably identified in the Lorenz-corrected data (intensity*q^2).

[00126] The spaces between and among the sub-micron particles in an opaloid (i.e., the inter-particle pores, collectively the inter-particle pore volume, typically expressed in units of cc/g or as a porosity in vol%) may define an interconnected pore volume that is characteristic of the opaloid. **Figure 3a** shows a schematic of a cross-section of a neat opaloid comprising monodisperse sub-micron particles 10 in a three-dimensional packing arrangement, having

an inter-particle pore volume 13. The pore volume 13 may have a complex and/or irregular geometry. The challenge of quantitatively characterizing the pore size of porous materials with complex or irregular pore geometries is well-known. Pore size in this case may be considered a population property that is inherently polydisperse and may be described by a pore size distribution. A variety of standard evaluation methods are available to those of ordinary skill in the art, such as quantitative image analysis, BET/BJH analysis, capillary flow porometry (including bubble point analysis), liquid/liquid porometry, thermoporometry by differential scanning calorimetry, and mercury porosimetry. Each of these quantification methods makes simplifying assumptions about the pore geometry, and most produce a pore size distribution from which characteristic pore size parameters may be extracted, such as a median or mode pore size (via BET/BJH analysis), the largest through-pore (e.g., via bubble point determination), or the mean flow pore size (via capillary flow porometry). In some embodiments, the mode pore size(s) of opaloids may be characterized via BET/BJH analysis as a preferred method. **Figure 7** shows a representative pore size distribution from BET/BJH analysis of a neat opaloid prepared from silica sub-micron particles with a diameter of approximately 12 nm. The mode pore size of the distribution shown in **Figure 7** is approximately 5 nm. The three-dimensional packing arrangement of the neat opaloid may be further characterized by comparing the pore diameter (d) to the particle diameter (D), for example using the ratio d/D. **Figure 8** shows the expected values of d/D for different tightly packed arrangements with different coordination numbers (n). For many opaloid packing arrangements, the pore diameter is expected to be smaller than the particle diameter (i.e., d/D ≤ 1). However, for the same reasons that the ID may be larger than D, d/D may be larger than 1, for example the opaloid may have d/D ≤ 1.1 or d/D ≤ 1.5 or d/D ≤ 2.0.

[00127] The challenge of characterizing the particle size (e.g., the particle diameter, D) of the sub-micron particles in an opaloid is also complex and well-known to those of ordinary skill in the art. A variety of standard tools are available, such as dynamic light scattering of the colloidal dispersion from which the opaloid is produced (in which case care must be taken to prevent agglomeration from skewing the data), or direct microscopy of the opaloid itself, such as in **Figure 4**. In the case of particles of known shape (e.g., spherical particles), and known level of surface roughness (e.g., essentially smooth), the specific surface area (SSA, in units of m^2/g, as measured by BET) may be measured, and if the density of the particles (ρ) is known (or if it can be measured, for example by helium pycnometry), then a representative particle size may be calculated using, for example, the standard equations for the volume and area of a sphere (V_{sphere} and A_{sphere}, respectively) based on its diameter (D). The relevant equations for a sphere are as follows:

$$A_{sphere} = \pi D^2$$

$$V_{sphere} = \frac{\pi D^3}{6}$$

$$SSA = \frac{\pi D^2}{\rho\left(\frac{\pi D^3}{6}\right)} = \frac{6}{\rho D}$$

$$D = \frac{6}{(SSA)\rho}$$

Figure 9 illustrates how SSA may be used to estimate the particle size of an opaloid. Five neat opaloids were produced from solid silica sub-micron particles with nominal diameters (as reported by the manufacturers) of 7 nm, 12 nm, 22 nm, 45 nm, and 100 nm. **Figure 9a** compares the SSA measured by BET (solid dots) to the expected values (open squares). The expected values were calculated assuming the sub-micron particles are perfectly smooth, solid spheres of the nominal diameter and assuming a density of silica of 2.2 g/cc. **Figure 9b** compares the particle diameter calculated from the SSA data to the nominal diameters reported by the manufacturers. The dashed line in **Figure 9b** is the 45° line passing through the origin and is included as a guide to the eye. As shown in **Figure 9b**, the SSA method for determining particle size works well for particles that are essentially smooth, solid spheres and may be utilized in such relatively simple cases. However, this method may not be as accurate for particles with a large degree of internal porosity or high surface roughness. In such complex cases characterizing the particle size of the constituent sub-micron particles in an opaloid may be done with direct observation via scanning electron microscopy, which may be combined with quantitative image analysis. The calculations described in the foregoing paragraph, and illustrated in **Figure 9**, may be used to calculate the effective diameter of the sub-micron particles of the opaloid. In the case that the sub-micron particles contain intra-particle pores, then the density to be used in the calculation is the sub-micron particle apparent density. The sub-micron particle apparent density is the matrix density of the particle multiplied by the intra-particle porosity of the sub-micron particle.

[00128] In the description of opaloid morphology above, many of the properties may be considered population properties, such as inter-particle distance (ID), pore diameter (d), and particle diameter (D). Such properties may be represented by distributions, which may be characterized using standard summary statistics known to those of ordinary skill in the art. Such summary statistics include the median value, the volume-weighted mode value, the volume-weighted average, the number-weighted mode value, the number-weighted average, and the related 10/25/75/90 percentile values. When comparing two different population properties (for example, when comparing pore diameter to particle diameter), consistent summary statistics may be used (for example, making the comparison using the mode value for both properties). In some cases, the volume-weighted mode value may be preferred.

Advantages and Challenges of Opaloids

[00129] As described above, opaloids may have many advantageous properties, especially when the opaloid comprises sub-micron particles (including nanoparticles) that themselves comprise ceramics or glass. Such properties may include:

1. Narrow distribution of small pore sizes (e.g., comprising the spaces between adjacent sub-micron particles, and optionally porosity within sub-micron particles)
2. Relatively high porosity, especially considering their small pore size (e.g., porosity of around 30 vol% - 70 vol%, due to the packing arrangement of the constituent sub-micron particles)
3. Crush-resistance, enabling porosity to be retained even under mechanical compression
4. Stability at high temperatures (e.g., including dimensional stability due to the tight packing and temperature stability of the constituent sub-micron particles)
5. Stability in a wide range of chemical environments (e.g., due to the chemical properties of the constituent sub-micron particles)
6. Wettability with various fluids including water (e.g., due to the wettability of the constituent sub-micron particles)

[00130] However, practical and high-integrity opaloids are very challenging to produce. Significant challenges include:

a. Fabricating large areas with high integrity (e.g., relatively free or free of through-plane defects such as cracks). In this case, “large areas” means larger than between 1 millimeter or a few centimeters in extent in each of two orthogonal directions, and “through-plane defects” can be characterized as through-plane cracks or holes that compromise the integrity of the opaloid and contribute to it having e.g., greater haze, a much lower bubble point, higher liquid or gas permeance, and/or poorer ability to selectively remove small species via filtration.
b. Making flexible, free-standing structures that enable e.g., industrial roll-to-roll processing. Bending stiffness may be quantified by e.g., a Kawabata bend test. Furthermore, flexibility may also be evaluated by wrapping the composite membrane around a mandrel of defined diameter, then unwrapping the composite membrane, repeating these cycles of wrapping and unwrapping a desired number of times, and then using a performance test to evaluate the suitability of the composite membrane for the desired application. A non-limiting example of such a performance test is the Organic Solvent Nanofiltration (OSN) test described below.
c. Making mechanically robust structures that can withstand shipping, handling, storage, installation, and operation in the intended application, especially when the

opaloid is very thin. Tensile testing may be used, for example, to evaluate mechanical robustness.

d. Enabling sufficiently rapid fabrication (e.g., coating and drying times of a few minutes or less, for example less than 1 minute) for e.g., economical, high-volume production (e.g., thousands of square meters per year, hundreds of thousands of square meters per year, millions of square meters per year, or more).

Introduction to Membrane-Reinforced Opaloids

[00131] The inventors have surprisingly discovered that some or all of the aforementioned challenges a – d can be overcome, while simultaneously retaining some or all of the aforementioned advantageous properties 1 – 6, by producing composite membranes in which an opaloid is reinforced with a microporous polymer scaffold. **Figure 10a** shows a schematic of a microporous polymer scaffold 14, for example ePTFE, comprising scaffold matrix 15, for example nodes interconnected by fibrils, and scaffold pores 16. As illustrated in **Figure 10b**, the inventors have shown that opaloid 9 comprising sub-micron particles 10 and inter-particle pores 13 can be formed within the scaffold pores 16 of the microporous polymer scaffold to form composite membranes 20 of the present disclosure. Such composite membranes may be referred to as Membrane-Reinforced Opaloids (MROs). **Figure 10b** further shows that the MROs (i.e., the composite membranes 20) comprise composite membrane pores 22, which comprise inter-particle pores 13 of the opaloid 9 within the scaffold pores 16, and interfacial particle-scaffold pores 24 (i.e., pores whose boundaries are defined by both the structural elements of the scaffold and the constituent particles of the opaloid; in practice these are pores at the interface between the opaloid and the scaffold matrix). Additionally, cracks or defects 26 may be present. In an MRO, an opaloid may fill at least a portion of the pore volume of a microporous polymer scaffold. The opaloid may comprise a continuous opaloid phase (e.g., with a continuous pore volume defined by the inter-particle pores) that extends over a large area (meaning larger than between 1 millimeter or a few centimeters in extent in each of two orthogonal directions) within the pore volume of the microporous polymer scaffold.

[00132] The inventors have surprisingly discovered that the quality of MROs may be dramatically improved when they comprise a microporous polymer scaffold characterized by extremely tight pores (i.e., a microporous polymer scaffold with a bubble point of greater than about 2 bar). Such MROs may be referred to as High-Integrity MROs. In High-Integrity MROs, cracks or defects 26 (as shown in **Figure 10**) can be minimized or eliminated. The minimization or elimination of such cracks or defects may be demonstrated, for example, using capillary flow porometry of the MRO and/or direct visualization of the MRO via microscopy such as scanning electron microscopy, as will be shown below.

[00133] The production of MROs with high integrity and high quality via the use of membrane reinforcements with extremely tight pores was surprising in numerous respects:

1. The extremely tight structure and high surface area of the microporous polymer scaffold provided a large number of potential nucleation sites for defects within the opaloid. Nevertheless, through-plane defects (e.g., cracks) were surprisingly minimized (e.g., as measured by capillary flow porometry).

   The extremely tight structure and high surface area of the microporous polymer scaffold provided a large number of interfaces with the potential to disrupt the formation and structure of the opaloid. Nevertheless, the MROs surprisingly and substantially retained both the narrow distribution of small pores (e.g., as measured by BET/BJH), and the tight particle packing arrangement (e.g., as measured by SAXS) associated with the neat opaloid.

   The rapid drying of the MROs under hot-air convection (e.g., in a few minutes or less, consistent with the needs of high-volume production), imposed turbulent surface forces and significant mechanical stresses on the MRO. Nevertheless, defects were surprisingly minimized (e.g., as measured by capillary flow porometry, BET/BJH, SAXS, and haze), and there was no obvious loss of particles during drying or subsequent handling despite the absence of a binder (e.g., a polymeric binder).
2. The extremely tight structure and high surface area of the microporous polymer scaffold provided a high-surface-area matrix of hydrophobic material throughout the composite membrane. Nevertheless, the resulting MROs were surprisingly highly wettable with water.
3. The extremely tight structure and high surface area of the microporous polymer scaffold provided a large number of interfaces to nucleate defects during mechanical stress testing, and the lack of a binder provided limited support to cohere the particles. Nevertheless, the resulting MROs were flexible and free-standing and able to survive significant handling and mechanical stress without significant loss of particles or desirable properties. In addition, the MROs showed exceptional robustness when subjected to liquid flow under very high trans-membrane pressures up to about 50 bar with no obvious change in liquid permeance after exposure to such high pressures.
4. The use of reinforcements with extremely tight structures surprisingly produced a “step change” in the ability of the MROs to selectively separate small molecules from a solvent (e.g., as measured through organic solvent nanofiltration).

As described above, both the sub-micron particles and the microporous polymer scaffolds are main elements of the membrane-reinforced opaloids of the present invention. These elements will be described in greater detail in the next two sections.

Description of Sub-micron Particles

[00134] The following description of the sub-micron particles is applicable to all embodiments, examples and aspects of the composite membranes described herein. The sub-micron particles within the plurality of scaffold pores may be substantially monodisperse in size. The sub-micron particles may comprise a mixture of substantially monodisperse populations (e.g., resulting in a multi-modal pore size distribution). As used herein, the term population may be used to refer to sub-groups within the sub-micron particles, for example sub-micron particles having different sizes within a population having otherwise about the same materials, and/or shape, and/or source within the supply chain. Alternatively, populations may be used, for example, to refer to sub-groups having different sizes, and/or materials, and/or shape, and/or source within the supply chain.

[00135] The sub-micron particles may have a particle diameter (or effective particle diameter) of about 1 nm to about 1 μm. Therefore, the term sub-micron particle is also intended to include nanoparticles, where nanoparticles are particles typically comprising a particle diameter (or effective diameter) of about 1 nm to about 100 nm. The sub-micron particles may have a particle diameter (or effective particle diameter) of about 1 nm to 500 nm (noting that the term “about” applies to both the bottom and top of the range), or about 1 nm to about 200 nm, or about 10 nm to 500 nm, or about 1 nm to 100 nm, or about 1 nm to 80 nm, or about 5 nm to 70 nm, or about 4 nm to 50 nm, or about 5 nm to 50 nm, or about 5 nm to 75 nm, or about 2 nm to 60 nm, or about 2 nm to 50 nm, or about 2 nm to 25 nm. The sub-micron particles may have a particle diameter (or effective particle diameter) of up to and including 45 nm, or up to and including 25 nm, or up to and including 15 nm, or up to and including 10 nm, or up to and including 8 nm. Without wishing to be bound by theory, it is hypothesized that larger particles may result in weaker drying forces, and therefore tighter (higher bubble point pressure) microporous polymer scaffolds may not necessarily be required to prevent defects (e.g., cracks) within the composite membrane during fabrication when such particles are used.

[00136] The sub-micron particles may comprise at least two different populations of sub-micron particles, where a first population of sub-micron particles is characterized by a first particle diameter (or effective particle diameter) and a second population of sub-micron particles is characterized by a second particle diameter (or effective diameter). The first and second particle diameters (or effective diameters) may be the same, or the first and second particle diameters (or effective diameters) may be different.

[00137] As used herein, the particle diameter is taken to mean the particle diameter as measured by the test methods described herein. It is also intended to encompass non-spherical particles, where such particles may be regarded as having an effective particle diameter. As used herein, the effective particle diameter is the diameter of a hypothetical spherical particle of same composition that, using a given particle-size determination method, would give the same diameter as a substance composed of spherical or non-spherical particles at the same concentration.

[00138] The sub-micron particles are not intended to be limited to a particular shape and may include sub-micron particles of any shape as required for the composite membranes' intended purpose. The sub-micron particles may be substantially spherical in shape. The sub-micron particles may have a polygonal structure. The sub-micron particles may have an aspect ratio of about 1, or of about 1.2, or of about 1.4, or of about 1.6, or of about 2, or of about 2.5, or of about 3.

[00139] The sub-micron particles may be porous or non-porous. The sub-micron particles may be hydrophilic or hydrophobic. The sub-micron particles may be oleophilic or oleophobic.

[00140] The sub-micron particles may be stable at very high pH (e.g., above about pH 10, or above about pH 11, or above about pH 12, or above about pH 13, or above about pH 14). The sub-micron particles may be stable at very low pH (e.g., below about pH 5, or below about pH 4, or below about pH 3, or below about pH 2, or below about pH 1, or below about pH 0).

[00141] The sub-micron particles may comprise a wide variety of materials including ceramics and glasses (noting that some common definitions of ceramics include glasses as a subset of ceramics). Sudha et al. describe ceramics as follows in "Corrosion of ceramic materials" (in Fundamental Biomaterials: Ceramics, Editor(s): Sabu Thomas, Preetha Balakrishnan, M.S. Sreekala,Woodhead Publishing Series in Biomaterials, Woodhead Publishing, 2018, Pages 223-250), "Ceramics materials can be defined as inorganic, nonmetallic materials comprising metal, nonmetal, or metalloid atoms held by ionic or covalent bonds. The ceramic structure is based on electric neutrality. They are generally prepared using clays and other minerals from the earth or chemically processed crystalline oxide, nitride, or carbide powders, i.e., aluminium and oxygen (alumina—Al_2O_3), silicon and nitrogen (silicon nitride—Si_3N_4), silicon and carbon (silicon carbide—SiC), etc. Ceramic materials are typically categorized as traditional ceramic and advanced ceramic. Traditional ceramic materials include clay, porcelain, feldspar, silica, calcite, and nepheline... Advanced ceramics includes alumina, zirconia, silicon carbide, silicon nitride, and titania-based materials, which can replace the metals and plastics in the modern era due to their exceptional properties that make them highly resistant to melting, bending, stretching and possess unique individual properties

in their own way... Ceramic materials are broadly classified into two types based on the arrangement of atoms that constitute the particular substance. (a) Crystalline ceramic materials: Most of the ceramic materials have crystalline structure and are more brittle than metals. The arrangement of atoms in the crystalline ceramic was highly ordered throughout the material. Crystalline ceramics were not amenable to set of processing/production. These materials were generally synthesized either by compacting powders into a body followed by sintering at higher temperature to form a solid desired shape or by the reaction "in situ." The techniques adapted to form crystalline ceramics include slip casting, tape casting, injection molding, dry pressing, and so on. (b) Noncrystalline/Amorphous ceramic materials: The processing of glass is totally different from the crystalline ceramic preparation and involves several steps. Noncrystalline ceramic, being glasses, can be usually prepared from melts. The glasses were processed into desired shape either by casting them in the molten state or by blowing the toffee-like viscosity state into a mold. These noncrystalline ceramic materials were also called "Super cooled liquids" because the orientations of molecules are random and highly disordered in the frozen solid state..."

[00142] Examples of suitable ceramics may include silica, alumina, titania, ceria, zirconia, yttria-stabilized zirconia, other oxides, and other classes of ceramics including carbides, nitrides, sulfides, borides, phosphides, selenides, titanates, carbonates, nitrates, sulfates, borates, and phosphates, or combinations thereof.

[00143] The sub-micron particles may be colloidal sub-micron particles. The sub-micron particles may be imbibed within the scaffold pore volume comprising the scaffold pores. The sub-micron particles may be suspended in a liquid as a colloidal precursor (e.g., a colloidal suspension or colloidal dispersion) at least during the imbibing process, where the colloidal precursor may comprise a fluid continuous phase and the sub-micron particles dispersed or suspended within the continuous phase. The composite membrane may comprise the fluid (or liquid) continuous phase in the inter-particle pores within the opaloid. Such arrangements of sub-micron particles are usually produced from a colloidal precursor that was itself a colloidal dispersion or colloidal suspension. However, the sub-micron particles are not necessarily dispersed or suspended in a fluid (or the fluid continuous phase) within the scaffold pore volume. As such, the composite membrane may comprise an opaloid within the scaffold pores that is fully dried, i.e., the fluid continuous phase between the sub-micron particles of the opaloid having been substantially removed. The three-dimensional arrangements of sub-micron particles described by the term opaloids within the scaffold pores, as used herein, are not particularly restricted in their method of manufacture, and if the same or similar arrangement of sub-micron particles is made without the use of a precursor that is a colloidal

dispersion or colloidal suspension, it may nevertheless be considered an opaloid as defined herein.

[00144] The sub-micron particles may be coated in a material, for example to aid in colloidal stabilization of the colloidal suspension or colloidal dispersion, and/or to aid in the formation of the opaloid within the scaffold pores. The material may comprise, for example, a polymeric material (e.g., a dispersing agent).

Description of Microporous Polymer Scaffolds

[00145] The following description of the microporous polymer scaffolds is applicable to all embodiments, examples and aspects of the composite membranes described herein. As used herein, the term "microporous polymer scaffold" refers to a thin, flexible, freestanding, porous polymer structure that may be configured in a variety of forms such as a porous web (i.e., a long, thin, flexible material typically supplied in roll form), a porous sheet (e.g., a flat sheet), or a porous tube (e.g., a round tube). The microporous polymer scaffold may be in the form of a porous web or porous flat sheet. As used herein, the term "porous" is meant to denote a structure comprising voids (i.e., pores) within a solid matrix. The pores each have a pore volume, and the plurality of pores define the total pore volume of the microporous polymer scaffold (i.e., the scaffold pore volume). The solid matrix (i.e., the scaffold matrix) refers to the solid portion of the microporous polymer scaffold, excluding its pore volume.

[00146] The microporous polymer scaffold may have a first major exterior surface (i.e., a first surface) and a second major exterior surface (i.e., a second surface) that opposes the first surface (in the case of a tube these two surfaces correspond to the inner and outer diameters of the tube). The microporous polymer scaffold may have a thickness, which is the distance between the first and second major exterior surfaces. The plurality of pores have inner surfaces defined by their interfaces with the scaffold matrix. The inner surface of a pore refers to the surface of the pore that is not on an exterior surface of the scaffold.

[00147] As used herein, the term "microporous" refers to a structure, such as a polymer scaffold or membrane, that comprises pores that are not visible to the naked eye and that create passageways extending from the first major surface to the second major surface (i.e., from one exterior surface of the layer to the opposite exterior surface of the layer). Such passageways may be described as "through pores." The scaffold pore volume may also comprise pores that are not "through pores" (i.e., some pores may not be connected to both exterior surfaces through the scaffold pore volume). Such pores that are connected to only one exterior surface may be described as "dead-end pores," and such pores that are not connected to either exterior surface may be described as "closed-cell pores." Within the scaffold pore volume, all of the pores may be interconnected and may form a continuous

porous network, or all of the pores may be isolated from each other, or there may be any intermediate level of interconnection among the pores. In some embodiments, the term "microporous" may have a maximum pore size as defined by its bubble point that is less than about 1000 µm. The scaffold pores may have an average pore size on a volume basis (e.g., as measured by BET/BJH) from about 0.01 to about 100 µm, e.g., from about 0.01 to about 1 µm, or about 0.02 to about 25 µm, or about 0.01 to about 10 µm, or about 0.05 to about 20 µm, or about 0.1 to about 80 µm, or about 0.1 to about 50 µm, or about 0.1 to about 30µm, or about 0.2 to about 60 µm, or about 0.5 to about 50 µm, or any intermediate range or value between about 0.01 to 100 µm. The scaffold pores may have a median pore size on a volume basis (e.g., as measured by BET/BJH) from about 0.01 to about 100 µm, e.g., from about 0.01 to about 1 µm, or about 0.02 to about 25 µm, or about 0.01 to about 10 µm, or about 0.05 to about 20 µm, or about 0.1 to about 80 µm, or about 0.1 to about 50 µm, or about 0.1 to about 30µm, or about 0.2 to about 60 µm, or about 0.5 to about 50 µm, or any intermediate range or value between about 0.01 to 100 µm. The scaffold pores may have a primary mode pore size (i.e., the pore size corresponding to the peak of the largest mode) on a volume basis (e.g., as measured by BET/BJH) from about 0.01 to about 100 µm, e.g., from about 0.01 to about 1 µm, or about 0.02 to about 25 µm, or about 0.01 to about 10 µm, or about 0.05 to about 20 µm, or about 0.1 to about 80 µm, or about 0.1 to about 50 µm, or about 0.1 to about 30µm, or about 0.2 to about 60 µm, or about 0.5 to about 50 µm, or any intermediate range or value between about 0.01 to 100 µm. The scaffold pores may have a primary mode pore size (i.e., the pore size corresponding to the peak of the largest mode) on a number basis (e.g., as measured by BET/BJH) from about 0.01 to about 100 µm, e.g., from about 0.01 to about 1 µm, or about 0.02 to about 25 µm, or about 0.01 to about 10 µm, or about 0.05 to about 20 µm, or about 0.1 to about 80 µm, or about 0.1 to about 50 µm, or about 0.1 to about 30µm, or about 0.2 to about 60 µm, or about 0.5 to about 50 µm, or any intermediate range or value between about 0.01 to 100 µm. The scaffold pores may have a mean flow pore size (e.g., as measured by Capillary Flow Porometry) from about 0.01 to about 100 µm, e.g., from about 0.01 to about 1 µm, or about 0.02 to about 25 µm, or about 0.01 to about 10 µm, or about 0.05 to about 20 µm, or about 0.1 to about 80 µm, or about 0.1 to about 50 µm, or about 0.1 to about 30µm, or about 0.2 to about 60 µm, or about 0.5 to about 50 µm, or any intermediate range or value between about 0.01 to 100 µm.

[00148] The scaffold matrix may comprise a continuous network of interconnected material elements, and the scaffold pores may be void spaces between these material elements. The material elements may comprise a wide variety of structural components that form the building blocks of the overall polymer structure. The material elements are not particularly limited, and may comprise, for example, fibers, bundles of fibers, nodes, and fibrils. In one embodiment, the microporous polymer scaffold may have a microstructure comprising fibers, bundles of

fibers, and a plurality of scaffold pores, where the fibers and bundles of fibers are interconnected, and the plurality of scaffold pores are void spaces between the fibers and bundles of fibers. In another embodiment, the microporous polymer scaffold may have a microstructure comprising nodes, fibrils, and a plurality of scaffold pores, where the nodes are interconnected by the fibrils, and the plurality of scaffold pores are void spaces between the nodes and fibrils.

[00149] A suitable microporous polymer scaffold depends largely on the intended application. The microporous polymer scaffold may support and mechanically reinforce composite materials or membranes (e.g., a composite membrane such as a membrane-reinforced opaloid), improving its structural integrity, handleability, and durability. The microporous polymer scaffold may enable the composite membrane to be thin (e.g., less than about 150 microns) and/or have a large area while retaining handleability and other desirable properties. The microporous polymer scaffold may have good mechanical properties and be thermally, chemically, and electrochemically stable in the environment in which the composite membrane is to be used. The microporous polymer scaffold may also be tolerant of any manufacturing steps required in the production of the composite membrane, as well as in the subsequent storage, shipping, and handling of the composite membrane.

[00150] The microporous polymer scaffold may be stable at very high pH (e.g., above about pH 10, or above about pH 11, or above about pH 12, or above about pH 13, or above about pH 14). Additionally, the microporous polymer scaffold may be stable at very low pH (e.g., below about pH 5, or below about pH 4, or below about pH 3, or below about pH 2, or below about pH 1, or below about pH 0).

[00151] The microporous polymer scaffold may be formed by any suitable method applicable for the intended application. The method of manufacturing the microporous polymer scaffold is not particularly limited, and any conventional method known in the art may be used to form the microporous polymer scaffold. Non-limiting examples of suitable processing methods include roll-to-roll processing, paste processing, gel processing, and expansion. The microporous polymer scaffold may be a microporous polymer membrane or polymer substrate. Depending largely on the method of manufacture, the microporous polymer scaffold may have a machine direction (MD) and a transverse direction (TD), where the MD is orthogonal to the TD, and the MD and TD are each orthogonal to the thickness direction. For webs, MD aligns with the long direction, and TD aligns with the width direction.

[00152] The microporous polymer scaffold may be formed from/of any suitable material for the intended application. The material is not particularly limited and may be any material known to those of skill in the art to form the microporous polymer scaffold. In some embodiments, the microporous polymer scaffold may comprise polymeric materials. The polymeric materials may comprise a polymer or a mixture of polymers. The polymeric

materials may comprise a homopolymer or a copolymer. The polymeric materials may comprise inorganic polymeric materials and/or organic polymeric materials. The polymeric materials may comprise fluorine and/or heteroatoms. The polymeric materials may comprise aromatic moieties and/or non-aromatic (e.g., aliphatic or olefinic) moieties. The polymeric materials may comprise side chains and/or functional groups. The polymeric materials may comprise a polymer that is fibrillatable (e.g., PTFE). As used herein, the term "fibrillatable" refers to the ability of a polymer to form a fibril microstructure, such as, for example, by solid state deformation or paste processing. The microporous polymer scaffold may be formed from a non-fluorinated polymer, a partially fluorinated polymer, a perfluorinated polymer, and any combination thereof. The microporous polymer scaffold may comprise polyolefins such as polyethylene (PE) or polypropylene (PP). The microporous polymer scaffold may comprise a polytetrafluoroethylene (PTFE), a polyethylene (PE), or a copolymer of PTFE and PE. The microporous polymer scaffold may comprise an expanded polytetrafluoroethylene (ePTFE) or an expanded polyethylene (ePE). In embodiments where the polymer is non-fluorinated, the non-fluorinated polymer may be selected from a hydrocarbon polymer.

[00153] One non-limiting method to produce porous polytetrafluoroethylene (PTFE) membranes is through paste processing with subsequent expansion to form expanded polytetrafluoroethylene (ePTFE). ePTFE is referred to herein for ease of discussion, but it is to be appreciated that expanded modified PTFE, expanded blends of PTFE, expanded copolymers of PTFE, and PTFE homopolymers are all considered to be within the purview of the invention. Patents have been issued on expandable blends of PTFE, expandable modified PTFE, and expanded copolymers of PTFE, such as, for example, U.S. Patent No. 5,708,044 to Branca; U.S. Patent No. 6,541,589 to Baillie; U.S. Patent No. 7,531,611 to Sabol et al.; U.S. Patent No. 8,647,144 to Ford; U.S. Patent No. 8,158,235, U.S. Patent No. 7,306,729 and U.S. Patent No. 9,139,669 to Xu et al.

[00154] A non-limiting method to produce porous polyethylene membranes is through a wet or gel process known in the industry. In this process, polyethylene is mixed with a hydrocarbon liquid and other additives. This mixture is heated above the polymer melt temperature and extruded into a sheet. This sheet can then be orientated biaxially before and/or after the hydrocarbon liquid is extracted, producing a microporous membrane. Various process details are known in literature as in U.S. Patent No. 5,248,461, U.S. Patent No. 4,873,034, U.S. Patent No. 5051183, U.S. Patent No. 6566012, Casting and stretching of filled and unfilled UHMW-polyethylene films, Ir.F.H. Assinck, Centre for polymers and composites, Eindhoven University of Technology, Nov 1995 and Porous biaxially drawn ultra-high molecular weight polyethylene films, N.S.J.A. Gerrits, Department of Materials Technology, DSM Research; and P.J. Lemstra, Department of Polymer Technology, Eindhoven University of Technology, October 1990.

[00155] The microporous polymer scaffold may have a mass per area of 0.5 g/m^2 to 50 g/m^2, or 0.5 g/m^2 to 40 g/m^2, or 0.5 g/m^2 to 30 g/m^2, or 0.5 g/m^2 to 20 g/m^2, or 0.5 g/m^2 to 10 g/m^2, or 0.5 g/m^2 to 5 g/m^2, or 5 g/m^2 to 50 g/m^2, 5 g/m^2 to 40 g/m^2, or 5 to 30 g/m^2, or 5 g/m^2 to 20 g/m^2, or 5 g/m^2 to 10 g/m^2.

[00156] The microporous polymer scaffold may have a non-contact thickness of up to about 1000 µm. The microporous polymer scaffold may have a non-contact thickness of from about 1 µm to about 1000 µm, or from about 2 µm to about 1000 µm, or from about 2 µm to about 500 µm. The microporous polymer scaffold may have a non-contact thickness of greater than 2 µm and up to about 1000 µm, greater than 2 µm and up to about 900 µm, greater than 1 µm and up to about 800 µm, greater than 1 µm and up to about 700 µm, greater than 1 µm and up to about 600 µm, greater than 1 µm and up to about 500 µm, greater than1 µm and up to about 400 µm, greater than 1 µm and up to about 300 µm, greater than 1 µm and up to about 200 µm, or greater than 1 µm and up to about 150 µm, or greater than 1 µm and up to about 100 µm, or greater than 1 µm and up to about 75 µm, or greater than 1 µm and up to about 50 µm, or greater than12 µm and up to about 25 µm, or greater than 1 µm and up to about 10 µm, or greater than 1 µm and up to about 5 µm, or up to about2 µm, or up to about 1 µm. In some embodiments, the microporous polymer scaffold may have a non-contact thickness of any value including and between about 2 µm to about 500 µm, or between about 2 µm and about 100 µm, or about 2 µm and about 50 µm, or about 2 µm and about 25 µm.

[00157] The non-contact thickness of the microporous polymer scaffold is measured as indicated in the test methods described herein.

[00158] The microporous polymer scaffold may have a porosity of at least 40 vol%, or at least 50 vol%, or at least 60 vol%, or at least 67 vol%, or at least 70 vol %, or at least 75 vol%, or at least 80 vol%, or at least 82 vol%, or at least 84 vol%, or at least 86 vol%, or at least 88 vol%, or at least 90 vol%, or at least 91 vol%, or at least 95 vol%, or at least 98 vol%, or any intermediate value or range of values in the range from 40 vol% to 98 vol%. In some embodiments, the microporous polymer scaffold may have a porosity from about 40 vol% to about 98 vol%, or from about 40 vol% to about 91 vol%, or from about 40 vol %to about 90 vol%, or from about 40vol% to about 85 vol%, or from about 40 vol% to about 80 vol%, or from about 40 vol% to about 75 vol%, or from about 40 vol% to about 70 vol%, or from about 40 vol% to about 60 vol%, or from about 50 vol% to about 98 vol%, or from about 50 vol% to about 91 vol%, or from about 50 vol %to about 90 vol%, or from about 50 vol% to about 85 vol%, or from about 70 vol % to about 90 vol%, or from about 50 vol% to about 80 vol%, or from about 50 vol% to about 75 vol%, or from about 50 vol% to about 70 vol%, or from about 50 vol% to about 60 vol%. In some embodiments, the microporous polymer scaffold may have a porosity from about 83 vol% to about 91 vol%.

[00159] The microporous polymer scaffold may have a bubble point pressure equal to or greater than 0.5 bar, or equal to or greater than 1 bar or equal to or greater than 2 bar. The microporous polymer scaffold may have a bubble point pressure of from about 0.5 bar to about 10 bar, or from about 1 bar to about 10 bar, or from about 2 bar to about 15 bar, or from about 2 bar to about 10 bar, or from about 2 bar to about 5 bar, or from about 3 bar to about 9 bar, or from about 3 bar to about 8 bar, or from about 4 bar to about 9 bar, or from about 4 bar to about 8 bar. The microporous polymer scaffold may have a bubble point pressure of equal to or greater than about 4 bar, or equal to or greater than about 5 bar, or equal to or greater than about 6 bar, or equal to or greater than about 7 bar, or equal to or greater than about 8 bar, or equal to or greater than about 9 bar, or equal to or greater than about 10 bar.

[00160] The microporous polymer substrate has a first direction, a second direction, and a thickness direction, where the first direction is orthogonal to the second direction, and the first and second directions are each orthogonal to the thickness direction, where the second direction is the direction in which the microporous polymer substrate has its minimum matrix tensile strength. In some embodiments, the microporous polymer substrate may have a matrix tensile strength (MTS) in the second direction of at least 50 MPa. The microporous polymer substrate may have a matrix tensile strength in the second direction of at least 100 MPa, or at least 300 MPa, or at least about 400 MPa, or at least about 500 MPa. The microporous polymer substrate may have a matrix tensile strength between about 50 MPa to about 500 MPa, or about 150 MPa to about 450 MPa, or about 250 MPa to about 450 MPa, or any intermediate values and ranges between 50 MPa to about 500 MPa.

[00161] Without wishing to be bound by theory, it is believed that one of the primary functions of the microporous polymer scaffold is to prevent the development of cracks that may be caused by stresses that develop during the drying process of the colloidal dispersion or colloidal suspension as the opaloid is being formed within the scaffold pores. This process of crack formation will be discussed in greater detail in the next section.

Crack Formation During Drying

[00162] Without wishing to be bound by theory, it is believed that one of the primary sources of defects in opaloids is cracks that are caused by stresses during drying, as illustrated in **Figure 11**. As used herein, the term “crack” may describe a fracture within an opaloid phase, which may form during or after the particles consolidate to form the opaloid. In appearance, a crack may be relatively linear or branching, and the contours of the two sides may appear highly complementary (i.e., may appear to “fit together”) consistent with a fractured solid that has been pulled apart. **Figure 11** depicts a schematic of a colloidal dispersion being concentrated to form an opaloid. As the system approaches and exceeds the colloidal glass

transition point (where the packing density is equal to or greater than the colloidal glass transition packing density), the sub-micron particles become effectively immobilized, and the continued evaporation of the liquid phase results in the formation of menisci that cause compressive stress to build up on the arrangement of sub-micron particles (e.g., due to capillary forces). Differential compression may result in tension and/or shear forces acting on the arrangement of particles. If the opaloid is in contact with a rigid surface then additional tension and/or shear forces may arise as the rigid surface further restrains the arrangement of sub-micron particles. The aforementioned forces may exceed the cohesive forces holding the particles together, resulting in the formation of large cracks (e.g., as shown in **Figure 2**). Without wishing to be bound by theory, it is believed that microporous polymer scaffolds with tighter structures (e.g., those with bubble points greater than 2 bar) are better at mechanically reinforcing the arrangement of sub-micron particles during the drying process, thereby minimizing the formation of large cracks (for example, in the case of opaloids prepared from colloidal precursors).

Overview of Membrane-Reinforced Opaloid Morphology & Properties

[00163] The following description of membrane-reinforced opaloids are applicable to all embodiments, examples and aspects of the composite membranes described herein. MROs may comprise a microporous polymer scaffold where the scaffold matrix is intimately integrated with the opaloid. **Figure 12** shows such an MRO, in which the sub-micron particles 10 (comprising silica sub-micron particles with a diameter of approximately 22 nm) of the opaloid 9 are arranged so as to conform to the shape of the scaffold matrix 15 (having the node and fibril microstructure of ePTFE). The pore volume of such an MRO may be dominated by the inter-particle pore volume 13. The intimacy of the integration may be evaluated by measuring (e.g., via quantitative image analysis) the distances from the inner surface of the polymer scaffold to the centers of the nearest sub-micron particles (i.e., the integration distances, d_i, as shown in the image). In **Figure 12**, these distances are generally very small (e.g., less than about 1 particle diameter, D), demonstrating intimate integration with the microporous polymer scaffold as defined herein. **Figure 13** shows another such MRO, in which the sub-micron particles 9 comprise a blend of two populations of substantially monodisperse sub-micron particles (silica sub-micron particles 27 having a diameter of approximately 7 nanometers and perfluoroalkoxy alkane sub-micron particles 28 having a diameter of approximately 90 nanometers) in an ePTFE microporous polymer scaffold 15, where the ePTFE had a bubble point of about 1.9 bar.

[00164] In some embodiments, MROs may have large defects (e.g., cracks). **Figure 14** shows a surface scanning electron micrograph of an MRO comprising silica sub-micron

particles with a diameter of approximately 12 nm and an ePTFE microporous polymer scaffold where the ePTFE had a bubble point of about 1.9 bar. Large defects (e.g., cracks) 26 may be observed in the sample. Defects may be considered large when their widest width is from about 45 nm and about 55 nm, or from about 45 nm and about 60 nm, or from about 45 nm and about 70 nm, or from about 45 nm and about 75 nm, or from about 45 nm and about 100 nm, or from about 45 nm and about 200 nm, or from about 45 nm and about 250 nm, or from about 45 nm and about 300 nm, or from about 45 nm and about 500 nm, or from about 45 nm and about 750 nm, or from about 45 nm and about 1 micron. Additionally, defects may be considered large when their widest width is from about 50 nm and about 60 nm, or from about 50 nm and about 70 nm, or from about 50 nm and about 75 nm, or from about 50 nm and about 100 nm, or from about 50 nm and about 200 nm, or from about 50 nm and about 250 nm, or from about 50 nm and about 300 nm, or from about 50 nm and about 500 nm, or from about 50 nm and about 750 nm, or from about 50 nm and about 1 micron. Defects may be considered large when their widest width is from about 60 nm and about 70 nm, or from about 60 nm and about 75 nm, or from about 60 nm and about 100 nm, or from about 60 nm and about 200 nm, or from about 60 nm and about 250 nm, or from about 60 nm and about 300 nm, or from about 60 nm and about 500 nm, or from about 60 nm and about 750 nm, or from about 60 nm and about 1 micron. Defects may also be considered large when their widest width is from about 70 nm and about 75 nm, or from about 70 nm and about 100 nm, or from about 70 nm and about 200 nm, or from about 70 nm and about 250 nm, or from about 70 nm and about 300 nm, or from about 70 nm and about 500 nm, or from about 70 nm and about 750 nm, or from about 70 nm and about 1 micron. Defects may be considered large when their widest width is from about 75 nm and about 100 nm, or from about 75 nm and about 200 nm, or from about 75 nm and about 250 nm, or from about 75 nm and about 300 nm, or from about 75 nm and about 500 nm, or from about 75 nm and about 750 nm, or from about 75 nm and about 1 micron. Further, defects may be considered large when their widest width is from about 100 nm and about 200 nm, or from about 100 nm and about 250 nm, or from about 100 nm and about 300 nm, or from about 100 nm and about 500 nm, or from about 100 nm and about 750 nm, or from about 100 nm and about 1 micron. Defects may be considered large when their widest width is from about 200 nm and about 250 nm, or from about 200 nm and about 300 nm, or from about 200 nm and about 500 nm, or from about 200 nm and about 750 nm, or from about 200 nm and about 1 micron. Defects may be considered large when their widest width is from about 250 nm and about 300 nm, or from about 250 nm and about 500 nm, or from about 250 nm and about 750 nm, or from about 250 nm and about 1 micron. Defects may be considered large when their widest width (W) is from about 4.5 particle diameters and about 6 particle diameters (i.e., when $4.5*D < W < 6*D$), or when $4.5*D < W < 10*D$, or when $4.5*D < W < 20*D$, or when $4.5*D < W < 50*D$, or when $4.5*D < W < 100*D$, or

when 4.5*D < W < 200*D, or when 4.5*D < W < 500*D. Defects may be considered large when 5*D < W < 10*D, or when 5*D < W < 20*D, or when 5*D < W < 50*D, or when 5*D < W < 100*D, or when 5*D < W < 200*D, or when 5*D < W < 500*D. Defects may be considered large when 10*D < W < 20*D, or when 10*D < W < 50*D, or when 10*D < W < 100*D, or when 10*D < W < 200*D, or when 10*D < W < 500*D. Defects may be considered large when 20*D < W < 50*D, or when 20*D < W < 100*D, or when 20*D < W < 200*D, or when 20*D < W < 500*D. Defects may be considered large when 50*D < W < 100*D, or when 50*D < W < 200*D, or when 50*D < W < 500*D, or when 100*D < W < 200*D, or when 100*D < W < 500*D, or 200*D < W < 500*D. When large defects extend through the entirety of the thickness) or substantially through the thickness of the MRO, they may compromise the integrity of the MRO as described below, and as indicated by metrics such as a dramatic reduction of the bubble point of the MRO (e.g., to values below about 10 bar). It has been surprisingly discovered that such defects can be minimized or eliminated by fabricating MROs that comprise a microporous polymer scaffold with a bubble point greater than 2 bar. Therefore, as described above, MROs that comprise a microporous polymer scaffold that had a bubble point greater than 2 bar may be considered High-Integrity Membrane-Reinforced Opaloids. Similarly, MROs with bubble points greater than about 10 bar may be considered High-Integrity Membrane-Reinforced Opaloids.

[00165] MROs may comprise an opaloid in which the packing arrangement of the sub-micron particles is similar to the packing arrangement of a neat (i.e., unreinforced) opaloid formed from the same colloidal dispersion or colloidal suspension without the microporous polymer scaffold. **Figure 15** shows SAXS data for two opaloids, one neat and the other an MRO reinforced with an ePTFE microporous polymer scaffold with a bubble point of 7.6 bar, both prepared from an aqueous colloidal dispersion of silica sub-micron particles with a diameter of approximately 12 nm. As indicated by the two leftmost triangles, two major SAXS peaks are observed at virtually identical q values in each case, indicating that the packing arrangement of particles in the MRO (as described by the ID values and the presence of longer-range order) is comparable to that of the neat opaloid.

[00166] MROs may also comprise an opaloid in which the pore phase is similar to the pore phase of the neat opaloid formed from the same colloidal dispersion or colloidal suspension without the microporous polymer scaffold. **Figure 16** shows BET/BJH data for four opaloids: neat (i.e., unreinforced), and MROs reinforced with ePTFE microporous polymer scaffolds that had bubble points of 1.9 bar, 4.8 bar, and 7.6 bar. All the pore size distributions have mode pore diameters between about 5 nm and 7 nm, and all overlap to a significant degree. Compared to the neat system (i.e., unreinforced, with no microporous polymer scaffold and therefore no bubble point of the microporous polymer scaffold), as the bubble point of the microporous polymer scaffold increased from 1.9 bar to 4.8 bar to 7.6 bar, the pore volume of

the composite membrane shifted to the right (i.e., the pore volume at pore diameters above about 7 nm increased). This is consistent with the hypothesis that microporous polymer scaffolds with tighter structures can disrupt the long-range order of the opaloid more significantly than scaffolds with less tight structures, while maintaining the local three-dimensional packing arrangement of sub-micron particles. To better quantify this trend, the parameter ϕ was defined as shown in **Figure 17a**, which compares two of the data sets from **Figure 16**: the data set for the neat (i.e., unreinforced) sample, and the data set for the MRO reinforced with an ePTFE microporous polymer scaffold that had a bubble point of 1.9 bar. As shown in the insets in **Figure 17a**, ϕ was defined as the fraction of the pore volume of the composite membrane (P, expressed in mL/g) that is contained in pores that are larger than the largest pore observed in the corresponding neat opaloid. This definition was developed for MROs in which the microporous polymer scaffold was substantially filled by the opaloid. For MROs with a significant fraction of pores that are not filled by the opaloid, a suitable background subtraction would be required as will be understood by one of ordinary skill in the art. **Figure 17b** shows how the value of ϕ increased with the bubble point of the microporous polymer scaffold when 3 MROs were fabricated, each of which comprised particles with a nominal diameter of 12 nm but comprising ePTFE microporous polymer scaffolds with different bubble points selected from 1.9 bar, 4.8 bar, and 7.6 bar. Without wishing to be bound by theory, the results depicted in **Figure 17b** are consistent with the hypothesis that microporous polymer scaffolds with tighter structures may disrupt the opaloid more significantly than scaffolds with less tight structures. **Figure 17c** shows how the value of ϕ also increased with particle diameter when 3 MROs were fabricated, each of which comprised an ePTFE microporous polymer scaffold with a bubble point of 1.9 bar but comprising particles of different nominal diameters selected from 7nm, 12nm, and 22 nm. The results shown in **Figure 17c** demonstrates that opaloids may be disrupted more significantly when the ratio of the particle size (D) to the pore size of the microporous polymer scaffold increases (i.e., when fewer particles can fit within a typical pore of the microporous polymer scaffold). Without wishing to be bound by theory, in both cases (i.e., pertaining to both **Figure 17b** and **Figure 17c**), it is believed that the increase in ϕ (i.e., the increase in large pores) may be caused by a larger fraction of interfacial particle-scaffold pores compared to inter-particle pores.

[00167] MROs (such as, but not limited to, High-Integrity MROs) may have few or no gross defects (e.g., cracks) that extend through the thickness of the MRO. **Figure 18** shows such an MRO 20, in which several defects 26 are observed. It is to be noted that in Figure 16 the defects appear localized, and there is no evidence of gross cracks spanning the entire thickness of the MRO. The magnification of the image is low to enable virtually the full thickness of the membrane to be viewed, although at this magnification the individual sub-

micron particles (comprising silica with a diameter of approximately 7 nm) cannot be readily resolved, and neither can the microporous polymer matrix (comprising ePTFE) due to limited contrast with the opaloid. The homogeneity of the image is further evidence of intimate integration between the opaloid and the microporous polymer scaffold, and also evidence of a continuous opaloid phase throughout the MRO, indicating that the extent of the continuous opaloid phase is the same as the length and width of the prepared sample, which was over 15 cm in this case.

[00168] **Figures 19, 20, and 21** show that High-Integrity MROs can be made with materials other than just SiO_2 nanoparticles and ePTFE microporous polymer scaffolds. **Figures 19a and 19b** show a surface SEM and a cross-section SEM, respectively, of a High-Integrity MRO comprising yttria-stabilized zirconia sub-micron particles (particle size 32 nm) in an ePTFE microporous polymer scaffold that had a bubble point (of the scaffold itself) of about 4.8 bar. **Figure 20** shows a surface SEM of a High-Integrity MRO comprising yttria-stabilized zirconia sub-micron particles (particle size 32 nm) in a polyethylene microporous polymer scaffold that had a bubble point pressure (of the scaffold itself) of about 3.1 bar. **Figure 21** shows a surface SEM of a High-Integrity MRO comprising yttria-stabilized zirconia (YSZ, particle size 32nm) in an ePTFE microporous polymer scaffold where the ePTFE had a bubble point of about 3.3 bar. **Figures 22a** and **22b** show SAXS data collected for the High-Integrity MRO in **Figure 21**. As discussed previously, the scattering vector or peak position, q (in units of nm^{-1}), is proportional to the sine of the scattering angle, θ, and inversely proportional to the wavelength, λ, according to the expression: $q = 4\pi\sin(\theta)/\lambda$. Values of q can be converted to real space correlation distances with the relationship $d = 2\pi/q$. The triangle indicates a peak position at 19.2 nm, corresponding to an inter-particle distance. The presence of this structure factor peak, and its length scale, which is comparable to the particle size, are characteristic of an opaloid.

[00169] MROs may be produced with large areas, for example 10s of centimeters or more in extent in each of two orthogonal directions. **Figure 23a** shows a sample of an MRO sitting on a black lab bench. The MRO comprises an ePTFE microporous polymer scaffold that had a bubble point of about 7.6 bar, and silica sub-micron particles with a diameter of about 7 nm. The width of the sample was about 68 millimeters and the length of the sample was about 100 millimeters. The size of the samples appeared to be limited only by the size of practical industrial batch and roll-to-roll processes (which can reach e.g., greater than 1 meter in width and e.g., thousands of meters in length). **Figure 23b** shows a sample of the same material bent 180° back on itself to illustrate the flexibility of the material. **Figure 23c** shows a sample of the same material lying flat on a business card with the words beneath the sample clearly legible with minimal distortion, illustrating that the sample was substantially optically clear,

which is evidence of intimate integration between the opaloid and the microporous polymer scaffold, as well as high integrity as will be described below.

[00170] MROs may be produced with high integrity as indicated by a high degree of optical clarity, for example if the refractive indices of the microporous polymer matrix and the opaloid are closely matched and if large defects have been minimized. These conditions may be satisfied in the case of an MRO comprising ePTFE microporous reinforcement and further comprising an opaloid made up of silica sub-micron particles. **Figure 23c** shows such an MRO, which is substantially clear. **Figure 24** shows optical haze measurements of three MROs, each comprising silica sub-micron particles with a diameter of approximately 12 nm, and each comprising a different ePTFE microporous polymer scaffold with one of three different bubble points: 1.9, 4.8, and 7.6 bar. As the scaffold bubble point increased, the haze decreased significantly. Without wishing to be bound by theory, the haze is attributed primarily to the presence of defects large enough to scatter visible light. Therefore, lower haze in these composite membranes is evidence of higher integrity (i.e., fewer and/or smaller defects). MROs may be considered to have high integrity when the haze value is between a lower value of 0% and an upper value of 65%, or an upper value of 55%, or an upper value of 50%, or an upper value of 45%, or an upper value of 40%, or an upper value of 35%, or an upper value of 30%, or an upper value of 25%, or an upper value of 20%, or an upper value of 15%, or an upper value of 10%, or an upper value of 5%. The composite membranes of the present disclosure may have a haze value of from 5 % to about 65 %.

[00171] MROs may also be produced with high integrity as indicated by a high composite membrane bubble point. MROs with very small pore diameters, for example as shown in **Figure 16**, should have extremely high bubble points (e.g., > 20 bar according to the Young-Laplace equation as illustrated in **Figure 32**). However, if there are large defects through the thickness of the MRO (e.g., cracks), then a much lower bubble point may be detected. **Figure 25** shows capillary flow porometry measurements of three MROs, each comprising silica sub-micron particles with a diameter of approximately 12 nm, and each comprising a different ePTFE microporous polymer scaffold with one of three different bubble points: 1.9, 4.8, and 7.6 bar. The MRO comprising the microporous polymer scaffold with a bubble point of 1.9 bar has a bubble point pressure of only approximately 9 bar, indicating the presence of a significant population of large defects through the thickness of the membrane. However, the MROs comprising the microporous polymer scaffolds with bubble points of 4.8 and 7.6 bar have bubble points of about 24 bar and >28 bar, respectively, indicating that large defects (e.g. cracks) have been minimized or eliminated.

[00172] MROs with high integrity (i.e., comprising microporous polymer scaffolds with bubble point greater than 2 bar) may enable dramatic improvements in the ability to selectively separate small molecules from a solvent (e.g., through organic solvent nanofiltration). **Figure**

26 shows a schematic of an experimental apparatus for performing Organic Solvent Nanofiltration (OSN). A challenge solution produced by dissolving a probe molecule (e.g., rose bengal) in pure ethanol was passed through the MRO samples under a pressure gradient, and the rejection of the rose bengal by the MRO was determined based on the relative concentrations of rose bengal in the permeate and retentate. In these OSN tests, the MRO was used as the filter medium (i.e., the layer within the system that selectively separated the target molecule from the solvent, also referred to as "rejecting" the target molecule). **Figure 27** shows the results of such Organic Solvent Nanofiltration measurements on three MROs, each comprising silica sub-micron particles with a diameter of approximately 12 nm, and each comprising a different ePTFE microporous polymer scaffold with one of three different bubble points: 1.9, 4.8, and 7.6 bar. The MRO comprising the microporous polymer scaffold with a bubble point of 1.9 bar had a relatively low rejection of about 2.4%. However, the MROs comprising the microporous polymer scaffolds with bubble points of 4.8 and 7.6 bar showed rose bengal rejections of 89% and 95%, respectively, indicating that large defects (e.g. cracks) have been minimized or eliminated.

[00173] To briefly recap, the results shown in **Figures 24**, **25,** and **26** illustrate the dramatic improvement in the integrity of MRO samples when the bubble point of the microporous polymer scaffold was greater than 2 bar. The resulting MROs showed significantly lower haze (**Figure 24**), dramatically higher bubble points (**Figure25**), and a step change in the ability to filter small molecules (**Figure 26**).

[00174] MROs are porous, and therefore the liquid permeance (measured in liters/(m^2*hour*bar) or LMH/bar) through MROs under a fixed pressure gradient may be expected to be inversely proportional to the viscosity of the permeating liquid. The same experimental apparatus shown in **Figure 26** was used to measure the liquid permeance of 5 liquids through a high-integrity MRO with a thickness of approximately 2.5 microns comprising silica sub-micron particles with a diameter of approximately 7 nm and an ePTFE membrane with a bubble point of 7.6 bar. The permeance was measured at a constant trans-membrane pressure of 4 bar. The 5 fluids were methanol (viscosity ~0.54 cP), ethanol (viscosity ~1.07 cP), isopropanol (viscosity ~2.04 cP), isobutanol (viscosity ~3.95 cP), and 2-ethyl-1-hexanol (viscosity ~6.27 cP), where the "~" symbol is used to mean "approximately." **Figure 28** compares the measured liquid permeance data (round circles) to the expected trend (solid squares). The expected trend is normalized to the permeance of the ethanol measurement (at ~1.07 cP) and calculated assuming that permeance is inversely proportional to viscosity. The measured data agree very well with the expected trend, providing strong evidence that the primary mechanism of liquid permeance is viscous flow through porous media, as expected.

[00175] MROs with high integrity may be mechanically robust, for example with respect to liquid permeance under extremely high pressures. **Figure 29a** shows a high-pressure flow cell that was used to measure liquid permeance at trans-membrane pressures up to 50 bar. Ethanol was passed through a High-Integrity MRO sample under trans-membrane pressures of 10 bar, 20 bar, 40 bar, 50 bar, 40 bar, 20 bar, and 10 bar (in that order) for about 10 minutes at each setpoint. The MRO had a thickness of about 5 microns and comprised silica sub-micron particles with a diameter of about 7 nm and an ePTFE microporous polymer scaffold with a bubble point of approximately 7.6 bar. **Figure 29b** shows the resulting liquid flux (in $L*m^{-2}*h$), and permeance (in LMH/bar) through the MRO. The flux data clearly show the step changes associated with changes in trans-membrane pressure, and show virtually no hysteresis in flux after exposure to trans-membrane pressures up to 50 bar. Similarly, the permeance data show relatively constant permeance throughout the experiment when the flux is normalized for the trans-membrane pressure. This level of mechanical robustness is surprising given how thin the sample was (only about 5 microns) and that the neat (i.e., unreinforced) version of these opaloids are brittle materials, as illustrated in **Figure 2**. This data provides more evidence of the highly advantageous properties, such as high mechanical robustness, of High-Integrity MROs. Other measurements of permeance or mass transfer may also be used to characterize MROs, such as Gurley measurements and/or other standard air flow measurements.

Detailed Description of Membrane-Reinforced Opaloid Morphology

[00176] The following description of membrane-reinforced opaloid morphology is applicable to all embodiments, examples and aspects of the composite membranes described herein. Each scaffold pore having a pore volume may define the volume of an individual pore within the microporous polymer scaffold. The microporous polymer scaffold also has a scaffold pore volume, where the scaffold pore volume is a characteristic of the microporous polymer scaffold (as a whole) and comprises the total pore volume of the microporous polymer scaffold (i.e., comprises the cumulative pore volume of all scaffold pores). The scaffold pore volume is not necessarily constant; for example, it may change as a result of the process to produce the MRO. For example, the scaffold may deform as a result of stresses during coating and/or drying, resulting in either an increase or decrease in its pore volume. For instance, the thickness of the scaffold may decrease (i.e., “collapse”) in response to capillary forces during wetting and/or drying.

[00177] In an MRO as discussed herein, an opaloid is at least partially contained within the plurality of scaffold pores of the microporous polymer scaffold. The opaloid within the plurality of scaffold pores may have undergone a colloidal glass transition. In some embodiments, a

neat opaloid is formed from the same or similar sub-micron particles as the MRO. The opaloid within at least one of the plurality of scaffold pores may have a packing arrangement of sub-micron particles similar to the packing arrangement of a neat opaloid. In this context, the term "similar" is taken to mean comprising structural, material, or performance characteristics that are generally the same as, or within the same range (as understood by one of ordinary skill in the art), when compared to an opaloid formed from the same sub-micron particles. As defined herein, a three-dimensional arrangement of sub-micron particles is one that may comprise at least 4 constituent particles, and may comprise at least one particle that is not aligned substantially in-plane with its three nearest-neighbor particles.

[00178] The opaloid within the plurality of scaffold pores may comprise a three-dimensional packing arrangement of the sub-micron particles with an inter-particle distance (ID), or distribution of inter-particle distances. The pores of the composite membrane may be defined at least in part by this inter-particle distance. As used herein, the inter-particle distance may be the distance between the centers of adjacent sub-micron particles (or if the sub-micron particles are non-spherical, then between the centroids of adjacent sub-micron particles). The inter-particle distance may be expressed in e.g., mm, μm, or nm and may be measured as per the test methods described herein. The inter-particle distance (ID) may be, for example, less than about 2 times the particle diameter or effective particle diameter D. The ID may be, for example, less than about 1.1 times the particle diameter or effective particle diameter D (i.e., less than about 1.1*D). The ID may be less than about 1.2*D. The ID may be less than about 1.3*D. The ID may be less than about 1.4*D. The ID may be less than about 1.5*D. The ID may be less than about 1.6*D. The ID may be less than about 1.8*D. The ID may be less than about 2.2*D. The ID may be less than about 2.4*D. The ID may be less than about 2.6*D. The ID may be less than about 2.8*D. The ID may be less than about 3*D. The ID may be between about 0.6*D to about 3*D, or between about 0.7 *D to about 3*D, or between about 0.8*D to about 2*D, or between about 0.9*D to about 1.5*D, or between about 1*D to about 1.3*D. The ID may be, for example, greater than about 0.5 times the effective particle diameter D and less than about 1.75 times the effective particle diameter D. The ID may be, for example, greater than about 0.5 times the effective particle diameter D and less than about 1.5 times the effective particle diameter D. The ID may be, for example, greater than about 0.55 times the effective particle diameter D and less than about 3 times the effective particle diameter D. The ID may be, for example, greater than about 0.55 times the effective particle diameter D and less than about 2.5 times the effective particle diameter D. The ID may be, for example, greater than about 0.55 times the effective particle diameter D and less than about 2 times the effective particle diameter D. The ID may be, for example, greater than about 0.55 times the effective particle diameter D and less than about 1.75 times the effective particle

diameter D. The ID may be, for example, greater than about 0.55 times the effective particle diameter D and less than about 1.5 times the effective particle diameter D. The ID may be, for example, greater than about 0.6 times the effective particle diameter D and less than about 3 times the effective particle diameter D. The ID may be, for example, greater than about 0.6 times the effective particle diameter D and less than about 2.5 times the effective particle diameter D. The ID may be, for example, greater than about 0.6 times the effective particle diameter D and less than about 2 times the effective particle diameter D. The ID may be, for example, greater than about 0.6 times the effective particle diameter D and less than about 1.75 times the effective particle diameter D. The ID may be, for example, greater than about 0.6 times the effective particle diameter D and less than about 1.5 times the effective particle diameter D. The ID may be, for example, greater than about 0.65 times the effective particle diameter D and less than about 3 times the effective particle diameter D. The ID may be, for example, greater than about 0.65 times the effective particle diameter D and less than about 2.5 times the effective particle diameter D. The ID may be, for example, greater than about 0.65 times the effective particle diameter D and less than about 2 times the effective particle diameter D. The ID may be, for example, greater than about 0.65 times the effective particle diameter D and less than about 1.75 times the effective particle diameter D. The ID may be, for example, greater than about 0.65 times the effective particle diameter D and less than about 1.5 times the effective particle diameter D. The ID may be, for example, greater than about 0.7 times the effective particle diameter D and less than about 3 times the effective particle diameter D. The ID may be, for example, greater than about 0.7 times the effective particle diameter D and less than about 2.5 times the effective particle diameter D. The ID may be, for example, greater than about 0.7 times the effective particle diameter D and less than about 2 times the effective particle diameter D. The ID may be, for example, greater than about 0.7 times the effective particle diameter D and less than about 1.75 times the effective particle diameter D. The ID may be, for example, greater than about 0.7 times the effective particle diameter D and less than about 1.5 times the effective particle diameter D.

[00179] The composite membranes of the present disclosure may comprise a microporous polymer scaffold that may be intimately integrated with the opaloid (and as defined herein, the opaloid may therefore be intimately integrated with the microporous polymer scaffold). Within a microporous polymer scaffold pore containing the opaloid, the sub-micron particles of the opaloid may be arranged so as to conform to the surface(s) of the microporous polymer scaffold defining the polymer scaffold pore, resulting in an interface between the opaloid and the surface(s) of the microporous polymer scaffold defining the polymer scaffold pore. The opaloid may comprise sub-micron particles at the interface between the opaloid and the inner surfaces of the microporous polymer scaffold pore. Each of these sub-micron particles may

be characterized by an integration distance, d_i, where d_i may be the magnitude (i.e., the length, expressed in nm) of the shortest of the normal vectors extending from the inner surfaces of the microporous polymer scaffold pore to the surface of the sub-micron particle. The opaloid may be considered to be intimately integrated with the microporous polymer scaffold if the median integration distance d_i is less than about 1 sub-micron particle diameter or effective diameter D, or less than about 0.5*D, or less than about 2*D, or less than about 3*D. The median integration distance may be in the range from about 0.5*D to about 3*D, or from about 0.75*D to about 2.5*D, or from about 1*D to about 3*D, or from about 1*D to about 2*D. For an opaloid that is intimately integrated with the microporous polymer scaffold, the median integration distance may be within the same order of magnitude as the sub-micron particle diameter D. The integration distance may be measured using scanning electron microscopy combined with quantitative image analysis as described herein.

[00180] The opaloid within the plurality of scaffold pores may be contained within the scaffold pores. Composite membranes of the present disclosure may be such that at least a portion of the scaffold pores are at least partially filled with sub-micron particles. For example, a plurality of scaffold pores may be at least partially filled with sub-micron particles. As used herein, at least partially filled is meant to encompass composite membranes (e.g., MROs) where a percentage of the scaffold pores are filled with sub-micron particles, for example from about 1% to about 100%, or from 1% to about 90%, or from about 1% to about 80%, or from about 1% to about 75%, or from about 1% to about 50%, or from about 1% to about 25%, or from about 5% to about 60%, or from about 5% to about 40%, or from about 10% to about 45%. or from about 1% to about 15%, or from about 1% to about 10%, or from about 1% to about 5%. At least partially filled can also be taken to encompass composite membranes where the plurality of scaffold pores have an opaloid within their pore volume, but the pore volume of an individual scaffold pore is not completely filled with an opaloid. In some embodiments, more than one opaloid may be positioned within the pore volume. The opaloids may be the same or different compositionally. In addition, the opaloids may have the same or different sub-micron particle size, material, or the same or different size in terms of the extent (e.g. distance and/or area) of each opaloid.

[00181] In some embodiments, all of the scaffold pores of the microporous polymer scaffold may be filled or substantially filled with sub-micron particles. However, due to the limited packing density of the particles, even a scaffold pore that is completely filled with particles may still have a finite level of porosity due to inter-particle pores. By analogy, one may think of a barrel that is “filled” with marbles or wiffle balls; the barrel may be filled such that substantially no more marbles or wiffle balls can fit within it, yet the barrel still contains substantial pore volume due to e.g., “inter-particle pores” (for example, between the marbles

or between the wiffle balls), and/or due to e.g., “intra-particle pores” (for example, within the wiffle balls).

[00182] The composite membrane comprises a plurality of composite membrane pores that are at least in part defined by the opaloid. The opaloid within the scaffold pore volume may comprise a three-dimensional packing arrangement having spaces between the sub-micron particles in the opaloid. The spaces between the sub-micron particles may be defined as inter-particle pores. The inter-particle pores may be typically described in units of vol% or cc/g. The inter-particle pores may define an interconnected pore volume. The interconnected pore volume may be a characteristic of the opaloid. The composite membrane pores may be at least in part defined by the interconnected pore volume of the opaloid. The inter-particle pores of the opaloid may be characterized by an inter-particle pore diameter, d. The opaloid may comprise a ratio (d/D) of the inter-particle pore diameter, d, to particle diameter or effective particle diameter, D, of, for example, about $d/D \leq 0.5$, or about $d/D \leq 0.8$, or about $d/D \leq 1$, or about $d/D \leq 1.1$, or about $d/D \leq 1.2$, or about $d/D \leq 1.5$, or about $d/D \leq 1.8$, or about $d/D \leq 2$. The inter-particle pore diameter to particle diameter or effective particle diameter ratio (d/D) may be from about 0.20 to about 2.0, or about 0.20 to about 1.80, or about 0.2 to about 1.50, or about 0.20 to about 1.20, or about 0.20 to about 1.10, or about 0.20 to 1.0, or about 0.20 to about 0.90, or about 0.20 to 0.80, or about 0.20 to about 0.70. The inter-particle pore diameter to particle diameter or effective particle diameter ratio (d/D) may be from about 0.225 to about 2,0 or about 0.225 to about 1.80, or about 0.225 to about 1.50, or about 0.225 to about 1.20, or about 0.225 to about 1.10, or about 0.225 to 1.0, or about 0.225 to about 0.90, or about 0.225 to 0.80, or about 0.225 to about 0.70. The inter-particle pore diameter to particle diameter or effective particle diameter ratio (d/D) may be from about 0.25 to about 2,0 or about 0.25 to about 1.80, or about 0.25 to about 1.50, or about 0.25 to about 1.20, or about 0.25 to about 1.10, or about 0.25 to 1.0, or about 0.25 to about 0.90, or about 0.25 to 0.80, or about 0.25 to about 0.70. The inter-particle pore diameter to particle diameter or effective particle diameter ratio (d/D) may be from about 0.30 to about 2.0, or about 0.30 to about 1.80, or about 0.30 to about 1.50, or about 0.30 to about 1.20, or about 0.30 to about 1.10, or about 0.30 to 1.0, or about 0.30 to about 0.90, or about 0.30 to 0.80, or about 0.30 to about 0.70. The inter-particle pore diameter to particle diameter or effective particle diameter ratio (d/D) may be from about 0.35 to about 2.0, or about 0.35 to about 1.80, or about 0.35 to about 1.50, or about 0.35 to about 1.20, or about 0.35 to about 1.10, or about 0.35 to 1.0, or about 0.35 to about 0.90, or about 0.35 to 0.80, or about 0.35 to about 0.70. The inter-particle pore diameter to particle diameter or effective particle diameter ratio (d/D) may be from about 0.40 to about 2.0, or about 0.40 to about 1.80, or about 0.40 to about 1.50, or about 0.40 to about 1.20, or about 0.40 to about 1.10, or about 0.40 to 1.0, or about 0.40 to about 0.90, or about 0.40 to 0.80, or

about 0.40 to about 0.70. The inter-particle pore diameter to particle diameter or effective particle diameter ratio (d/D) may be from about 0.50 to about 2.0, or about 0.50 to about 1.80, or about 0.50 to about 1.50, or about 0.50 to about 1.20, or about 0.50 to about 1.1, or about 0.50 to 1.0, or about 0.50 to about 0.90, or about 0.50 to 0.80, or about 0.50 to about 0.70. The inter-particle pore diameter and particle diameter may be measured or characterized by the methods described herein.

[00183] As used herein, the term "filled" is meant to denote that substantially all (i.e., greater than about 95%) of the pore volume of a scaffold pore is occupied by the opaloid (inclusive of both the solid portion and porosity of the opaloid). The composite membrane may, therefore, comprise composite membrane pores derived from the inter-particle spacing of the sub-micron particles of the opaloid within the scaffold pore volume (i.e., inter-particle pores), plus any intra-particle pore volume, and any interfacial particle-scaffold pores between the sub-micron particles of the opaloid and scaffold pore walls. In some embodiments, where for example, significant defects (e.g., cracks) are present in the opaloid, then the composite membrane pores may additionally be derived from any defects (e.g., cracks), if any, in the opaloid. In some embodiments, where for example, the pore volume of each of the plurality of scaffold pores is only partially filled, then the composite membrane pores may additionally be derived from any unfilled pore volume of the scaffold pores.

[00184] The aforementioned inter-particle pores, intra-particle pore volume, and the interfacial particle-scaffold pores within the scaffold pore volume (collectively, the "opaloid pores") may define a void volume that is characteristic of the opaloid within the scaffold pore volume (i.e., the opaloid void volume, which may be expressed in, for example, cc/g or cc per square meter). The aforementioned opaloid void volume and the solid volume of the sub-micron particles of the opaloid (together, the "opaloid"), may define a volume that is characteristic of the opaloid phase within the scaffold pore volume (i.e., the opaloid volume, which may be expressed in, for example, cc/g or cc per square meter). To calculate the opaloid void fraction (or opaloid porosity), the numerator should be the opaloid void volume and the denominator should be the opaloid volume. The opaloid porosity within the scaffold pores having opaloid incorporated therein may be from about 15 vol% to about 70 vol%, or about 15 vol% to about 65 vol%, or about 15 vol% to about 60 vol%, or about 15 vol% to about 55 vol%, or about 15 vol% to about 50 vol%. The opaloid porosity within the scaffold pores having opaloid incorporated therein may be from about 20 vol% to about 70 vol%, or about 20 vol% to about 65 vol%, or about 20 vol% to about 60 vol%, or about 20 vol% to about 55 vol%, or about 20 vol% to about 50 vol%. The opaloid porosity within the scaffold pores having opaloid incorporated therein may be from about 25 vol% to about 70 vol%, or about 25 vol% to about 65 vol%, or about 25 vol% to about 60 vol%, or about 25 vol% to about 55 vol%, or about 25

vol% to about 50 vol%. The opaloid porosity within the scaffold pores having opaloid incorporated therein may be from about 30 vol% to about 50 vol%, or from about 30 vol% to about 55 vol%, or from about 30 vol% to about 60 vol%, or from about 30 vol% to about 65 vol%, or from about 30 % to about 66%, or about 30 vol% to about 70 vol%. The opaloid porosity within the scaffold pores having opaloid incorporated therein may be from about 35 vol% to about 50 vol%, or from about 35 vol% to about 55 vol%, or from about 35 vol% to about 60 vol%, or from about 35 vol% to about 65 vol%, or from about 35 % to about 66%, or about 35 vol% to about 70 vol%. The opaloid porosity within the scaffold pores having opaloid incorporated therein may be from about 40 vol% to about 50 vol%, or from about 40 vol% to about 55 vol%, or from about 40 vol% to about 60 vol%, or from about 40 vol% to about 65 vol%, or from about 40 % to about 66%, or about 40 vol% to about 70 vol%. The opaloid porosity within the scaffold pores having opaloid incorporated therein may be from about 45 vol% to about 50 vol%, or from about 45 vol% to about 55 vol%, or from about 45 vol% to about 60 vol%, or from about 45 vol% to about 65 vol%, or from about 45 % to about 66%, or about 45 vol% to about 70 vol%. In some embodiments, the opaloid porosity within the scaffold pores having opaloid incorporated therein may be about 50 vol%. The opaloid within the plurality of scaffold pores may comprise sub-micron particles having a packing density. Opaloid packing density may be calculated by taking a ratio where the numerator is the sum of the solid volume of the sub-micron particles and the intra-particle void volume, and the denominator is the opaloid volume. The sub-micron particles within the opaloid may have a packing density within the scaffold pore volume that may be greater than or equal to the packing density of the corresponding neat opaloid, and/or greater than or equal to a colloidal glass transition packing density (or volume fraction) for the sub-micron particles when in a colloidal system.

[00185] The opaloid within the scaffold pore volume may have a packing density of sub-micron particles of about 0.4, or about 0.45, or about 0.49, or about 0.5, or about 0.55, or about 0.58, or about 0.60, or about 0.65, or about 0.7, or about 0.75, or about 0.8, or about 0.85. The opaloid within the scaffold pore volume may have a packing density of sub-micron particles of from about 0.4 to about 0.85, or from about 0.5 to about 0,85, or from about 0.4 to about 0.8, or from about 0.4 to about 0.75, or from about 0.5 to about 0.8,

[00186] The opaloid within the scaffold pore volume may have a pore size (d) to inter-particle distance (ID) ratio (d/ID) from about 0.07 to about 4.0, or from about 0.07 to about 2.5, or from about 0.07 to about 1.75, or from about 0.07 to about 1.0, or from about 0.07 to about 0.75, or from about 0.07 to about 0.5, or from about 0.1 to about 4.0, or from about 0.1 to about 2.5, or from about 0.1 to about 1.75, or from about 0.1 to about 1.0, or from about 0.1 to about 0.75, or from about 0.1 to about 0.5, or from about 0.15 to about 4.0, or from about

0.15 to about 2.5, or from about 0.15 to about 1.75, or from about 0.15 to about 1.0, or from about 0.15 to about 0.75, or from about 0.15 to about 0.5, or from about 0.2 to about 4.0, or from about 0.2 to about 2.5, or from about 0.2 to about 1.75, or from about 0.2 to about 1.0, or from about 0.2 to about 0.75, or from about 0.2 to about 0.5, or from about 0.25 to about 4.0, or from about 0.25 to about 2.5, or from about 0.25 to about 1.75, or from about 0.25 to about 1.0, or from about 0.25 to about 0.75, or from about 0.25 to about 0.5, or from about 0.3 to about 4.0, or from about 0.3 to about 2.5, or from about 0.3 to about 1.75, or from about 0.3 to about 1.0, or from about 0.3 to about 0.75, or from about 0.3 to about 0.5.

[00187] The composite membrane may have a porosity, where the porosity may be defined by the void spaces formed by the interconnected pore volume (e.g., the inter-particle pores as defined above) of the opaloid, any intra-particle pore volume, any interfacial particle-scaffold pores, any defects (e.g., cracks), if any, in the opaloid, and, in some examples, any unfilled scaffold pores or unfilled scaffold pore volumes. The composite membrane may comprise a porosity of between about 10 vol% to about 45 vol%, or about 10 vol% to about 50 vol%, or about 10 vol% to about 55 vol%, or about 10 vol% to about 60 vol%, or about 10 vol% to about 65 vol%, or about 10 vol% to about 70 vol%, or about 10 vol% to about 75 vol%. The composite membrane may comprise a porosity from about 15 vol% to about 45 vol%, or from about 15 vol% to about 50 vol%, or from about 15 vol% to about 55 vol%, or from about 15 vol% to about 60 vol%, or from about 15 vol% to about 65 vol%, or from about 15 vol% to about 70 vol%, or from about 15 vol% to about 75 vol%. The composite membrane may comprise a porosity from about 20 vol% to about 45 vol%, or from about 20 vol% to about 50 vol%, or from about 20 vol% to about 55 vol%, or from about 20 vol% to about 60 vol%, or from about 20 vol% to about 65 vol%, or from about 20 vol% to about 70 vol%, or from about 20 vol% to about 75 vol%. The composite membrane may comprise a porosity from about 25 vol% to about 45 vol%, or from about 25 vol% to about 50 vol%, or from about 25 vol% to about 55 vol%, or from about 25 vol% to about 60 vol%, or from about 25 vol% to about 65 vol%, or from about 25 vol% to about 70 vol%, or from about 25 vol% to about 75 vol%. The composite membrane may comprise a porosity from about 30 vol% to about 45 vol%, or from about 30 vol% to about 50 vol%, or from about 30 vol% to about 55 vol%, or from about 30 vol% to about 60 vol%, or from about 30 vol% to about 65 vol%, or from about 30 vol% to about 70 vol%, or from about 30 vol% to about 75 vol%. The composite membrane may comprise a porosity from about 35 vol% to about 45 vol%, or from about 35 vol% to about 50 vol%, or from about 35 vol% to about 55 vol%, or from about 35 vol% to about 60 vol%, or from about 35 vol% to about 65 vol%, or from about 35 vol% to about 70 vol%, or from about 35 vol% to about 75 vol%. In some embodiments, the composite membrane porosity may be about 40 vol%.

[00188] The opaloid itself may be considered to have an opaloid pore volume and pore size. The opaloid pores may be described by considering the specific pore volume (cc/g) in a specific pore size range in the pore size distribution characterized by N_2 sorption (as described by the test methods disclosed herein). In analyzing the pore size distribution of the composite membrane there will be a peak in the specific pore volume, which may be associated with the inter-particle pore size (d) within the opaloid based on the aforementioned criteria for the inter-particle pore size. The peak may, in some embodiments, be the mode pore size (nm) with the highest specific pore volume (for example, in cases where the composite membrane pore size is dominated by the inter-particle pores of the three-dimensional packing arrangement of the opaloid). In other embodiments, the peak may instead be one of several peaks, each of which indicates the contribution from, for example, any of any defects (e.g., cracks) in the opaloid, and any unfilled pore volume of the scaffold pore. The opaloid pore size may be characterized by a mode pore size. The opaloid pore size may be within about 0.15 times to about 2 times the sub-micron particle diameter or equivalent diameter, D. The opaloid pore size may be within about 0.15 to about 1.5 times the sub-micron particle diameter or equivalent diameter, D (i.e., about 0.15*D to about 1.5*D). The opaloid pore size may be within about 0.2*D to about 1.0*D, or about 0.25*D to about 0.75*D, or about 0.3*D to about 0.7*D. The opaloid pore size may be about 0.7*D for small sub-micron particles (i.e., D of about 7 nm), and about 0.4*D for intermediate sub-micron particles (i.e., D of about 12 nm to about 45 nm), and about 0.3*D for larger sub-micron particles (i.e., D of about 100 nm). The opaloid pore size may be about 0.15*D, or about 0.2*D, or about 0.3*D, or about 0.4*D, or about 0.5*D, or about 0.6*D, or about 0.7*D, or about 0.8*D, or about 0.9*D, or about 1*D, or about 1.1*D, or about 1.2*D, or about 1.3*D, or about 1.4*D, or about 1.5*D, about 1.75*D, or about 2D, or any range in between. In some embodiments, the opaloid pore size may be about 0.25*D to about 0.75*D.

[00189] The opaloid pores may have a mode pore size of from about 1 nm to about 1 μm, or from about 1 nm to about 50 nm, or from about 1 nm to about 100 nm, or from about 2 nm to about 50 nm. The opaloid pores may have a mode pore size of from about 2 nm to about 20 nm, or about 2 nm to about 25 nm, or about 2 nm to about 30 nm, or about 2 nm to about 40 nm, or about 2 nm to about 60 nm, or about 2 nm to about 80 nm, or about 2 nm to about 100 nm. The opaloid pores may have a mode pore size of from about 5 nm to 20 nm, or from about 5 nm to about 30 nm, or from about 5 nm to about 40 nm, or from about 5 nm to about 50 nm, or from about 5 nm to about 60 nm, or from about 5 nm to about 80 nm, or from about 5 nm to about 100 nm. The opaloid pores may have a mode pore size of from about 10 nm to 20 nm, or about 10 nm to about 30 nm, or about 10 nm to about 40 nm, or about 10 nm to about 50 nm, or about 10 nm to about 60 nm, or about 10 nm to about 80 nm, or about 10 nm to about 100 nm. The opaloid pores may have a mode pore size of from about 20 nm to about

30 nm, or about 20 nm to about 40 nm, or about 20 nm to about 50 nm, or about 20 nm to about 60 nm, 20 nm to about 80 nm, or about 10 nm to about 100 nm. The opaloid pores may have a mode pore size of from about 30 nm to about 40 nm, or about 30 nm to about 50 nm, or about 30 nm to about 60 nm, 30 nm to about 80 nm, or about 30 nm to about 100 nm. The opaloid pores may have a mode pore size of from about 40 nm to about 50 nm, or about 40 nm to about 60 nm, 40 nm to about 80 nm, or about 40 nm to about 100 nm. The opaloid pores may have a mode pore size of from about 50 nm to about 70 nm, 50 nm to about 80 nm, or about 50 nm to about 100 nm.

[00190] In analyzing the pore size distribution of the composite membrane, the opaloid pore size may also be compared to the maximum pore size of neat opaloid comprising the same sub-micron particles and the fraction (Φ) of composite membrane pores that have an opaloid pore size larger than the maximum neat opaloid pore size and less than 80 nm (as may be determined by the methods described herein), where the maximum neat opaloid pore size is the maximum pore size less than or equal to 80 nm in a neat opaloid comprising the same sub-micron particles. As used herein, 80 nm was the maximum pore size measured using N_2 sorption pore size distributions, for all particle sizes investigated. Φ may be less than about 0.7, or less than about 0.6, or less than about 0.5, or less than about 0.4, or less than about 0.3, or less than about 0.2. Φ may depend on the pore size of the microporous polymer scaffold, on the sub-micron particle diameter D, and/or on the ratio of the two.

[00191] The opaloid may comprise a continuous opaloid phase that extends continuously within at least a portion of the scaffold pores in at least one direction at least about 1 mm, or at least about 5 mm, or at least about 10 mm, or at least about 20 mm, or at least about 40 mm, or at least about 50 mm, or at least about 75 mm, or at least about 100 mm, or at least 150 mm, or at least 200 mm, or at least 300 mm or, from about 1 mm to about 300 mm, or from about 1 mm to about 250 mm, from about 1mm to about 200 mm, from about 1 mm to about 150 mm, from about 1 mm to about 100 mm, from about 1 mm to about 75 mm, from about 1 mm to about 50 mm, from about 1 mm to about 40 mm, from about 1 mm to about 30 mm, from about 1 mm to about 20 mm, from about 1 mm to about 10 mm, from about 1 mm to about 5 mm, or any intermediate value from about 1 mm to about 300 mm (i.e., the "extent" of the opaloid). In this context, the term "extends continuously" (i.e. the extent of the opaloid) is not intended to describe the distance along a continuous path of the opaloid within the scaffold pores (which may, for example, comprise a torturous or indirect path within the scaffold pore volume) but rather, the term "extends continuously" is intended to encompass the displacement between two points of the opaloid within the scaffold pores that are connected by such a continuous path within the scaffold pore volume.

[00192] As used herein, the continuous opaloid phase comprises a continuous pore volume defined by the inter-particle spacing of the opaloid. The opaloid may comprise a continuous opaloid phase that extends over an area of the scaffold pores and/or the scaffold pore volume, where the area of the continuous opaloid phase may be at least about 1 mm, or at least about 5 mm, or at least about 10 mm, or at least about 20 mm, or at least about 40 mm, or at least about 50 mm, or at least about 75 mm, or at least about 100 mm, or at least 150 mm, or at least 200 mm, or at least 300 mm or from about 1 mm to about 300 mm, or from about 1 mm to about 250 mm, from about 1mm to about 200 mm, from about 1 mm to about 150 mm, from about 1 mm to about 100 mm, from about 1 mm to about 75 mm, from about 1 mm to about 50 mm, from about 1 mm to about 40 mm, from about 1 mm to about 30 mm, from about 1 mm to about 20 mm, from about 1 mm to about 10 mm, from about 1 mm to about 5 mm, or any intermediate value from about 1 mm to about 300 mm, in displacement in two orthogonal directions of the composite membrane. The displacement over which the area extends in each orthogonal direction may be a different value selected from the aforementioned ranges. The extent of the opaloid may be measured, for example, by using representative SEM images to confirm that the opaloid phase is continuous, and then measuring the macroscopic extent of the opaloid phase visually (and confirming with, for example, a tape measure or ruler, or similar measuring device).

[00193] The composite membrane may have a bubble point pressure of from about 1 bar and about 15 bar, or about 1 bar and about 20 bar, or about 1 bar and about 25 bar, about 1 bar and about 27 bar, or about 1 bar and about 30 bar. The composite membrane may have a bubble point pressure of from about 5 bar and about 15 bar, or about 5 bar and about 20 bar, or about 5 bar and about 25 bar, about 5 bar and about 27 bar, or about 5 bar and about 30 bar. The composite membrane may have a bubble point pressure of from about 10 bar and about 15 bar, or about 10 bar and about 20 bar, or about 10 bar and about 25 bar, about 10 bar and about 27 bar, or about 10 bar and about 30 bar. The composite membrane may have a bubble point pressure of from about 15 bar and about 20 bar, or about 15 bar and about 25 bar, about 15 bar and about 27 bar, or about 15 bar and about 30 bar. The composite membrane may have a bubble point pressure of fromabout 20 bar and about 25 bar, about 20 bar and about 27 bar, or about 20 bar and about 30 bar. The composite membrane may have a bubble point pressure of from about 25 bar and about 27 bar, or about 25 bar and about 30 bar. The bubble point pressure of the composite membrane is measured as indicated in the test methods described herein.

[00194] The bubble point pressure of the composite membrane may be considered to be a measure of a characteristic pore size of the composite membrane (i.e., the largest through-pore), for example, a composite membrane having a high bubble point pressure (for example,

having a bubble point pressure that is equal to or greater than 10 bar) may be considered to have relatively few large defects that extend through the thickness. That is to say, if the composite membrane does comprise any defects (e.g., cracks), these are few in number and may be considered to be largely limited to localized defects (i.e., those that do not span the full thickness of the composite membrane). Accordingly, such composite membranes of the present disclosure may be referred to as high-integrity membrane-reinforced opaloids.

[00195] The composite membranes described herein have a total surface area, where the total surface area comprises contributions from the microporous polymer scaffold and the sub-micron particles (e.g., the opaloid). The composite membranes of the present disclosure may have a surface area in which the contribution of the sub-micron particles (i.e., the opaloid) within the pore volume of the microporous polymer scaffold comprises from about 10% to about 20%, or about 10% to about 30%, or about 10% to about 40%, or about 10% to about 50%, or about 10% to about 60%, or about 10% to about 70%, or about 10% to about 80%, or about 10% to about 90% of the surface area based on the total surface area of the composite membrane. The composite membranes may have a surface area in which the contribution of the sub-micron particles (i.e., the opaloid) within the pore volume of the microporous polymer scaffold comprises from about 20% to about 30%, or about 20% to about 40%, or about 20% to about 50%, or about 20% to about 60%, or about 20% to about 70%, or about 20% to about 80%, or about 20% to about 90%. The composite membranes may have a surface area in which the contribution of the sub-micron particles (i.e., the opaloid) within the pore volume of the microporous polymer scaffold comprises from about 30% to about 40%, or about 30% to about 50%, or about 30% to about 60%, or about 30% to about 70%, or about 30% to about 80%, or about 30% to about 90%. The composite membranes may have a surface area in which the contribution of the sub-micron particles (i.e., the opaloid) within the pore volume of the microporous polymer scaffold comprises from about 40% to about 50%, or about 40% to about 60%, or about 40% to about 70%, or about 40% to about 80%, or about 40% to about 90%. The composite membranes may have a surface area in which the contribution of the sub-micron particles (i.e., the opaloid) within the pore volume of the microporous polymer scaffold comprises from about 50% to about 60%, or about 50% to about 70%, or about 50% to about 80%, or about 50% to about 90%. The composite membranes may have a surface area in which the contribution of the sub-micron particles (i.e., the opaloid) within the pore volume of the microporous polymer scaffold comprises from about 60% to about 70%, or about 60% to about 80%, or about 60% to about 90%, or about 70% to about 80%, about 70% to about 90%, or about 80% to about 90%, or about 85% to about 90%.

[00196] The composite membrane may have a contact thickness of equal to or less than about 150 μm. The composite membrane may have a contact thickness ranging from about 1 μm to about 150 μm, or from 2 μm to about 100 μm, or from about 2 μm to about 90 μm, or from about 2 μm to about 80 μm, or from about 2 μm to about 75 μm, or from about 3 μm to about 75 μm, or from about 4 μm to about 75 μm, or from about 5 μm to about 75 μm, or from about 5 μm to about 70 μm, or from about 5 μm to about 65 μm, or from about 5 μm to about 60 μm, or from about 5 μm to about 55 μm, or from about 10 μm to about 55 μm, or from about 10 μm to about 50 μm, or from about 10 μm to about 45 μm, or from about 10 μm to about 40 μm. In the present disclosure, μm has its usual meaning, i.e., μm refers to micrometers or microns.

[00197] The contact thickness of the composite membrane is measured as indicated in the test methods described herein. The thickness direction of the composite membrane is the same as the thickness direction of the microporous polymer scaffold.

[00198] The composite membrane may have a volumetric scaffold filling ratio, which is the volume of the sub-micron particles (i.e., the solid volume of the sub-micron particles of the opaloid within the pore volume of the microporous polymer scaffold) to the volume of the matrix of the microporous polymer scaffold (i.e., the volume occupied by the solid matrix of the microporous polymer scaffold excluding its pore volume), of from about 0.7 and about 1.1. The composite membrane may have a volumetric scaffold filling ratio of from about 0.75 and about 1.05, or from about 0.8 and about 1.

[00199] The composite membrane may comprise a plurality of microporous polymer scaffolds. The number of microporous polymer scaffolds is not particularly limited, and the composite membrane may comprise one microporous polymer scaffold, or two microporous polymer scaffolds, or three microporous polymer scaffolds, or four microporous polymer scaffolds, or from 1 and 20 microporous polymer scaffolds, or from 1 and 10 microporous polymer scaffolds. At least one of the plurality of microporous polymer scaffolds may have a bubble point pressure of equal to or greater than two (2) bar, and the sub-micron particles incorporated within the scaffold pore volume.

[00200] The composite membrane may comprise other layers and components besides the microporous polymer scaffold and the sub-micron particles, such that the composite membrane is suitable for its intended function.

Additional Properties of MROs

[00201] The following description of properties of the membrane reinforced opaloids of the present disclosure are applicable to all embodiments, examples and aspects of the composite membranes described herein.

[00202] The composite membranes of the present disclosure may exhibit a first peak in tensile force versus displacement, as indicated by the triangles on Figure 30a, Figure 30b, and Figure 30c. This tensile peak may correspond to a significant fracturing or yielding of the opaloid phase, indicating the long-range extent of the opaloid along the gauge length of the tensile test.

[00203] As shown by **Figure 30a**, **Figure 30b**, and **Figure 30c**, the composite membranes of the present disclosure may have a tensile strength that is substantially the same as a tensile strength of the microporous polymer scaffold when measured on an absolute basis (i.e., units of Newtons/mm, where the millimeter refers to the sample width), but the strength may be higher or lower than the original (e.g., unimbibed) microporous polymer scaffold. The absolute strength (AS) of the microporous polymer scaffold may be calculated from its matrix tensile strength (MTS), mass-per-area (MpA), and skeletal density (ρ_s) as follows.

$$AS = MTS * (MpA/\rho_s)$$

[00204] Tensile testing may be used to assess the presence of continuous opaloid phases in composite articles. As indicated by the triangles in **Figure 30a**, **Figure 30b**, and **Figure 30c**, tensile testing of composite membranes and subsequent analysis demonstrated a first tensile peak (e.g., yield point) that may be associated with the yielding of a continuous opaloid phase with macroscopic extent. The strain associated with this peak may be referred to as the composite opaloid yield strain. The presence of the first tensile peak (which may be referred to as the opaloid yield peak) may be an indication that the opaloid extends macroscopically in the direction of the tensile pull by at least a length equivalent to the gauge length.

[00205] The composite membranes of the present disclosure may have a Young's modulus that is larger than a Young's modulus of the original microporous polymer scaffold (e.g., before fabrication of the MRO). For example, the composite membrane may have a Young's modulus that is at least two times larger, or at least three times larger than the Young's modulus of the microporous polymer scaffold.

[00206] Tensile properties may contribute to improved handling and durability in applications (e.g., in industrial applications as described below). For example, **Figure 30a**, **Figure 30b**, and **Figure 30c** show that the composite membranes may have a break strain that is significantly larger than the composite opaloid yield strain. A large difference between the break strain and the composite opaloid yield strain may enable the composite membrane to avoid catastrophic failure (e.g., it may fail more slowly and/or predictably, enabling

appropriate monitoring and/or intervention). The ratio of the break strain divided by the composite opaloid yield strain may be at least about 1.2, or at least about 1.4, or at least about 1.6, or at least about 1.8, or at least about 2.0, or at least about 2.5, or at least about 3.0, or at least about 4, or at least about 5, or at least about 6, or at least about 7, or at least about 8, or at least about 9, or at least about 10, or at least about 12, or at least about 14, or at least about 16, or at least about 18, or at least about 20. The ratio of the break strain divided by the composite opaloid yield strain may be about 1.2 to about 20, or about 1.4 to about 20, or about 1.6 to about 20, or about 1.2 to about 18, or about 1.4 to about 18, or about 1.6 to about 18, or about 1.2 to about 16, or about 1.4 to about 16, or about 1.6 to about 16, or about 1.2 to about 14, or about 1.4 to about 14, or about 1.6 to about 14, or about 1.2 to about 12, or about 1.4 to about 12, or about 1.6 to about 12, or about 1.2 to about 10, or about 1.4 to about 10, or about 1.6 to about 10. Furthermore, the higher Young's modulus of the composite membranes relative to the original scaffold may contribute to improved handleability because, for example, the composite membrane may be less prone to wrinkling than the original scaffold. Furthermore, the composite membranes may exhibit significantly lower Young's modulus and/or higher ductility than the neat opaloid, which may be characterized by high modulus and/or low displacement before brittle failure. The lower Young's modulus and/or higher ductility of the composite membranes (relative to the neat opaloid) may contribute to improved handleability because, for example, the composite membrane may be less prone to breaking during installation or use.

[00207] The composite membrane may have low compressibility (i.e., the composite membrane resists compression under mechanical load). One non-limiting way to quantify compressibility under load is by the ratio of the contact thickness, T_C, to the non-contact thickness, T_{NC} (i.e., Compressibility (%) = $(1 - T_C/T_{NC}) \cdot 100$). The compressibility of the composite membrane as determined in this manner may be from about 0.2% to about 1%, or about 0.2% to about 3%, or about 0.2% to about 5%, or about 0.2% to about 10%, or about 0.2% to about 15%, or about 0.2% to about 20%, or about 0.2% to about 25%, or about 0.2% to about 30%, or about 0.2% to about 40%, or about 0.2% to about 50%, or about 0.2% to about 60%, or about 0.2% to about 70%, or about 0.2% to about 80%. The compressibility of the composite membrane may be from about 0.5% to about 1%, or about 0.5% to about 3%, or about 0.5% to about 5%, or about 0.5% to about 10%, or about 0.5% to about 15%, or about 0.5% to about 20%, or about 0.5% to about 25%, or about 0.5% to about 30%, or about 0.5% to about 40%, or about 0.5% to about 50%, or about 0.5% to about 60%, or about 0.5% to about 70%, or about 0.5% to about 80%. The compressibility of the composite membrane may be from about 1% to about 3%, or about 1% to about 5%, or about 1% to about 10%, or about 1% to about 15%, or about 1% to about 20%, or about 1% to about 25%, or about 1%

to about 30%, or about 1% to about 40%, or about 1% to about 50%, or about 1% to about 60%, or about 1% to about 70%, or about 1% to about 80%. The compressibility of the composite membrane may be from about 3% to about 5%, or about 3% to about 10%, or about 3% to about 15%, or about 3% to about 20%, or about 3% to about 25%, or about 3% to about 30%, or about 3% to about 40%, or about 3% to about 50%, or about 3% to about 60%, or about 3% to about 70%, or about 3% to about 80%. The compressibility of the composite membrane may be from about 5% to about 10%, or about 5% to about 15%, or about 5% to about 20%, or about 5% to about 25%, or about 5% to about 30%, or about 5% to about 40%, or about 5% to about 50%, or about 5% to about 60%, or about 5% to about 70%, or about 5% to about 80%. The compressibility of the composite membrane may be from about 10% to about 15%, or about 10% to about 20%, or about 10% to about 25%, or about 10% to about 30%, or about 10% to about 40%, or about 10% to about 50%, or about 10% to about 60%, or about 10% to about 70%, or about 10% to about 80%. The compressibility of the composite membrane as determined in this manner may be from about 15% to about 20%, or about 15% to about 25%, or about 15% to about 30%, or about 15% to about 40%, or about 15% to about 50%, or about 15% to about 60%, or about 15% to about 70%, or about 15% to about 80%. The compressibility of the composite membrane as determined in this manner may be from about 20% to about 25%, or about 20% to about 30%, or about 20% to about 40%, or about 20% to about 50%, or about 20% to about 60%, or about 20% to about 70%, or about 20% to about 80%. The compressibility of the composite membrane as determined in this manner may be from about 30% to about 40%, or about 30% to about 50%, or about 30% to about 60%, or about 30% to about 70%, or about 30% to about 80%, or about 40% to about 50%, or about 40% to about 60%, or about 40% to about 70%, or about 40% to about 80%, or about 50% to about 60%, or about 50% to about 70%, or about 50% to about 80%, or about 60% to about 70%, or about 60% to about 80%, or about 70% to about 80%.

Fabrication of MROs

[00208] The following passage describes in more detail some example methods by which MROs may be produced. It is intended to provide guidance to one of ordinary skill in the art to facilitate production of MROs but should not be construed as being limited to a particular embodiment or aspect.

[00209] Fabricating a composite membrane by providing a microporous polymer scaffold and depositing the opaloid in the pores of the microporous polymer scaffold may be preferred over other methods (e.g., co-extrusion or co-deposition of particles with a polymeric binder, or compounding the particles with loose fibers because, for example, the strength of the composite membrane (e.g., the tensile strength of the composite membrane per unit of mass

or per unit thickness) may be significantly increased. The MRO may be produced by incorporating the sub-micron particles into the microporous polymer scaffold via a method that comprises imbibing. As used herein, the term "imbibing" refers to a process of depositing a material within the pores of a microporous polymer scaffold using a liquid carrier, but not substantially incorporating the imbibed material into the matrix of the microporous polymer scaffold, such that the microporous polymer scaffold remains largely intact. For example, the microporous polymer scaffold may be wetted with an imbibing fluid, where the imbibing fluid comprises the sub-micron particles and a liquid carrier. To achieve a high loading of opaloid in the MRO, a high concentration of sub-micron particles in the imbibing fluid may be used (e.g., in some embodiments, the imbibing fluid may be prepared with minimal dilution of the sub-micron particles). As used herein, a microporous polymer scaffold that is "wetted" with a fluid has some or all of its pores filled with the fluid. The wetted microporous polymer scaffold may then be dried, such that the liquid carrier is substantially removed, resulting in the sub-micron particles being deposited within the pores of the microporous polymer scaffold. As will be appreciated by one skilled in the art, to produce an MRO a variety of imbibing conditions must be chosen so that the material deposited in the pores comprises an opaloid (e.g., the concentration of sub-micron particles in the liquid carrier within the pores, the packing density the sub-micron particles are enabled to achieve in the pores (e.g., enabled in part by a high colloidal stability of the colloidal precursor), the ratio of the volume of sub-micron particles in the pores to the skeletal and total volume of the microporous polymer scaffold, and the distribution of the imbibing fluid in the microporous polymer scaffold).

[00210] The imbibed microporous polymer scaffold may be dried by heating it to a high temperature, such as to 250°C, for a sufficient period of time such as 1 minute to 120 minutes. It will be appreciated by one of ordinary skill in the art that other conventional drying methods may be used, and that drying conditions, in particular time and temperature, may be modified depending on the needs of the process and on the limitations of the materials (e.g., including their melting points and/or glass transition temperatures and/or decomposition temperatures). The method may further comprise a step of heat treating the dried MRO.

[00211] The sub-micron particles may be imbibed into the microporous polymer scaffold from one side of the microporous polymer scaffold (e.g., by applying a thin film of the imbibing fluid on one side of the microporous polymer scaffold via Mayer bar coating), or from both sides (first and second surfaces) of the microporous polymer scaffold (e.g., by dip coating the microporous polymer scaffold in the imbibing fluid). The sub-micron particles may be imbibed such that the opaloid is substantially contained within the pores of the microporous polymer scaffold (i.e., the thickness of opaloid deposited on the first or second surface of the microporous polymer scaffold, outside the pore volume of the microporous polymer scaffold, sometimes referred to as "buttercoat" layers, is minimal). The thickness of a minimal

buttercoat layer may be less than 2 microns, or less than 1 micron, or less than 0.5 microns, or less than 0.2 microns, or less than 0.1 microns.

[00212] The imbibing process may comprise a backer that is a film or fabric, such as a woven material or a non-woven material, such as a web, that serves as a processing aid in the production of the MRO by physically supporting it through at least a portion of the imbibing process. The use of a backer may enable a higher loading of opaloid in the microporous polymer scaffold. The backer may be a polymer film. The imbibing process may comprise a step in which the microporous polymer scaffold wetted with imbibing fluid is in contact with the backer. The backer may be adhered to the MRO, and the force of adhesion may be such that the backer can be removed from (e.g., peeled off of) the MRO without substantially damaging the MRO.

[00213] The liquid carrier in the fluid is not particularly limited, and any suitable liquid carriers known in the art may be used. Suitable liquid carriers may include water and organic liquids. Organic liquids may include alcohols and mixtures of alcohols (such as a C1-C5 alcohols), dimethyl sulfoxide, dimethyl acetamide, acetonitrile, toluene, dimethyacetamide (DMAc), methyl ethyl ketone (MEK), acetone, dimethylformamide (DMF), tetrahydrofuran (THF), and N-methyl-2-pyrrolidone (NMP). More than one liquid carrier may be used, such as two, or three, or four liquid carriers. The C1-C5 alcohol (e.g., isomers of methanol, ethanol, propanol, butanol, and pentanol) may be any one selected from methanol, ethanol, propan-1-ol, propan-2-ol, butan-1-ol, pentan-1-ol, and a combination thereof.

[00214] If the imbibing fluid does not spontaneously and readily wet the microporous polymer scaffold, then a variety of techniques may be employed to assist in achieving good wetting, such as by applying a differential pressure to force the liquid into the microporous polymer scaffold, raising the temperature of the liquid to lower its viscosity and surface tension, and/or pre-wetting the microporous polymer scaffold with another miscible liquid. As described above, imbibing microporous polymer scaffolds, especially low surface energy scaffolds, relies on good wetting. "Wetting" results when the contact angle, θ, between the liquid and the solid is less than about 90 degrees. Spontaneous wetting occurs when the surface energy between the solid and liquid, γ_{SL} is less than the surface energy between the solid and air, γ_{SA}. The typical relationship between these parameters and the liquid-air surface energy, γ_{LA} (i.e., the surface tension of the liquid), is given by the relationship below (Young's equation):

$$\gamma_{SL} = \gamma_{SA} - \gamma_{LA}*\cos(\theta)$$

[00215] To achieve good wetting, the surface tension of the imbibing fluid should be sufficiently low to penetrate the microporous polymer scaffold. For example, a surface tension of less than or equal to about 30 dynes/cm is typically required to penetrate expanded

microporous PTFE. Higher surface tension imbibing fluids may accordingly be suitable for higher energy scaffolds such as microporous polyethylene or microporous polypropylene.

[00216] Imbibing fluids that are aqueous or substantially aqueous are preferred in some cases, for example because of the availability of stable and highly concentrated colloidal dispersions, or because of safety and environmental reasons. For example, when the sub-micron particles comprise a ceramic or glass then an aqueous or substantially aqueous imbibing fluid may be preferred to minimize the need for oligomeric or polymeric dispersing agents. To enable an aqueous or substantially aqueous imbibing fluid to wet a microporous polymer scaffold with minimal dilution, a suitable wetting agent may be emulsified in the aqueous or substantially aqueous imbibing fluid with the aid of a surfactant. Suitable wetting agents include alcohols and mixtures of alcohols that exhibit a low water solubility, such as those alcohols having five to ten carbon atoms in the longest continuous chain, e.g., alcohols with C5-C10 linear chains, and the like. For example, pentanols, hexanols, octanols, and the like, are within the range of suitable wetting agents. Herein, these wetting agents may be referred to as “insoluble alcohols.” Similarly, suitable wetting agents also include carboxylic acids and mixtures of carboxylic acids that exhibit a low water solubility, such as those carboxylic acids having five to ten carbon atoms in the longest continuous chain, e.g., carboxylic acids with C5-C10 linear chains, and the like. For example, pentanoic acid, hexanoic acid, octanoic acid, and the like, are within the range of suitable wetting agents. Herein, these wetting agents may be referred to as “insoluble carboxylic acids.” Such insoluble wetting agents are most effective when present in the imbibing fluid above their solubility limit so as to form an “oil phase” that may be emulsified. Further, the imbibing fluid can incorporate with the water insoluble alcohol(s) and/or carboxylic acid(s) other water insoluble organics, such as alkanes, etc. In some embodiments, the wetting agent may also exhibit a low γ_{SL} relative to the targeted low surface energy scaffold.

[00217] The surfactant(s) can be a single surfactant or a combination of surfactants. Suitable surfactants are defined as those that are able to emulsify the desired wetting agent. For example, for the alcohols described above, several classes of anionic surfactants can be used, including, but not limited to, those having a structure of $R(EO)_nOSO_3^-$ or $ROSO_3^-$ where R can be any organic chain, "O" is oxygen, "S" is sulfur, "EO" is ethylene oxide and $n \geq 1$. In an alternate embodiment, non-ionic surfactants having the structure $R(EO)_nOH$, where $n \geq 1$, are also suitable for this invention. In a preferred embodiment, nonionic surfactants with hydrophilic-lipophilic balance ("HLB") values of ten or greater were found most effective to emulsify the wetting agents described above. The concentration of surfactant can be adjusted in order to achieve good emulsification of the desired wetting agent. For example, when 4% by weight of n-hexanol wetting agent (based on the total aqueous solution weight) is used, a concentration of about 2 wt% of sodium dodecyl ether sulfate was found to be suitable. In an

alternate formulation, 6 wt% of an ethoxylated alcohol was able to emulsify 4 wt% n-hexanol wetting agent. Other examples of suitable surfactants include Tergitol™ TMN10 and Barlox™ 8S.

[00218] In addition to the aqueous delivery system provided by the surfactant and the wetting agent, a stabilizing agent can be added. A stabilizing agent is typically soluble in both the wetting agent and water, and it allows a greater amount of wetting agent to be stabilized in the aqueous system than without the stabilizer. In one embodiment, glycols were found to be effective stabilizers, such as but not limited to dipropylene glycol ("DPG"), dipropylene glycol monomethyl ether, and propylene glycol. A wide range of stabilizer concentrations can be used depending on the amount of additional stability desired. For instance, if a small increase in stability is desired, a small amount of the stabilizer should be used. Conversely, higher stabilizer concentrations generally further increase the emulsion stability. Exceptions to these general guidelines do however exist. For example, DPG may be an effective stabilizer when used in concentrations ranging from less than about 1% wt. up to about 10% wt. based on total aqueous emulsion weight for hexanol-based systems

[00219] The imbibing fluid may contain additives such as dispersing agents to stabilize the colloidal dispersion or colloidal suspension. The purpose of such dispersing agents is typically to reduce viscosity, reduce or prevent agglomeration of particles, and/or reduce or prevent settling of particles. Preparation of the colloidal dispersion or colloidal suspension, and maintaining the particles as suspended or dispersed, may require the use of high-shear mixing. Various means of high-shear mixing for the preparation of colloidal dispersions and colloidal suspensions are available and are well-known to those of ordinary skill in the art, such as rotor-stators, Cowles mixers, wet jet mills, and media mills.

Applications including Supported Liquid Membranes (SLMs)

[00220] As described above, MROs of the present disclosure have an extraordinary set of properties that may enable high performance in a variety of applications. Such applications may include filtration media and electrochemical separators. The inventors have also recognized that the list of desirable properties above may make MROs a nearly ideal membrane support for so-called Supported Liquid Membranes (SLMs), especially MROs comprising sub-micron particles that comprise ceramics and/or glasses. A supported liquid membrane is a membrane system where a liquid is immobilized within the pores of a microporous membrane, typically via capillary forces. In use, SLMs are typically not submerged in the supported liquid; instead, the supported liquid is contained in the pores of the membrane support, while outside of the SLM (e.g. adjacent to the SLM) there may be, for example, a gas phase or other fluid that is immiscible with the supported liquid. SLMs have been explored for a wide variety of applications including gas separation and electrochemical

separators. The extremely small pores, relatively high porosity, crush resistance, and wettability may enable composite membranes (MROs) of the present disclosure to durably retain relatively large amounts of liquid even when subjected to high differential pressure and high compressive stress. Furthermore, the chemical and thermal stability of the MROs of the present disclosure may make them suitable for applications in challenging environments.

[00221] In some embodiments, the supported liquid within the SLM must be able to remain in the pores of the support even if subjected to significant compression or to a significant pressure drop across the SLM (i.e., a significant trans-membrane pressure). For example, the liquid may be retained within the composite membrane pores via capillary forces. The liquid may be retained in the composite membrane pores when subjected to significant trans-membrane pressure, for example a trans-membrane pressure of at least between about 1 bar to about 28 bar, or between about 5 bar to about 25 bar, or between about 10 bar to about 20 bar, or about 2 bar to about 15 bar, or about 7 bar to about 28 bar.

[00222] The supported liquid in the SLM may also have adequate durability for the intended application (e.g., the liquid itself does not unacceptably degrade when exposed to the thermal, chemical, electrochemical, radiation, and other stresses of the intended application). The liquid may comprise high-performance fluids such as ionic liquids, deep eutectic solvents, or low-vapor-pressure oils. Ionic liquids can, for example, be liquid at less than about 100°C (i.e., so-called “room-temperature ionic liquids” or RTILs), have tuneable properties such as viscosity and solubility, and can be stable at high voltage and/or high temperatures.

[00223] Furthermore, the membrane support for the liquid must also have adequate durability (e.g., chemical and mechanical durability) to survive in the intended application without unacceptable loss of function. In some embodiments, it will also be readily wettable with the liquid to be supported.

[00224] The composite membrane (i.e., the MRO) may be a membrane support for a supported liquid membrane. In some embodiments, the composite membranes having sub-micron particles with a particle diameter of from about 1 to 100 nm, or about 2 to 80 nm, or about 3 to 60 nm, or about 4 to 40nm, or about 5 to 35 nm, or about 5 to 30 nm, or about 5 to 25 nm may be a membrane support for a supported liquid membrane. The membrane support for the SLM may comprise sub-micron particles that comprise a ceramic and/or a glass.

[00225] The composite membrane may further comprise a liquid within the composite membrane pores. The liquid may have adequate durability (e.g., regarding thermal, chemical, electrochemical, radiation, and other stresses).

[00226] The composite membrane pores may be substantially filled or partially filled with the liquid. In some embodiments, the SLM has no residual porosity, meaning the liquid has

completely filled the pore volume of the membrane support of the SLM. In some embodiments, the SLM has up to 5% residual porosity. In some case the residual porosity is up to 1%, up to 2%, up to 3%, up to 5%, up to 7%, up to 10%, up to 15%, up to 20%, up to 25%, up to 30% up to 40 or up to 45% or up to 50% or up to 60% or up to 70% or up to 80% or up to 90% or up to 95% or up to 98% or up to 99%.

[00227] The liquid may be retained within the composite membrane pores.

[00228] There are numerous methods by which an MRO could be used in the fabrication of a SLM. In one embodiment, an MRO is first fabricated. Then the pores of the MRO are filled with the liquid to be supported. The pores may be filled with the liquid by spontaneous wetting, or the wetting may be assisted by any of a variety of means that will be evident to one of ordinary skill in the art, such as by applying a differential pressure to force the liquid into the MRO, raising the temperature of the liquid to lower its viscosity and surface tension, pre-wetting the MRO with another miscible liquid, and so on. As described above, non-limiting examples of high-performance liquids to be supported in the SLM may include deep eutectic solvents, low-vapor-pressure oils, and ionic liquids (ILs) including room-temperature ionic liquids (RTILs). Such high-performance liquids are typically customized to the desired application based on, for example, their durability in the application as well as other properties such as transport properties (e.g., ionic conductivity, selective ionic conductivity, gas permeability, selective gas permeability, solute permeability, selective solute permeability, and so on).

Volumetric vs. Gravimetric Basis

[00229] When fabricating composite materials, mass-based formulations and mass-normalized units (e.g., specific surface area expressed in cc/g) are often used for convenience. However, when designing and analyzing composite materials, the volume fraction of different components is often more meaningful than mass fraction. For example, thickness and porosity, which are inherently volumetric properties, are important considerations to the calculation of permeance and conductance. As another example, matrix tensile strength (MTS), which is effectively a volume-normalized version of tensile strength, is a critical parameter for characterizing both the microporous polymer scaffold and the composite membrane (i.e., the MRO). To account for the differences in the skeletal densities of different components (e.g., different microporous polymer scaffolds and different sub-micron particles), the inventors believe that volume-normalized units may be preferred over other conventions such as mass-normalized units in some cases.

[00230] An example of a property that may be best expressed in volume-normalized units is the (mass-)specific pore volume. By multiplying the customary gravimetric units (i.e.,

cc_{pore}/g_{solid}) by the skeletal density (expressed in g_{solid}/cc_{solid}) the volume-specific pore volume (expressed in cc_{pore}/cc_{solid}) may be obtained. The relationship between volume-specific pore volume and porosity is shown in **Figure 31**. This plot illustrates the ideal level of porosity that may be achieved by the opaloids in the MROs of the present disclosure, as follows. The graph may be divided into three regions: 1) a concave-down region for low values of porosity, 2) the region surrounding the inflection point at 50 vol% porosity, and 3) a concave-up region for high values of porosity. Composite membranes in Region 1 shown in **Figure 31** may have unfavorable properties because their porosity is too low (e.g., low ion conductance), and they may be challenging to fabricate due to the difficulty of achieving such extremely high packing densities (e.g., denser than the theoretical limit of 26 vol% porosity for monodisperse spheres arranged in a hexagonal close-packed structure). Conversely, composite membranes in Region 3 may lack structural integrity (e.g., crush resistance) and be hard to fabricate and handle, especially in thin form factors, because of the extremely large amount of void volume per unit of solid (i.e., per unit of structure-defining material elements). Composite membranes in Region 2 may be preferred because the level of porosity is high enough to enable effective transport (e.g., high ion conductance and/or good mass transport), but the level of porosity is still low enough to maintain good structural integrity.

Test Methods

[00231] Non-Contact Thickness (e.g., of the Microporous Polymer Scaffold)

[00232] A sample of a microporous polymer scaffold was placed over a flat smooth metal anvil and tensioned to remove wrinkles. The height of microporous polymer structure on anvil was measured and recorded using a non-contact Keyence LS-7010M digital micrometer. Next, the height of the anvil without microporous polymer scaffold was recorded. The thickness of the microporous polymer scaffold was taken as a difference between micrometer readings with and without microporous polymer scaffold being present on the anvil.

[00233] Contact Thickness (e.g., of the Membrane-Reinforced Opaloid)

[00234] A sample of an MRO was analyzed with a Mitutoyo Litematic handheld micrometer with a measuring force of 0.01 Newtons to determine the contact thickness.

[00235] Mass per Area (e.g., of the Microporous Polymer Scaffold)

[00236] A microporous polymer scaffold was strained to a point sufficient to eliminate wrinkles, and then a 10 cm^2 piece was cut out using a die. The 10 cm^2 piece was weighed on a conventional laboratory balance. The mass-per-area (M/A) was then calculated as the ratio of the measured mass to the known area.

[00237] Bulk Density (e.g., of the Microporous Polymer Scaffold)

[00238] The bulk density of the microporous polymer scaffold was calculated by dividing its mass-per-area by its non-contact thickness.

[00239] Skeletal Density (e.g., of the Microporous Polymer Scaffold)

[00240] The skeletal density is the density of a solid calculated by excluding all open pores and internal void volume. A Micromeritics AccuPyc II 1340 Gas Pycnometer (Micromeritics Instrument Corp., Norcross, GA) using helium gas as the displacement medium was used to analyze the samples. The AccuPyc uses the theory of gas displacement to determine the volume occupied by a given sample. The sample was added to a 3.5 cm^3 sample cup and sealed in the analysis chamber. The sample was purged 50 times with helium gas at 19.5 psig and the gas expands into another precision internal volume. Once purged, the sample was then analyzed with 15 cycles of fill cycles at 19.5 psig, or until the sample volume equilibrium was detected (0.02% precision). The skeletal density was calculated by dividing the sample mass by the adjusted sample volume. The sample mass was determined by weighing on an analytical balance of +/- 0.1 mg sensitivity.

[00241] Sample Skeletal Density = Sample Mass / Sample Volume

[00242] Sample Volume = Sample Chamber Volume - (Expansion Chamber Volume/((Gauge Pressure After Fill/Gauge Pressure After Expansion) - 1))

[00243] Porosity (e.g., of the Microporous Polymer Scaffold)

[00244] The porosity of the microporous polymer scaffold was calculated by dividing the difference between skeletal density and bulk density of the membrane by the skeletal density of the membrane per the following formula:

[00245] Porosity = ((Skeletal Density – Bulk Density)/Skeletal Density)*100% [Vol%]

[00246] Absolute tensile strength (e.g., of the Microporous Polymer Scaffold) [first and second directions]

[00247] The tensile strength was determined in each direction by measuring the maximum tensile load of a sample as described in ASTM D638-5, then dividing the load by the original gauge width of the sample.

[00248] Matrix tensile strength (e.g., of the Microporous Polymer Scaffold) [first and second directions]

[00249] The absolute tensile strength (in units of N/mm or equivalent) was normalized to discount pore volume to determine the matrix tensile strength of the microporous polymer scaffold (in units of MPa or equivalent). The matrix tensile strength was calculated by dividing the absolute tensile strength of the sample by a ratio of its bulk density to the skeletal as shown in the following formula:

[00250] Matrix Tensile Strength = (Absolute Tensile Strength/Non-Contact Thickness)/(Bulk Density/Skeletal Density) [MPa]

[00251] Scanning Electron Microscopy (SEM)

[00252] Samples of neat opaloids and membrane-reinforced opaloids were carefully mounted to SEM stubs using double-sided conductive tape. Cross-sections of membrane-reinforced opaloids were prepared using a Gatan® Illion2 broad beam ion mill with ion beam accelerating voltages of 0.2-5kV at a milling temperature of -150°C to -160°C. The samples were then coated with a thin (2nm) conductive layer of platinum using a Cressington® 208HR sputter coater. SEM images were then obtained using a Hitachi® SU8000 and SU8230 FESEM at an accelerating voltage of 1-3kV, with working distances of 2-8mm, using upper and lower secondary electron detectors.

[00253] Small-Angle X-ray Scattering (SAXS)

[00254] Small-angle X-ray scattering (SAXS) measurements were performed on a Xenocs Xeuss 2.0 instrument. Samples were probed with Cu K-α radiation (λ = 0.154 nm). Typical operating conditions were 50kV and 0.6 mA. Sample-to-detector distances ranged from approximately 1200 to 6400 mm. Samples were held under vacuum during scattering experiments, which were performed directly on MROs and neat opaloids. The collection time varied based on the sample-to-detector distance, sample thickness, and operating voltage. Data were calibrated using a silver behenate standard. SAXS data were collected on a 2-D detector, and the intensity distribution provided information about structural length scales and anisotropy. For isotropic structures, the intensity was uniform over 360° (azimuthal angle) and could be integrated over 360° to obtain 1-D SAXS profiles. MROs and neat opaloids exhibited isotropic 2-D SAXS patterns. The scattering vector or peak position, q (in units of nm^{-1}), is proportional to the sine of the scattering angle, θ, and inversely proportional to the wavelength, λ, according to the expression: $q = 4\pi\sin(\theta)/\lambda$. Values of q can be converted to real space correlation distances with the relationship $d = 2\pi/q$. Lorenz-corrected intensities can be calculated by multiplying intensity by q^2. Primary inter-particle structural features may be identified by peaks in the Lorenz-corrected intensity spectra. Inter-particle distances (ID) larger than 100nm, but smaller than 300nm may be evaluated by use of Ultra Small-Angle X-ray Scattering (USAXS).

[00255] N_2 Sorption BET Specific Surface Area (SSA) and Pore Size Distributions

[00256] This technique is also known as BET/BJH. N_2 sorption was performed on a Quantachrome AutoSorb iQ MP-XR gas sorption instrument with nitrogen as the adsorbate at 77 K. A starting p/p_0 of 1e-5 was used in order to assess the pore structure of the samples down to the IUPAC-designated micropore regime (< 2 nm). Degassing was performed on the AutoSorb iQ using a step heating profile up to 150 °C under vacuum for four hours. Isotherms were collected with either standard resolution (47 adsorption points, 14 desorption points) or high resolution (65 adsorption points, 38 desorption points). High-resolution runs were carried out by utilizing a delta Vmax of 10 cc/g in addition to a larger number of partial pressure targets. The specific surface area was determined from the nitrogen adsorption data using the Brunauer-Emmett-Teller (BET) method. The range of data points used for this analysis was selected using the Rouquerol method according to ISO 9277:2010, "Determination of the specific surface area of solids by gas adsorption — BET method." Density functional theory (DFT) was utilized to calculate the pore size distribution over the IUPAC-designated micropore and mesopore regimes (pores < 50 nm). Based on the smallest fitting error for similar MROs in previous work, the kernel chosen for the DFT calculations was "N2 at 77 K on silica (cylinder pores, NLDFT adsorption branch)". For the data in the Figures, the mode pore size or primary pore size was the pore size (nm) with the highest specific pore volume (cc/g) in the pore size distribution.

[00257] Volume-specific surface area (e.g., of the Microporous Polymer Scaffold)

[00258] The specific surface area of the microporous polymer scaffold was normalized to account for differences in polymer densities by multiplying by the skeletal density of the microporous polymer scaffold:

[00259] Volume-specific surface area ($m^2_{surface}/cc$) = Specific surface area ($m^2_{surface}/g$) * Skeletal density (g/cc)

[00260] Area-normalized true surface area (e.g., of the Microporous Polymer Scaffold)

[00261] The area-normalized true surface area of the microporous polymer scaffold was calculated by multiplying its specific surface area by its mass per area:

[00262] Area-normalized true surface area ($m^2_{surface}/m^2$) = Specific surface area ($m^2_{surface}/g$) * Mass per area (g/m^2)

[00263] Haze

[00264] Haze values were determined by from visible light transmittance spectra, which were collected using a Jasco V670 UV-Vis spectrophotometer. MRO samples were loaded

onto IR cards with adhesive backers. Calibration standards 99AA02-1113-7774 and 99AA02-1113-7776 were used. The total transmittance, T_t; sample diffusion rate, T_4; and instrument diffusion rate, T_3; are given by the expression

$$T_i = \frac{\sum_{380}^{780} S(\lambda)y(\lambda)\tau_i(\lambda)d\lambda}{\sum_{380}^{780} S(\lambda)y(\lambda)d\lambda}$$

[00265] where *S* is the spectral power distribution of the light source, *y* is the spectral sensitivity of the human perception of brightness (or luminous efficiency function), and τ_i is the measured transmittance spectrum. For *S*, CIE standard illuminant D65 was used, which is representative of average daylight. For *y*, a 10-degree logarithmic quantal function was used. The diffuse transmittance, T_d, is given by $T_d = T_4 - T_3\frac{T_t}{100}$. Haze is defined as $\frac{T_d}{T_t}$ and corresponds to the ratio of transmitted light scattered at multiple angles (T_d) to all transmitted light (T_t).

[00266] Capillary flow porometry

[00267] Capillary flow porometry (CFP) measurements were performed using a Quantachrome capillary flow porometer. Adhesive backers (10 mm diameter) were applied to MROs and samples were die cut. Silicone oil (surface tension (γ_{lv}) about 19.75 mN/m) was applied and wet curves were collected over the full pressure range (about 0.25 to 392 psig or about 0.017 to 27 bar). Equivalent pore diameters were determined using the Young-Laplace equation with a contact angle value (θ) of 0°. **Figure 32** shows the calculated relationship between capillary pressure (DP) and pore diameter (d) for cylindrical pores assuming the Young-Laplace equation with a surface tension of 19.75 mN/m and a contact angle of zero degrees.

[00268] Bubble Point Pressure

[00269] The bubble point pressure is a means to characterize the pore size of a porous support material and may be measured according to a bubble point measurement as further explained below. For a given fluid and pore size of a porous material (such as the microporous polymer scaffolds and composite membranes of the present disclosure) at constant wetting, the pressure required to force an air bubble through the pore is in inverse proportion to the size of the through-pore (hole). The bubble point pressure can provide a measure of the largest pore size according to the Young-Laplace equation:

$$P = \frac{4\gamma_{lv}cos\theta}{d}$$

where *P* is the pressure required to dewet a liquid from a cylindrical pore, γ_{lv} is the liquid surface tension, θ is the contact angle, and *d* is the pore diameter.

[00270] The bubble point pressure was measured according to the general teachings of ASTM F316-03 using a Capillary Flow Porometer (Model 3G zh from Quantachrome Instruments). The sample holder comprised a porous metal plate (Part Number: 196450, Anton Paar), 25.4 mm in diameter and a plastic mask (Part Number ABF-300, Professional Plastics), 18mm inner diameter x 24.5 mm outer diameter. The sample was placed in between the metal plate and the plastic mask. The sample was then clamped down and sealed using an O-ring (Part Number: 193798, Anton Paar). The sample was wet with the test fluid (Silicone fluid, 10 cSt, having a surface tension of 19.75 dynes/cm).

[00271] Mean Flow Pore Diameter

[00272] The mean flow pore diameter was measured according to the general teachings of ASTM F316-03 using a Capillary Flow Porometer (Model 3G zh from Quantachrome Instruments). The dry gas flow data were determined by loading the dry sample into the sample holder, applying gas pressure to the dry sample, and measuring gas flow rate vs. gas pressure. The wet flow data were measured by loading the sample into the sample holder, wetting the sample with test fluid, applying gas pressure to the wet sample, and measuring the gas flow rate vs. gas pressure. The one-half dry flow data was determined by plotting one-half times the dry gas flow data as a function of gas pressure. The mean flow pore diameter was determined by identifying the intersection point of the one-half dry flow data and the wet flow data, and then using the Young-Laplace equation to convert the corresponding gas pressure from the intersection point to a pore diameter value.

[00273] Organic Solvent Nanofiltration Test (OSN)

[00274] Organic solvent nanofiltration experiments were performed according to the following method. Briefly, MRO samples were stacked on top of three layers of nonwoven membrane and loaded into a stir cell. The permeable spacer membranes were chosen to provide mechanical support to the MRO samples while having minimal impact on liquid permeance and solute rejection. Solvent (e.g., ethanol, molar mass = 46.1 g/mol) was flowed through the stir cell, pressurizing the stir cell (up to about 4 bar) to flow solvent at the desired flow rate. Next, a feed solution of rose bengal (RB; molar mass = 973.7 g/mol; ~ 18 g solution; concentration ~ 10 mg/L) was flowed through the stir cell and six 2-gram samples of permeate solution were collected incrementally as the solution was filtered. The masses of collected permeate samples, $M_{RB,p}$, and remaining unfiltered, concentrated retentate solution were recorded. Samples were diluted (~ 1 mg/L) and characterized by UV-Vis. The intensity of the RB absorbance peak at λ ~ 560 nm was converted to concentration (mg/L), $C_{RB,p,dilute}$, by dividing the measured absorbance by the Beer's Law coefficient, 0.23347. The incremental RB concentration in the permeate solution, $C_{RB,p,in}$, was determined from $C_{RB,p,in}$

= $C_{RB,p,dilute}(M_{EtOH} + M_{RB,p})/M_{RB,p}$, where M_{EtOH} is the mass of ethanol added to dilute the given RB sample to a concentration of 1 mg/L. The RB rejection of each sample was determined from 1 – $C_{RB,p,in}/C_{RB,r}$, where $C_{RB,r}$ is the corresponding RB concentration in the retentate solution that did not permeate through the filter. The percentage RB rejection was averaged over the six samples.

EXAMPLES

[00275] **Comparative Example 1 – Neat (i.e., non-reinforced) opaloid comprising SiO_2 sub-micron particles with diameter of about 7 nm**

[00276] Approximately 10g of an aqueous colloidal dispersion of nominally 7 nm diameter silica particles (Ludox® SM-AS, W. R. Grace) was poured into a small glass petri dish such that the bottom of the petri dish was covered with the colloidal dispersion. The dish was left open to dry inside a fume hood for 2-3 days until all the water had evaporated, leaving the dried silica in the dish. The result was a neat (non-reinforced) opaloid as shown in **Figure 2**. SAXS data for this neat opaloid is shown in **Figure 5**, and specific surface area data is shown in **Figure 9**.

[00277] **Comparative Example 2 – Neat (i.e., non-reinforced) opaloid comprising SiO_2 sub-micron particles with diameter of about 12 nm**

[00278] Approximately 10g of an aqueous colloidal dispersion of nominally 12 nm diameter silica particles (Ludox® AS-30, W. R. Grace) was poured into a small glass petri dish such that the bottom of the petri dish was covered with the colloidal dispersion. The dish was left open to dry inside a fume hood for 2-3 days until all the water had evaporated, leaving the dried silica in the dish. The result was a neat (non-reinforced) opaloid as shown in **Figure 1a**. SAXS data for this neat opaloid is shown in **Figure 5** and **Figure 15**. The pore size distribution of this opaloid is shown in **Figure 6**, **Figure 16**, and **Figure 17**. Specific surface area data for this opaloid is shown in **Figure 9**.

[00279] **Comparative Example 3 – Neat (i.e., non-reinforced) opaloid comprising SiO_2 sub-micron particles with diameter of about 22 nm**

[00280] Approximately 10g of an aqueous colloidal dispersion of nominally 22 nm diameter silica particles (Part Snowtex® ST-50, Nissan Chemical) was poured into a small glass petri dish such that the bottom of the petri dish was covered with the colloidal dispersion. The dish was left open to dry inside a fume hood for 2-3 days until all the water had evaporated, leaving the silica in the dish. The result was a neat (non-reinforced) opaloid as shown in Figure 1b. The SAXS data for this neat opaloid is shown in **Figure 5**, along with the specific surface area data shown in **Figure 9**.

[00281] **Comparative Example 4 – Neat (i.e., non-reinforced) opaloid comprising SiO_2 sub-micron particles with diameter of about 45 nm**

[00282] Approximately 10g of an aqueous colloidal dispersion of nominally 45 nm diameter silica particles (Snowtex® ST-30LH, Nissan Chemical) was poured into a small glass petri dish such that the bottom of the petri dish was covered with the colloidal dispersion. The dish was left open to dry inside a fume hood for 2-3 days until all the water had evaporated, leaving the dried silica in the dish. The result was a neat (non-reinforced) opaloid. SAXS data for this neat opaloid is shown in **Figure 5**, and specific surface area data is shown in **Figure 9**.

[00283] **Comparative Example 5 – Neat (i.e., non-reinforced) opaloid comprising SiO_2 sub-micron particles with diameter of about 100 nm**

[00284] Approximately 10g of an aqueous colloidal dispersion of nominally 100 nm diameter silica particles (Part Snowtex® MP-1040-H, Nissan Chemical) was poured into a small glass petri dish such that the bottom of the petri dish was covered with the colloidal dispersion. The dish was left open to dry inside a fume hood for 2-3 days until all the water had evaporated, leaving the dried silica in the dish. The result was a neat (non-reinforced) opaloid as shown in **Figure 1c** and **Figure 4**. SAXS data for this neat opaloid is shown in **Figure 5**, and specific surface area data is shown in **Figure9**.

[00285] **Comparative Example 6 – Membrane-Reinforced Opaloid comprising ePTFE microporous polymer scaffold with 1.9 bar bubble point and SiO_2 sub-micron particles with diameter of about 12 nm**

[00286] An ePTFE microporous polymer scaffold known in the art was processed by methods known to those skilled in the art following the teaching of U. S. Patent 8,158,235 to Gore with these modifications: 1) Blending PTFE fine powder (PTFE 601A, DuPont, Wilmington, DE) with a lubricant (Isopar K, Exxon, Houston, TX) in the proportion of 120 cc/lb. 2) Compressing the lubricated powder into a cylindrical shape. 3) Paste extruding at a reduction ratio of 126:1. 4) Calendering to a thickness of 0.008 inch. 5) Drying the tape in a convention oven set to 210C. 6) Longitudinally stretching the tape between two banks of rollers separated by a 344C heat zone at a ratio of 4.75:1 with a rate of 31%/sec. 7) Transversely stretching the longitudinally stretched tape in a 350C heat zone, while constraining the tape from shrinking in the longitudinal direction at a ratio of 21.4:1 with a rate of 76%/sec. 8) Subjecting the stretched tape to a 380C heat zone while constrained. The ePTFE microporous polymer scaffold (with attributes of scaffold A as shown in Table 1a and Table 1b) was restrained in a 6-inch diameter metal hoop and tensioned by hand to remove wrinkles, resulting in a scaffold restrained in the 6-inch hoop. An imbibing fluid was prepared by combining a silica nanoparticle colloidal dispersion (Ludox® AS-30, W. R. Grace) with an aqueous wetting package as follows. 1 g of Ludox® AS-30, 0.02 g Lonza Barlox 8S, and 0.02 g 1-hexanol were combined in a small sample vial and then shaken vigorously to emulsify the 1-hexanol. The nanoparticles were nominally 12 nanometers in diameter and the as-received colloidal dispersion was 30 mass% in water. The mixture was pipetted onto the surface of the

scaffold and spread evenly using the side of a plastic rod until it fully wet the ePTFE (about 30 seconds). Excess imbibing fluid was removed by wiping the surface of the ePTFE scaffold with a Kimwipe® tissue. The sample was dried with a heat gun at 200°F (93.3°C) until visibly dry and heated in a standard convection oven at 250°C for 1 hour to remove residual processing fluids and residual aqueous wetting package. The result was the membrane-reinforced opaloid as shown in **Figure 12** and **Figure 13**. The pore size distribution of this MRO is shown in **Figure 16** and **Figure 17**. The sample is optically hazy as shown in **Figure 24**. In **Figure 25**, the capillary flow porometry data shows the bubble point of the MRO. The performance of the MRO in an organic solvent nanofiltration test is shown in **Figure 27**.

[00287] **Example 7 – Membrane-Reinforced Opaloid comprising ePTFE microporous polymer scaffold with 7.6 bar bubble point and mass-per-area of about 2 g/m^2, and SiO_2 sub-micron particles with diameter of about 12 nm**

[00288] An ePTFE microporous polymer scaffold known in the art was processed by methods known to those skilled in the art following the teaching of U.S. Patent 7,306,729 to Gore. The ePTFE microporous polymer scaffold (with attributes of scaffold C as shown in Table 1a and Table 1b) was restrained in a 6-inch metal hoop and tensioned by hand to remove wrinkles, resulting in a scaffold restrained in the 6-inch hoop. A second ePTFE scaffold (with attributes of scaffold A as shown in Table 1a and Table 1b) was restrained in an 8-inch diameter plastic hoop, resulting in a scaffold restrained in the 8-inch hoop. The scaffold restrained in the 8-inch hoop was placed on top of the scaffold restrained in the 6 inch hoop such that the scaffolds were in contact. An imbibing fluid was prepared by combining a silica nanoparticle colloidal dispersion (Ludox® AS-30, W. R. Grace) with an aqueous wetting package as follows. 1 g of Ludox® AS-30, 0.02 g Lonza Barlox 8S, and 0.02 g 1-hexanol were combined in a small sample vial and then shaken vigorously to emulsify the 1-hexanol. The nanoparticles were nominally 12 nanometers in diameter and the as-received colloidal dispersion was 30 mass% in water. The mixture was pipetted onto the surface of the top ePTFE microporous polymer scaffold (scaffold A, the one restrained in the 8" hoop) and spread evenly using the side of a plastic rod until it fully wet both ePTFE layers (about 30 seconds). The scaffold restrained on the 8-inch plastic hoop was removed and discarded (resulting in the removal of excess imbibing fluid). The sample (i.e., the wetted ePTFE scaffold in the 6-inch hoop, with attributes of scaffold C) was dried with a heat gun at 200°F (93.3°C) until visibly dry and heated in a standard convection oven at 250°C for 1 hour to remove residual processing fluids and residual aqueous wetting package. The result was the membrane-reinforced opaloid. SAXS data for this sample is shown in Figure 13. The sample was optically transparent as shown in **Figure 24**. The d/ID ratio of this MRO may be about 0.43 based on an inter-particle distance (ID) of about 14 nm (from SAXS data in **Figure 15**), and a pore size (d) of about 6 nm (estimated based on BET/BJH data for

a comparable MRO in **Figure 16**). The sub-micron particles were without significant intra-particle pores, and SEMs indicate the pores of the microporous polymer scaffold were fully filled with the opaloid phase and the opaloid phase was without significant macroscopic defects (e.g., cracks). The packing density of the opaloid for this sample was calculated using the following equation: Packing Density = 1 – (Composite Membrane Volume – (Microporous Polymer Scaffold Mass/Microporous Polymer Scaffold Density)-((Composite Membrane Mass-Microporous Polymer Scaffold Mass)/Sub-Micron Particle Density))/(Composite Membrane Volume -(Microporous Polymer Scaffold Mass/Microporous Polymer Scaffold Density)). Packing density was about 0.443.

[00289] **Example 8 – Membrane-Reinforced Opaloid comprising ePTFE microporous polymer scaffold with 4.8 bar bubble point, and SiO_2 sub-micron particles with diameter of about 12 nm**

[00290] An ePTFE microporous polymer scaffold known in the art was processed by methods known to those skilled in the art following the teaching of U.S. Patent 7,306,729 to Gore. The ePTFE microporous polymer scaffold (with attributes of scaffold B as shown in Table 1a and Table 1b) was restrained in a 6-inch diameter metal hoop and tensioned by hand to remove wrinkles, resulting in a scaffold restrained in the 6-inch hoop. An imbibing fluid was prepared by combining a silica nanoparticle colloidal dispersion (Ludox® AS-30, W. R. Grace) with an aqueous wetting package as follows. 1 g of Ludox® AS-30, 0.02 g Lonza Barlox 8S, and 0.02 g 1-hexanol were combined in a small sample vial and then shaken vigorously to emulsify the 1-hexanol. The nanoparticles were nominally 12 nanometers in diameter and the as-received colloidal dispersion was 30 mass% in water. The mixture was pipetted onto the surface of the scaffold and spread evenly using the side of a plastic rod until it fully wet the ePTFE (about 30 seconds). Excess imbibing fluid was removed by wiping the surface of the ePTFE scaffold with a Kimwipe® tissue. The sample was dried with a heat gun at 200°F (93.3°C) until visibly dry and heated in a standard convection oven at 250°C for 1 hour to remove residual processing fluids and residual aqueous wetting package. The result was the membrane-reinforced opaloid. The pore size distribution of this MRO is shown in **Figure 16** and **Figure 17**. The sample was optically minimally hazy as shown in **Figure 24**. In **Figure 25**, the capillary flow porometry data shows a bubble point of the MRO greater than 24 bar. The performance of the MRO in an organic solvent nanofiltration test is shown **in Figure 27**.

[00291] **Example 9 – Membrane-Reinforced Opaloid Comprising ePTFE microporous polymer scaffold with 7.6 bar bubble point and mass-per-area of about 4 g/m^2, and SiO_2 sub-micron particles with diameter of about 12 nm**

[00292] An ePTFE microporous polymer scaffold known in the art was processed by methods known to those skilled in the art following the teaching of U.S. Patent 7,306,729 to Gore with the modification that the dried material before the machine direction expansion step

was layered with one duplicate layer to double its thickness and then processed through the remaining expansion steps. The ePTFE microporous polymer scaffold (with attributes of scaffold D as shown in Table 1a and Table 1b) was restrained in a 6-inch diameter metal hoop and tensioned by hand to remove wrinkles, resulting in a scaffold restrained in the 6-inch hoop. An imbibing fluid was prepared by combining a silica nanoparticle colloidal dispersion (Ludox® AS-30, W. R. Grace) with an aqueous wetting package as follows. 1 g of Ludox® AS-30, 0.02 g Lonza Barlox 8S, and 0.02 g 1-hexanol were combined in a small sample vial and then shaken vigorously to emulsify the 1-hexanol. The nanoparticles were nominally 12 nanometers in diameter and the as-received colloidal dispersion was 30 mass% in water. The mixture was pipetted onto the surface of the scaffold and spread evenly using the side of a plastic rod until it fully wet the ePTFE (about 30 seconds). Excess imbibing fluid was removed by wiping the surface of the ePTFE scaffold with a Kimwipe® tissue. The sample was dried with a heat gun at 200°F (93.3°C) until visibly dry and heated in a standard convection oven at 250°C for 1 hour to remove residual processing fluids and residual aqueous wetting package. The result was the membrane-reinforced opaloid. The pore size distribution of this MRO is shown in **Figure 16**. In **Figure 25**, the capillary flow porometry data shows the lack of an observable bubble point of the MRO. The performance of the MRO in an organic solvent nanofiltration test is shown in **Figure 27**. Packing density was calculated per the method described in Example 7. Packing density was about 0.572.

[00293] **Comparative Example 10 – Membrane-Reinforced Opaloid Comprising ePTFE microporous polymer scaffold with 1.9 bar bubble point and SiO_2 sub-micron particles with diameter of about 7 nm**

[00294] An ePTFE microporous polymer scaffold known in the art was processed by methods known to those skilled in the art following the teaching of U. S. Patent 8,158,235 to Gore with these modifications: 1) Blending PTFE fine powder (PTFE 601A, DuPont, Wilmington, DE) with a lubricant (Isopar K, Exxon, Houston, TX) in the proportion of 120 cc/lb. 2) Compressing the lubricated powder into a cylindrical shape. 3) Paste extruding at a reduction ratio of 126:1. 4) Calendering to a thickness of 0.008 inch. 5) Drying the tape in a convention oven set to 210C. 6) Longitudinally stretching the tape between two banks of rollers separated by a 344C heat zone at a ratio of 4.75:1 with a rate of 31%/sec. 7) Transversely stretching the longitudinally stretched tape in a 350C heat zone, while constraining the tape from shrinking in the longitudinal direction at a ratio of 21.4:1 with a rate of 76%/sec. 8) Subjecting the stretched tape to a 380C heat zone while constrained. The ePTFE microporous polymer scaffold (with attributes of scaffold A as shown in Table 1a and Table 1b) was restrained in a 6-inch diameter metal hoop and tensioned by hand to remove wrinkles, resulting in a scaffold restrained in the 6-inch hoop. An imbibing fluid was prepared by combining a silica nanoparticle colloidal dispersion (Ludox® SM-AS, W. R. Grace) with an

aqueous wetting package as follows. 1 g of Ludox® SM-AS, 0.02 g Lonza Barlox 8S, and 0.02 g 1-hexanol were combined in a small sample vial and then shaken vigorously to emulsify the 1-hexanol. The nanoparticles were nominally 7 nanometers in diameter and the as-received colloidal dispersion was 25 mass% in water. The mixture was pipetted onto the surface of the scaffold and spread evenly using the side of a plastic rod until it fully wet the ePTFE (about 30 seconds). Excess imbibing fluid was removed by wiping the surface of the ePTFE scaffold with a Kimwipe® tissue. The sample was dried with a heat gun at 200°F (93.3°C) until visibly dry and heated in a standard convection oven at 250°C for 1 hour to remove residual processing fluids and residual aqueous wetting package. The result was the membrane-reinforced opaloid with a pore size distribution shown in **Figure 17.**

[00295] **Comparative Example 11 – Membrane-Reinforced Opaloid comprising ePTFE microporous polymer scaffold with 1.9 bar bubble point and SiO_2 sub-micron particles with diameter of about 22 nm**

[00296] An ePTFE microporous polymer known in the art was processed by methods known to those skilled in the art following the teaching of U. S. Patent 8,158,235 to Gore with these modifications: 1) Blending PTFE fine powder (PTFE 601A, DuPont, Wilmington, DE) with a lubricant (Isopar K, Exxon, Houston, TX) in the proportion of 120 cc/lb. 2) Compressing the lubricated powder into a cylindrical shape. 3) Paste extruding at a reduction ratio of 126:1. 4) Calendering to a thickness of 0.008 inch. 5) Drying the tape in a convention oven set to 210C. 6) Longitudinally stretching the tape between two banks of rollers separated by a 344C heat zone at a ratio of 4.75:1 with a rate of 31%/sec. 7) Transversely stretching the longitudinally stretched tape in a 350C heat zone, while constraining the tape from shrinking in the longitudinal direction at a ratio of 21.4:1 with a rate of 76%/sec. 8) Subjecting the stretched tape to a 380C heat zone while constrained. The ePTFE microporous polymer scaffold (with attributes of scaffold A as shown in Table 1a and Table 1b) was restrained in a 6-inch diameter metal hoop and tensioned by hand to remove wrinkles, resulting in a scaffold restrained in the 6-inch hoop. An imbibing fluid was prepared by combining a silica nanoparticle colloidal dispersion (Snowtex® ST-50, Nissan Chemical) with an aqueous wetting package as follows. 0.5 g of Snowtex® ST-50, 0.5 g RO H_2O, 0.02 g Rhodapex ES-2K, and 0.02 g 1-hexanol were combined in a small sample vial and then shaken vigorously to emulsify the 1-hexanol. The nanoparticles were nominally 22 nanometers in diameter and the as-received colloidal dispersion was 50 mass% in water. The mixture was pipetted onto the surface of the scaffold and spread evenly using the side of a plastic rod until it fully wet the ePTFE (about 30 seconds). Excess imbibing fluid was removed by wiping the surface of the ePTFE scaffold with a Kimwipe® tissue. The sample was dried with a heat gun at 200°F (93.3°C) until visibly dry. The result was the membrane-reinforced opaloid with a pore size distribution shown in **Figure 17.**

[00297] **Example 12 – Membrane-Reinforced Opaloid comprising ePTFE microporous polymer scaffold with 7.6 bar bubble point and mass-per-area of about 8 g/m^2, and SiO_2 sub-micron particles with diameter of about 7 nm**

[00298] An ePTFE microporous polymer scaffold known in the art was processed by methods known to those skilled in the art following the teaching of U.S. Patent 7,306,729 to Gore with the modification that the dried material before the machine direction expansion step was layered with 4 duplicate layers to quadruple its thickness and then processed through the remaining expansion steps. The ePTFE microporous polymer scaffold (with attributes of scaffold E as shown in Table 1a and Table 1b) was restrained in an 8-inch diameter plastic hoop and tensioned by hand to remove wrinkles, resulting in a scaffold restrained in the 8-inch hoop. The membrane and hoop assembly was placed on a 6-inch metal hoop such that the membrane made contact with the edges of the metal hoop. An imbibing fluid was prepared by combining a silica nanoparticle colloidal dispersion (Ludox® SM-AS, W. R. Grace) with an aqueous wetting package as follows. 10 g of Ludox® SM-AS, 0.1 g Lonza Barlox 8S, and 0.1 g 1-Hexanol were combined in a small sample vial and then shaken vigorously to emulsify the 1-hexanol. The nanoparticles were nominally 7 nanometers in diameter and the as-received colloidal dispersion was 25 mass% in water. 1 g of the mixture was pipetted onto the surface of the scaffold and spread evenly using the side of a plastic rod until it fully wet the ePTFE (about 30 seconds). Excess imbibing fluid was removed by wiping the surface of the ePTFE scaffold with a Kimwipe® tissue. The hoop was flipped over such that the bottom of the scaffold was facing upwards. 0.5 g of the mixture was pipetted onto the surface of the scaffold and spread evenly using the side of a plastic rod (about 30 seconds). Excess imbibing fluid was removed by wiping the surface of the ePTFE scaffold with a Kimwipe® tissue. The sample was dried with a heat gun at 200°F (93.3°C) until visibly dry and heated in a standard convection oven at 250°C for 1 hour to remove residual processing fluids and residual aqueous wetting package. The result was the membrane-reinforced opaloid as shown in **Figure 18** and **Figure 23b and 23c**.

[00299] **Example 13 – Membrane-Reinforced Opaloid comprising ePTFE microporous polymer scaffold with 4.8 bar bubble point, and YSZ sub-micron particles with diameter of about 32 nm**

[00300] An ePTFE microporous polymer scaffold known in the art was processed by methods known to those skilled in the art following the teaching of U.S. Patent 7,306,729 to Gore. The ePTFE microporous polymer scaffold (with attributes of scaffold B as shown in Table 1a and Table 1b) was restrained in a 6-inch diameter metal hoop and tensioned by hand to remove wrinkles, resulting in a scaffold restrained in the 6-inch hoop. An imbibing fluid was prepared by combining a colloidal dispersion of yttria-stabilized zirconia nanoparticles (ZRYS3 available from Nyacol Nano Technologies, Inc.) with an aqueous wetting package as

follows. The nanoparticles were nominally 3 mol% yttria, 32 nanometers in diameter, and the as-received colloidal dispersion was 52 mass% in water. To the as-received colloidal dispersion, 2 mass% 1-hexanol and 2 mass% Tergitol TMN-10 were added, and the mixture was agitated vigorously to emulsify the 1-hexanol. 1 g of the mixture was pipetted onto the surface of the scaffold and spread evenly using the side of a plastic rod until it fully wet the ePTFE (about 30 seconds). Excess imbibing fluid was removed by wiping the surface of the ePTFE scaffold with a Kimwipe® tissue. The hoop was flipped over such that the bottom of the scaffold was facing upwards. 0.5 g of the mixture was pipetted onto the surface of the scaffold and spread evenly using the side of a plastic rod (about 30 seconds). Excess imbibing fluid was carefully removed from the surfaces of the microporous polymer scaffold by wiping with a lint-free cloth. The sample was then dried with a heat gun set to 125°C until visibly dry (up to about 1 minute), and then heat treated in a hot air convection oven at 150°C for an additional hour. The result was the membrane-reinforced opaloid shown in **Figure 19**.

[00301] **Example 14 – Membrane-Reinforced Opaloid comprising PE microporous polymer scaffold with 3.1 bar bubble point, and YSZ sub-micron particles with diameter of about 32 nm**

[00302] An ultrahigh molecular weight PE microporous polymer scaffold (with attributes of scaffold F as shown in Table 1a and Table 1b and made according to the method description in para [00154] of this disclosure was restrained in a 6-inch diameter metal hoop, resulting in a scaffold restrained in the 6-inch hoop. A substantially aqueous colloidal dispersion for imbibing was prepared comprising yttria-stabilized zirconia nanoparticles (ZRYS3 available from Nyacol Nano Technologies, Inc.). The nanoparticles are nominally 3 mol% yttria, 32 nanometers in diameter, and the as-received colloidal dispersion is 52 mass% in water. To the as-received colloidal dispersion, 2 mass% 1-hexanol and 2 mass% Tergitol TMN-10 were added, and the mixture was agitated vigorously to emulsify the 1-hexanol. 1 g of the mixture was pipetted onto the surface of the scaffold and spread evenly using the side of a plastic rod until it fully wet the ePTFE (about 30 seconds). Excess imbibing fluid was removed by wiping the surface of the ePTFE scaffold with a Kimwipe® tissue. The hoop was flipped over such that the bottom of the scaffold was facing upwards. 0.5 g of the mixture was pipetted onto the surface of the scaffold and spread evenly using the side of a plastic rod (about 30 seconds). Excess imbibing fluid was carefully removed from the surfaces of the microporous polymer scaffold by wiping with a lint-free cloth. The sample was then dried with a heat gun set to 100°C until visibly dry (up to about 1 minute), and then heat treated in a hot air convection oven at 115°C for an additional hour. The result was the membrane-reinforced opaloid shown in **Figure 20,** with properties described in Table 2a.

[00303] **Example 15 - Dimensional stability of MRO at elevated temperature**

[00304] A membrane-reinforced opaloid was made as per the teachings of Example 12. A square was cut from the hoop using a die punch. The square was placed unrestrained in a convection oven at 300°C for 15 minutes. The dimensions before and after heat treatment were measured with the ruler shown in **Figure 23a**. The final dimensions were indistinguishable from the initial dimensions, showing no dimensional change (e.g., no shrinkage) after exposure to high temperature. The membrane after exposure to heat is shown in **Figure 23a**.

[00305] **Example 16 – Membrane-Reinforced Opaloid comprising ePTFE microporous polymer scaffold with 7.6 bar bubble point and mass-per-area of about 2 g/m^2, and SiO_2 sub-micron particles with diameter of about 7 nm**

[00306] An ePTFE microporous polymer scaffold known in the art was processed by methods known to those skilled in the art following the teaching of U.S. Patent 7,306,729 to Gore. The ePTFE microporous polymer scaffold (with attributes of scaffold C as shown in Table 1a and Table 1b) was restrained in a 6-inch metal hoop, resulting in a scaffold restrained in the 6-inch hoop. A second ePTFE microporous polymer scaffold (with attributes of scaffold A as shown in Table 1a and Table 1b) was laid on an 8-inch plastic hoop and tensioned by hand to remove wrinkles, resulting in a scaffold restrained in the 8-inch hoop. The scaffold restrained in the 8-inch hoop was placed on top of the scaffold restrained in the 6 inch hoop such that the scaffolds were in contact. An imbibing fluid was prepared by combining a silica nanoparticle colloidal dispersion (Ludox® SM-AS, W. R. Grace) with an aqueous wetting package as follows. 1 g of Ludox® SM-AS, 0.02 g Lonza Barlox 8S, and 0.02 g 1-hexanol were combined in a small sample vial and then shaken vigorously to emulsify the 1-hexanol. Around 2 mL of the mixture was pipetted onto the surface of the scaffold restrained in the 8-inch hoopand spread evenly using the side of a plastic rod until it fully wet both ePTFE layers (about 30 seconds). The scaffold restrained on the 8" plastic hoop (with attributes of scaffold A) was removed and discarded, resulting in the removal of excess imbibing fluid. The sample was dried with a heat gun at 200°F (93.3°C) until visibly dry and heated in a standard convection oven at 250°C for 1 hour to remove residual processing fluids and residual aqueous wetting package. The liquid permeance of the resulting MRO is shown in **Figure 28.**

[00307] **Example 17 – Membrane-Reinforced Opaloid comprising ePTFE microporous polymer scaffold with 7.6 bar bubble point and mass-per-area of about 4 g/m^2, and SiO_2 sub-micron particles with diameter of about 7 nm**

[00308] An ePTFE microporous polymer scaffold known in the art was processed by methods known to those skilled in the art following the teaching of U.S. Patent 7,306,729 to Gore with the modification that the dried material before the machine direction expansion step was layered with one duplicate layer to double its thickness and then processed through the remaining expansion steps. The ePTFE microporous polymer scaffold (with attributes of

scaffold D as per Table 1a and Table 1b) was restrained in an 8-inch diameter plastic hoop and tensioned by hand to remove wrinkles, resulting in a scaffold restrained in the 8-inch hoop. The scaffold and hoop assembly was placed on a 6-inch metal hoop such that the scaffold made contact with the edges of the metal hoop. An imbibing fluid was prepared by combining a silica nanoparticle colloidal dispersion (Ludox® SM-AS, W. R. Grace) with an aqueous wetting package as follows. 10 g of Ludox® SM-AS, 0.1 g Lonza Barlox 8S, and 0.1 g 1-hexanol were combined in a small sample vial and then shaken vigorously to emulsify the 1-hexanol. 1 g of the mixture was pipetted onto the surface of the scaffold and spread evenly using the side of a plastic rod until it fully wet the ePTFE (about 30 seconds). Excess imbibing fluid was removed by wiping the surface of the ePTFE scaffold with a Kimwipe® tissue. The hoop was flipped over such that the bottom of the scaffold was facing upwards. 0.5 g of the mixture was pipetted onto the surface of the scaffold and spread evenly using the side of a plastic rod (about 30 seconds). The microporous polymer scaffold was restrained on the 6 inch metal hoop and removed from the 8 inch plastic hoop. Excess imbibing fluid was removed by wiping the surface of the ePTFE scaffold with a Kimwipe® tissue. The sample was dried with a heat gun at 200°F (93.3°C) until visibly dry and heated in a standard convection oven at 250°C for 1 hour to remove residual processing fluids and residual aqueous wetting package. The resulting MRO was characterized in a high-pressure liquid permeance test as shown in **Figure 29**.

[00309] **Example 18 – Membrane-Reinforced Opaloid comprising five ePTFE microporous polymer scaffolds with 7.6 bar bubble point and mass-per-area of about 2 g/m^2 each, and SiO_2 sub-micron particles with diameter of about 7 nm**

[00310] An ePTFE microporous polymer scaffold known in the art was processed by methods known to those skilled in the art following the teaching of U.S. Patent 7,306,729 to Gore. The ePTFE microporous polymer scaffold (with attributes of scaffold C as shown in Table 1a and Table 1b) was laid on a 6-inch metal hoop, resulting in a scaffold restrained in the 6-inch hoop. Four additional microporous ePTFE microporous polymer scaffolds with the same attributes were laid on top such that 5 layers of microporous polymer scaffolds were present. All layers were restrained in one 6-inch diameter metal hoop and tensioned by hand to remove wrinkles and to bring the membranes into intimate contact (i.e., to minimize or eliminate any air gap between the layers) , resulting in a 5 layer microporous polymer scaffold with intimate contact between layers restrained in the 6-inch hoop. An imbibing fluid was prepared by combining a silica nanoparticle colloidal dispersion (Ludox® SM-AS, W. R. Grace) with an aqueous wetting package as follows. 5 g of Ludox® SM-AS, 0.1 g Lonza Barlox 8S, and 0.1 g 1-hexanol were combined in a small sample vial and then shaken vigorously to emulsify the 1-hexanol. The mixture was pipetted onto the surface of the scaffold and spread evenly using the side of a plastic rod until it fully wet the ePTFE (about 120

seconds). Excess imbibing fluid was removed by wiping the surface of the ePTFE scaffold with a Kimwipe® tissue. The sample was dried with a heat gun at 200°F (93.3°C) until visibly dry and heated in a standard convection oven at 250°C for 1 hour to remove residual processing fluids and residual aqueous wetting package. The result was a multi-layer MRO that was optically clear.

[00311] **Example 19 – Membrane-Reinforced Opaloid comprising ePTFE microporous polymer scaffold with 7.6 bar bubble point and mass-per-area of about 4 g/m^2, and a blend of two SiO_2 sub-micron particles with diameters of about 3 nm and 12 nm**

[00312] An ePTFE microporous polymer scaffold known in the art was processed by methods known to those skilled in the art following the teaching of U.S. Patent 7,306,729 to Gore with the modification that the dried material before the machine direction expansion step was layered with one duplicate layer to double its thickness and then processed through the remaining expansion steps. The ePTFE microporous polymer scaffold (with attributes of scaffold D as shown in Table 1a and Table 1b) was restrained in a 6-inch diameter metal hoop and tensioned by hand to remove wrinkles, resulting in a scaffold restrained in the 6-inch hoop. An imbibing fluid was prepared by combining a first silica nanoparticle colloidal dispersion (LiSol 3, from Nyacol), a second silica nanoparticle colloidal dispersion (NexSil 12, from Nyacol), and an aqueous wetting package as follows. 3.2 g of NexSil 12, 1.8 g of LiSol 3, 0.1 g Lonza Barlox 8S, and 0.1 g 1-hexanol were combined in a small sample vial and then shaken vigorously to emulsify the 1-hexanol. The LiSol 3 nanoparticles were nominally 3 nanometers in diameter and the as-received colloidal dispersion was 7 mass% in water. The NexSil 12 nanoparticles were nominally 12 nanometers in diameter and the as-received colloidal dispersion was 30 mass% in water. The imbibing fluid was pipetted onto the surface of the scaffold and spread evenly using the side of a plastic rod until it fully wet the ePTFE (about 30 seconds). Excess imbibing fluid was removed by wiping the surface of the ePTFE scaffold with a Kimwipe® tissue. The sample was dried with a heat gun at 200°F (93.3°C) until visibly dry and heated in a standard convection oven at 250°C for 1 hour to remove residual processing fluids and residual aqueous wetting package. The result was a membrane-reinforced opaloid. The MRO was optically clear.

[00313] **Example 20 – Supported Liquid Membrane comprising MRO and a low-vapor-pressure oil**

[00314] An ePTFE microporous polymer scaffold known in the art was processed by methods known to those skilled in the art following the teaching of U.S. Patent 7,306,729 to Gore with the modification that the dried material before the machine direction expansion step was layered with one duplicate layer to double its thickness and then processed through the remaining expansion steps. The ePTFE microporous polymer scaffold (with attributes of

scaffold D as per Table 1a and Table 1b) was restrained in an 8-inch diameter plastic hoop and tensioned by hand to remove wrinkles, resulting in a scaffold restrained in the 8-inch hoop. The scaffold and hoop assembly was placed on a 6-inch metal hoop such that the scaffold made contact with the edges of the metal hoop. An imbibing fluid was prepared by combining a silica nanoparticle colloidal dispersion (Ludox® SM-AS, W. R. Grace) with an aqueous wetting package as follows. 10 g of Ludox® SM-AS, 0.1 g Lonza Barlox 8S, and 0.1 g 1-hexanol were combined in a small sample vial and then shaken vigorously to emulsify the 1-hexanol. 1 g of the mixture was pipetted onto the surface of the scaffold and spread evenly using the side of a plastic rod until it fully wet the ePTFE (about 30 seconds). Excess imbibing fluid was removed by wiping the surface of the ePTFE scaffold with a Kimwipe® tissue. The hoop was flipped over such that the bottom of the scaffold was facing upwards. 0.5 g of the mixture was pipetted onto the surface of the scaffold and spread evenly using the side of a plastic rod (about 30 seconds). Excess imbibing fluid was removed by wiping the surface of the microporous polymer scaffold with a Kimwipe® tissue. The microporous polymer scaffold was restrained on the 6 inch metal hoop and removed from the 8 inch plastic hoop. The sample was dried with a heat gun at 200°F (93.3°C) until visibly dry and heated in a standard convection oven at 250°C for 1 hour to remove residual processing fluids and residual aqueous wetting package. ~1 g of a low-vapor-pressure perfluoropolyether oil (Krytox® VPF1506 oil) was pipetted onto the surface of the MRO. The back of the pipet was used to spread the oil until it fully penetrated the membrane (~30 seconds). The excess oil was removed using a lint-free cloth. The oil was immobilized within the membrane. The result was a supported liquid membrane comprising a membrane-reinforced opaloid and a low-vapor-pressure oil.

[00315] **Example 21 – Supported Liquid Membrane comprising MRO and a room-temperature ionic liquid**

[00316] An ePTFE microporous polymer scaffold known in the art was processed by methods known to those skilled in the art following the teaching of U.S. Patent 7,306,729 to Gore with the modification that the dried material before the machine direction expansion step was layered with one duplicate layer to double its thickness and then processed through the remaining expansion steps. The ePTFE microporous polymer scaffold (with attributes of scaffold D as per Table 1a and Table 1b) was restrained in an 8-inch diameter plastic hoop and tensioned by hand to remove wrinkles, resulting in a scaffold restrained in the 8-inch hoop. The scaffold and hoop assembly was placed on a 6-inch metal hoop such that the scaffold made contact with the edges of the metal hoop. An imbibing fluid was prepared by combining a silica nanoparticle colloidal dispersion (Ludox® SM-AS, W. R. Grace) with an aqueous wetting package as follows. 10 g of Ludox® SM-AS, 0.1 g Lonza Barlox 8S, and 0.1 g 1-hexanol were combined in a small sample vial and then shaken vigorously to emulsify the 1-

hexanol. 1 g of the mixture was pipetted onto the surface of the scaffold and spread evenly using the side of a plastic rod until it fully wet the ePTFE (about 30 seconds). Excess imbibing fluid was removed by wiping the surface of the ePTFE scaffold with a Kimwipe® tissue. The hoop was flipped over such that the bottom of the scaffold was facing upwards. 0.5 g of the mixture was pipetted onto the surface of the scaffold and spread evenly using the side of a plastic rod (about 30 seconds). Excess imbibing fluid was removed by wiping the surface of the microporous polymer scaffold with a Kimwipe® tissue. The sample was dried with a heat gun at 200°F (93.3°C) until visibly dry and heated in a standard convection oven at 250°C for 1 hour to remove residual processing fluids and residual aqueous wetting package. ~1 g of a room-temperature ionic liquid (1-ethyl-3methylimidazolium acetate, Sigma Aldrich) was pipetted onto the surface of the MRO. The back of the pipet was used to spread the room-temperature ionic liquid until it fully penetrated the composite (~30 seconds). The excess room-temperature ionic liquid was removed using a lint-free cloth. The liquid was retained within the composite membrane. The result was a supported liquid membrane comprising a membrane-reinforced opaloid and a room-temperature ionic liquid.

[00317] **Example 22 – Membrane-Reinforced Opaloid comprising ePTFE microporous polymer scaffold with 3.3 bar bubble point, and mass-per-area of about 11.6 g/m^{2}and YSZ sub-micron particles with diameter of about 32 nm**

[00318] An ePTFE microporous polymer scaffold known in the art was processed by methods known to those skilled in the art following the teaching of U.S. Patent 3,953,566 to Gore. The ePTFE microporous polymer scaffold (with attributes of scaffold G as per Table 1a and Table 1b) was restrained in a 8-inch diameter metal hoop and tensioned by hand to remove wrinkles, resulting in a scaffold restrained in the 8-inch hoop. An imbibing fluid was prepared by combining a colloidal dispersion of yttria-stabilized zirconia nanoparticles (ZRYS3 available from Nyacol Nano Technologies, Inc.) with an aqueous wetting package as follows. The nanoparticles were nominally 3 mol% yttria, 32 nanometers in diameter (D), and the as-received colloidal dispersion was 52 mass% in water. To the as-received colloidal dispersion, 3 mass% 1-hexanol and 3 mass% Tergitol TMN-10 were added, and the mixture was agitated vigorously to emulsify the 1-hexanol. 1 g of the mixture was pipetted onto the surface of the scaffold and spread evenly using the side of a plastic rod until it fully wet the ePTFE (about 30 seconds). Excess imbibing fluid was removed by wiping the surface of the microporous polymer scaffold with a lint-free cloth. The hoop was flipped over such that the bottom of the scaffold was facing upwards. 0.5 g of the mixture was pipetted onto the surface of the scaffold and spread evenly using the side of a plastic rod (about 30 seconds). Excess imbibing fluid was carefully removed from the surfaces of the microporous polymer scaffold by wiping with a lint-free cloth. The sample was then dried in an oven set to 65°C until visibly

dry, and then heat treated in a hot air convection oven at 150°C for an additional 30 minutes. The result was the membrane-reinforced opaloid shown in **Figure 21.** Packing density was calculated per the method described in Example 7. Packing density was about 0.453. Based on BET/BJH measurement, the mode pore diameter (d) of this composite membrane was 10 nm. Based on SAXS measurement, the inter-particle distance (ID) was 23 nm. Therefore, d/ID was about 0.43, ID/D was about 0.72, and d/D was about 0.31.

[00319] **Example 23 – Membrane-Reinforced Opaloid comprising ePTFE microporous polymer scaffold with 3.6 bar bubble point and mass-per-area of about 0.7 g/m^2, and SiO_2 sub-micron particles with diameter of about 7 nm**

[00320] An ePTFE microporous polymer scaffold known in the art was processed by methods known to those skilled in the art following the teaching of U.S. Patent 7,306,729 Gore. The ePTFE microporous polymer scaffold (with attributes of scaffold H as shown in Table 1a and Table 1b) was laid on a 6-inch metal hoop and tensioned by hand to remove wrinkles, resulting in a scaffold restrained in the 6-inch hoop. A second ePTFE microporous polymer scaffold (with attributes of scaffold I as shown in Table 1a and Table 1b) was laid on an 8-inch plastic hoop and tensioned by hand to remove wrinkles, resulting in a scaffold restrained in the 8-inch hoop. The scaffold restrained in the 8-inch hoop was placed on top of the scaffold restrained in the 6 inch hoop such that the scaffolds were in contact. An imbibing fluid was prepared by combining a silica nanoparticle colloidal dispersion (Ludox® SM-AS, W. R. Grace) with an aqueous wetting package as follows. 40 g of Ludox® SM-AS, 0.8 g Lonza Barlox 8S, and 0.8 g 1-hexanol were combined in a small sample vial and then shaken vigorously to emulsify the 1-hexanol. Around 2 mL of the mixture was pipetted onto the surface of the scaffold restrained in the 8-inch hoop and spread evenly using the side of a glass rod until it fully wetted both layers of ePTFE (about 30 seconds). The scaffold restrained in the 8-inch hoop was removed and discarded. The fully wetted scaffold restrained in the 6-inch hoop was dried with a heat gun at 200°F (93.3°C) until visibly dry. The result was an MRO that was 0.6 microns thick and was optically clear.

[00321] **Example 24 – Membrane-Reinforced Opaloid comprising ePTFE microporous polymer scaffold with 3.6 bar bubble point and mass-per-area of about 4.6 g/m^2, and a blend of sub-micron particles comprising SiO_2 sub-micron particles with diameter of about 7 nm and Perfluoroalkoxy Alkane (PFA) sub-micron particles with diameter of about 90nm.**

[00322] An ePTFE microporous polymer scaffold known in the art was processed by methods known to those skilled in the art following the teaching of U.S. Patent 7, 306,729 to Gore. The ePTFE microporous polymer scaffold (with attributes of scaffold A as shown in Table 1a and Table 1b) was laid on a 6-inch metal hoop and tensioned by hand to remove wrinkles, resulting in a scaffold restrained in the 6-inch hoop. An imbibing fluid was prepared

by combining a silica nanoparticle colloidal dispersion (Ludox® SM-AS, W. R. Grace) and a Perfluoroalkoxy Alkane (PFA) nanoparticle colloidal dispersion (3M Dyneon PFA 6910GZ) with an aqueous wetting package as follows. 2.5 g of Ludox® SM-AS, 1.25 g of Dyneon PFA, 1.25 g of DI H_2O, 0.4 g Tergitol TMN-10, and 0.3 g 1-hexanol were combined in a small sample vial and then shaken vigorously to emulsify the 1-hexanol. The mixture was pipetted onto the surface of the scaffold restrained in the 6-inch hoop and spread evenly using the side of a plastic rod until it fully wet the ePTFE (about 30 seconds). Excess imbibing fluid was carefully removed from the surfaces of the microporous polymer scaffold by wiping with a lint-free cloth. The sample was dried with a heat gun at 200°F (93.3°C) until visibly dry. The result was an MRO as shown in **Figure 13.**

[00323] Properties of the opaloids and membrane-reinforced opaloids (composite membranes) of the examples are shown in Tables 2a and 2b.

[00324] The invention of this application has been described above both generically and with regard to specific embodiments. It will be apparent to those skilled in the art that various modifications and variations can be made in the embodiments without departing from the scope of the disclosure. Thus, it is intended that the embodiments cover the modifications and variations of this invention provided they come within the scope of the appended claims and their equivalents.

Table 1a - Physical Properties of Microporous Polymer Scaffolds of the Examples

Microporous polymer scaffold type	Polymer Type	Mass-per-area (g/m^2)	Non-contact thickness ()microns	Porosity (vol%)	Bubble point (bar)	Volume Specific Surface Area (m^2/cc)	Area normalized true surface area ($m^2_{surface}/ m^2$)
A	PTFE	4.6	24	91%	1.9	32.1	67.2
B	PTFE	4.4	14.8	87%	4.8	-	-
C	PTFE	2	7.9	89%	7.6	75.1	68.3
D	PTFE	4	12.2	85%	7.6	71.2	129.4
E	PTFE	8.5	22.2	83%	7.6	76.4	295.2
F	PE	3.1	19	83%	1.4	15.7	51
G	PTFE	11.6	34.3	85%	3.3	36.3	191.4
H	PTFE	0.7	3.6	91%	5.2	-	-
I	PTFE	3	15.1	91%	2.5	-	-

Table 1b - Tensile Properties of Microporous Polymer Scaffolds of the Examples

Microporous polymer scaffold type	MD Absolute Tensile Strength (N/mm)	TD Absolute Tensile Strength (N/mm)	Geometric Mean Absolute Tensile Strength (N/mm)	MD MTS (MPa)	TD MTS (MPa)	Geometric mean MTS (MPa)	Strength balance ratio (second/first directions)
A	0.570	0.642	0.605	272.4	307.2	289.3	0.9
B	0.760	0.512	0.624	380.2	256.2	312.1	0.7
C	0.365	0.401	0.382	401.3	440.9	420.6	0.9
D	0.711	0.732	0.722	391.1	402.7	396.9	1.0
E	1.466	1.471	1.468	379.5	380.6	380.0	1.0
F	0.331	0.432	0.378	101.5	132.7	116	0.8
G	1.87	0.946	1.33	356	180	253.1	0.5
H	-	-	-	315	297	-	0.9
I	-	-	-	302	273	-	0.9

MD refers to machine direction;

TD refers to transverse direction;

The first direction corresponds to the direction (MD or TD) with the higher tensile strength;

The second direction corresponds to the direction (MD or TD) with the lower tensile strength

Table 12*a* – Properties of Opaloids and Membrane-Reinforced Opaloids

Example	Microporous Polymer Scaffold	Microporous Polymer Scaffold Bubble Point (bar)	Sub-micron Particle Type	Sub-micron Particle Diameter (nanometers)	Mass pr Area (g/m^2)	Contact Thickness (micrometers)
1	None	N/A	Silica	7	N/A	N/A
2	None	N/A	Silica	12	N/A	N/A
3	None	N/A	Silica	22	N/A	N/A
4	None	N/A	Silica	45	N/A	N/A
5	None	N/A	Silica	100	N/A	N/A
6	A	~ 1.9	Silica	12	9.8	7.6
7	C	~ 7.6	Silica	12	3.2	2.2
8	B	~ 4.8	Silica	12	8.8	5.6
9	D	~ 7.6	Silica	12	7.1	4.4
10	A	~ 1.9	Silica	7	10.1	7.3
11	A	~ 1.9	Silica	22	9.1	6.7
12	E	~ 7.6	Silica	7	14.7	9.6
13	B	~ 4.8	Yttria-Stabilized Zirconia	32	-	-
14	F	~ 3.1	Yttria-Stabilized Zirconia	32	53.1	62

Table 22*b* – Properties of Opaloids and Membrane-Reinforced Opaloids

Example	Microporous Polymer Scaffold	Microporous Polymer Scaffold Bubble Point (bar)	Sub-micron Particle Type	Sub-micron Particle Diameter (nanometers)	Mass pr Area (g/m^2)	Contact Thickness (micrometers)
16	C	~ 7.6	Silica	7	3.6	2.4
17	D	~ 7.6	Silica	7	6.8	4.6
18	C (5 layers)	~ 7.6	Silica	7	-	-
19	D	~ 7.6	Silica	3 & 12	6.4	3.5
20	D	~ 7.6	Silica	7	-	-
21	D	~ 7.6	Silica	7	-	-
22	G	~ 3.3	Yttria-Stabilized Zirconia	32	-	-
23	H	~5.2	Silica	7	1.4	0.6
24	A	~1.9	Silica and PFA	7 (Silica) & 90 (PFA)	12	7

CLAIMS:

1. A composite membrane comprising:

a microporous polymer scaffold comprising a plurality of scaffold pores, each of said scaffold pores having a pore volume and the microporous polymer scaffold having a scaffold pore volume, wherein the microporous polymer scaffold has a bubble point pressure equal to or greater than 2 bar; and

an opaloid within the plurality of scaffold pores, wherein the opaloid comprises sub-micron particles within the scaffold pore volume; and

wherein the composite membrane comprises a plurality of composite membrane pores that are defined at least in part by the opaloid.

2. The composite membrane of claim 1, wherein the composite membrane comprises a bubble point of equal to or greater than 10 bar.

3. The composite membrane of claim 1 or claim 2, wherein the opaloid comprises a three-dimensional packing arrangement of sub-micron particles, and wherein the composite membrane pores are defined at least in part by an inter-particle distance within the packing arrangement.

4. The composite membrane of claim 3, wherein the inter-particle distance is from about 0.5 times to about 3 times the sub-micron particle diameter or effective diameter.

5. The composite membrane of claim 3 or 4, wherein the three-dimensional packing arrangement of sub-micron particles comprises a packing arrangement selected from face-centered cubic packing hexagonal close packing, body-centered cubic packing, simple cubic packing, random close packing, liquid like packing, and combinations thereof.

6. The composite membrane of any of claims 3 to 5, wherein the three-dimensional packing arrangement of sub-micron particles can be determined by a primary structure factor peak in Lorenz-corrected small angle X-ray scattering spectra of the composite membrane; and wherein the position of the primary structure factor peak maximum corresponds to an inter-particle distance within about 0.5 to about 3 times the sub-micron particle diameter or effective diameter.

7. The composite membrane of any of claims 1 to 6, wherein the sub-micron particles have a sub-micron particle diameter or effective diameter, and the composite membrane pores have a composite membrane pore size,

wherein the mode composite membrane pore size is from about 0.15 to about 2 times the sub-micron particle diameter or effective diameter.

8. The composite membrane of any preceding claim, wherein the porosity of the composite membrane is from about 10 to 75 %.

9. The composite membrane of any of preceding claim, wherein the opaloid comprises an opaloid pore size of about 0.15 to about 1.5 times the sub-micron particle diameter or equivalent diameter.

10. The composite membrane of any preceding claim, wherein the sub-micron particles have a diameter or an equivalent diameter of from 1 nm to 1μm.

11. The composite membrane of any preceding claim, wherein the composite membrane has a contact thickness of from about 0.5 μm to about 150 μm.

12. The composite membrane of any preceding claim, wherein the plurality of scaffold pores are at least partially filled with the opaloid.

13. The composite membrane of any of claims 1 to11, wherein the plurality of scaffold pores are filled with opaloid.

14. The composite membrane of claim 12 or claim 13, wherein the opaloid extends continuously within at least a portion of the scaffold pores in at least one direction by at least about 1mm.

15. The composite membrane of any preceding claim, wherein the composite membrane comprises a composite opaloid yield strain and a composite membrane break strain, and wherein the composite membrane break strain is greater than the opaloid yield strain.

16. The composite membrane according to any preceding claim, wherein the microporous polymer scaffold is selected from one of a non-fluorinated polymer, a partially fluorinated polymer, a perfluorinated polymer, and any combination thereof.

17. The composite membrane of any preceding claim, wherein the microporous polymer scaffold comprises polyolefins, optionally polyethylene (PE) or polypropylene (PP).

18. The composite membrane of any preceding claim, wherein the microporous polymer comprises any one selected from a polytetrafluoroethylene (PTFE), a polyethylene (PE), or a copolymer of PTFE and PE, expanded polyethylene (ePE), expanded polytetrafluoroethylene (ePTFE), or combinations thereof.

19. The composite membrane of any preceding claim, wherein the sub-micron particles comprise at least one of ceramics or glasses.

20. The composite membrane of claim 19, wherein the ceramic is selected from: silicon dioxide, aluminium oxide, titanium dioxide, cerium oxide, zirconium dioxide, yttria stabilized zirconium dioxide, other oxides, and other classes of ceramics including carbides, nitrides, sulfides, borides, phosphides, selenides, titanates, carbonates, nitrates, sulfates, borates, and phosphates, or combinations thereof.

21. The composite membrane of any preceding claim, wherein the sub-micron particles comprise sub-micron particles having at least two different populations of sub-micron particles, wherein a first population of sub-micron particles has a first particle diameter (or effective particle diameter) and a second population of sub-micron particles has a second particle diameter (or effective diameter).

22. The composite membrane of any preceding claim, further comprising a liquid within the composite membrane pores.

23. A membrane-reinforced opaloid comprising:

an opaloid; and

a microporous polymer scaffold; wherein the microporous polymer scaffold comprises a plurality of scaffold pores and has a bubble point pressure of equal to or greater than 2 bar;

wherein the opaloid extends at least partially within the plurality of scaffold pores.

24. The membrane-reinforced opaloid of claim 23, wherein the membrane-reinforced opaloid comprises opaloid pores defined at least in part by the opaloid extending within the plurality of scaffold pores, and wherein the membrane-reinforced opaloid comprises a bubble point pressure of equal to or greater than 10 bar.

25. The membrane-reinforced opaloid of claims 23 or 24, wherein the opaloid extends continuously within at least a portion of the scaffold pores in at least one direction by at least 1 mm.

26. A composite membrane comprising:

a microporous polymer scaffold, wherein the microporous polymer scaffold comprises a plurality of scaffold pores, each of said scaffold pores having a pore volume and the microporous polymer scaffold having a scaffold pore volume, wherein the microporous polymer scaffold comprises a bubble point pressure of equal to or greater than 2 bar;

and sub-micron particles, wherein the sub-micron particles are incorporated within the plurality of scaffold pores and comprise a three-dimensional packing arrangement within the scaffold pore volume, wherein the three-dimensional packing arrangement is characterized by at least one of:

a packing density of the sub-micron particles of from about 0.40 to about 0.85;

a pore size (d) to inter-particle distance (ID) ratio (d/ID) from 0.2 to 2.0, or

an inter-particle distance that is from 0.5 to about 3 times the particle diameter of the sub-micron particle diameter or effective diameter.

27. A method of manufacturing a composite membrane according to any one of claims 1 to 22, the method comprising:

(a) obtaining a microporous polymer scaffold having a bubble point pressure of equal to or greater than 2 bar, wherein the microporous polymer scaffold comprises a plurality of scaffold pores, each of said scaffold pores having a pore volume and the microporous polymer scaffold having a scaffold pore volume;

(b) incorporating sub-micron particles into the scaffold pore volume of the microporous polymer scaffold within the scaffold pores; and

(c) forming an opaloid within the scaffold pore volume, wherein the opaloid comprises the sub-micron particles.

28. The method of claim 27, wherein (b) comprises imbibing the microporous polymer scaffold with a colloidal system comprising the sub-micron particles.

29. The method of any of claims 27 or 28, comprising further processing the composite membrane after step (b), wherein the further processing comprises at least one of: heat treating, annealing, or drying of the composite membrane.

30. The method of claim 29, wherein the further processing of the composite membrane forms the opaloid according to step (c).

31. The method of claim 29 or 30, wherein the further processing of the composite membrane substantially removes the aqueous or organic continuous fluid phase from the opaloid within the scaffold pores.

32. The method of any of claims 27 to 31, wherein forming the opaloid comprises passing a colloidal dispersion or colloidal suspension through the colloidal glass transition point for the colloidal dispersion or colloidal suspension.

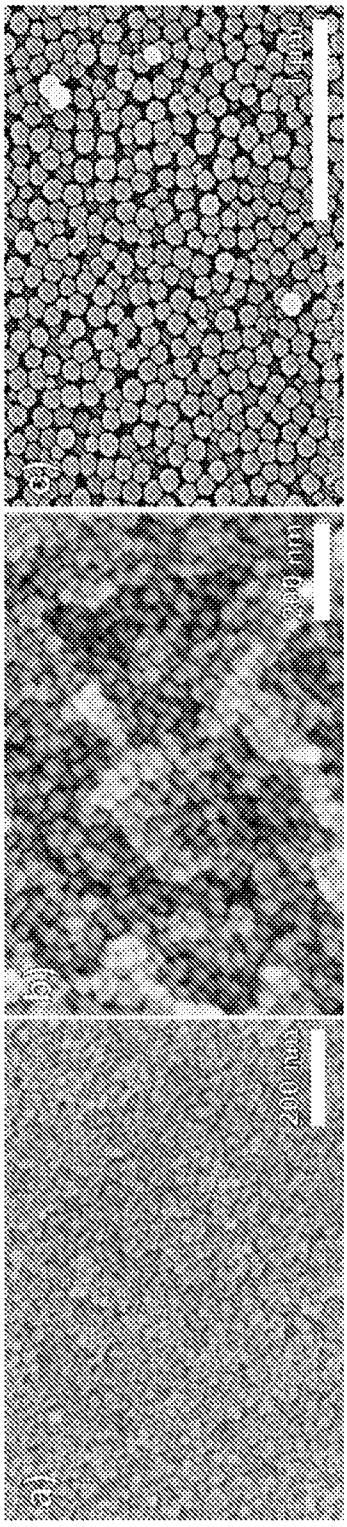


Figure 1

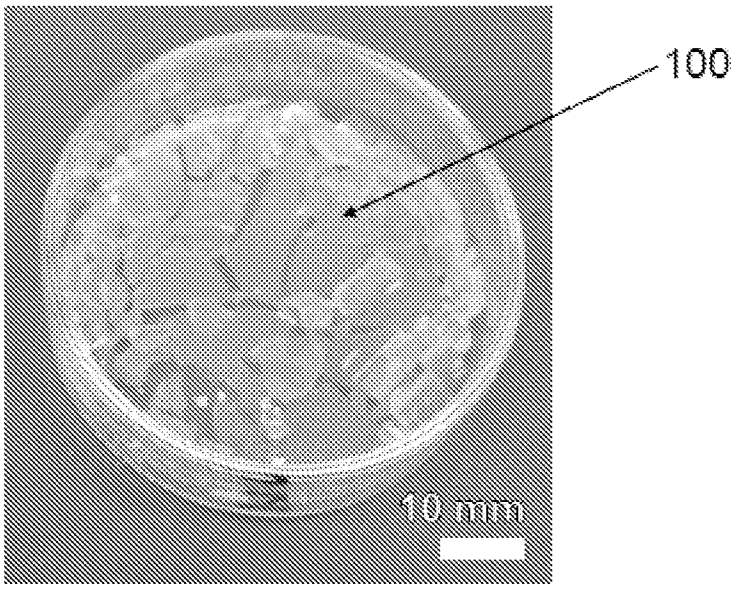


Figure 2

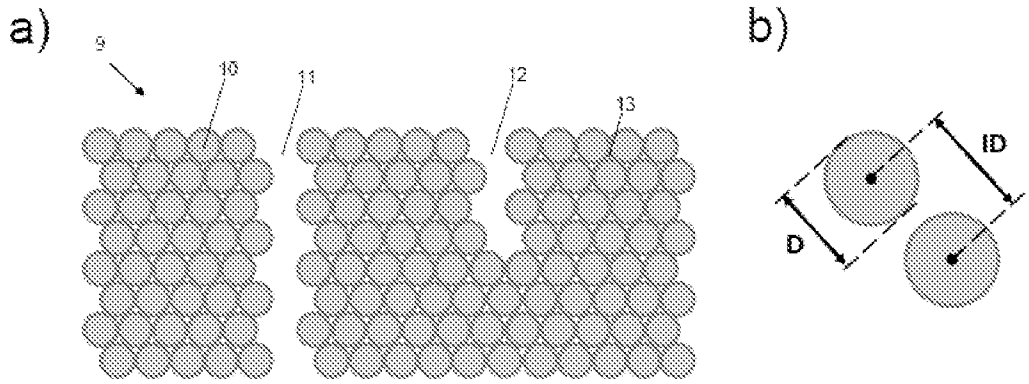


Figure 3

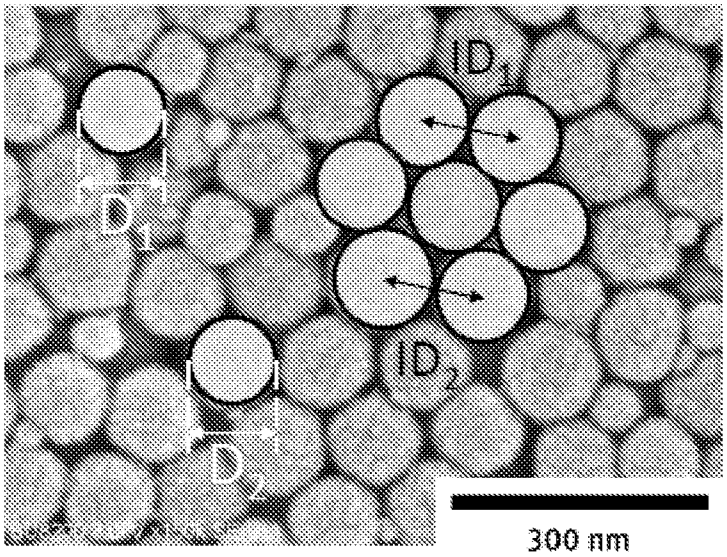


Figure 4

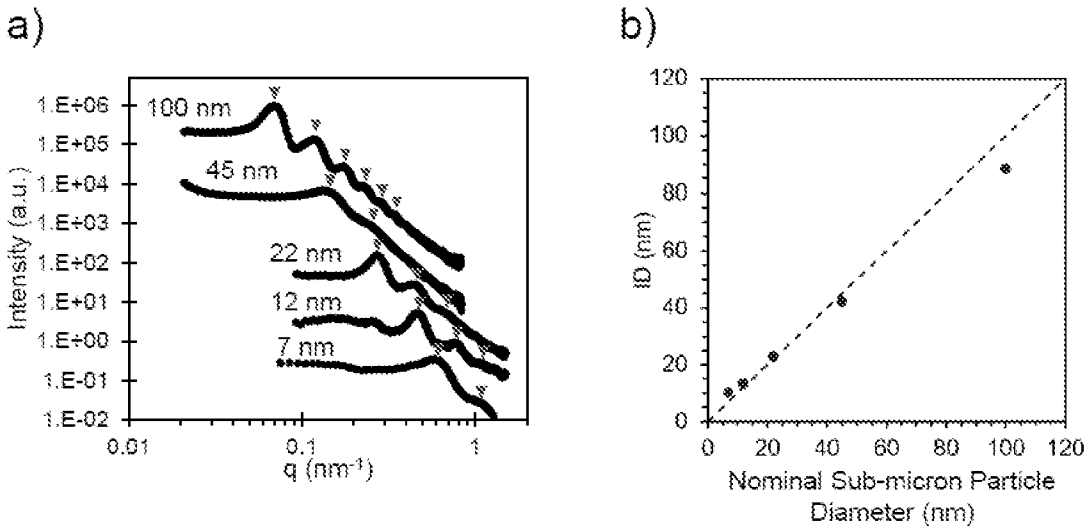
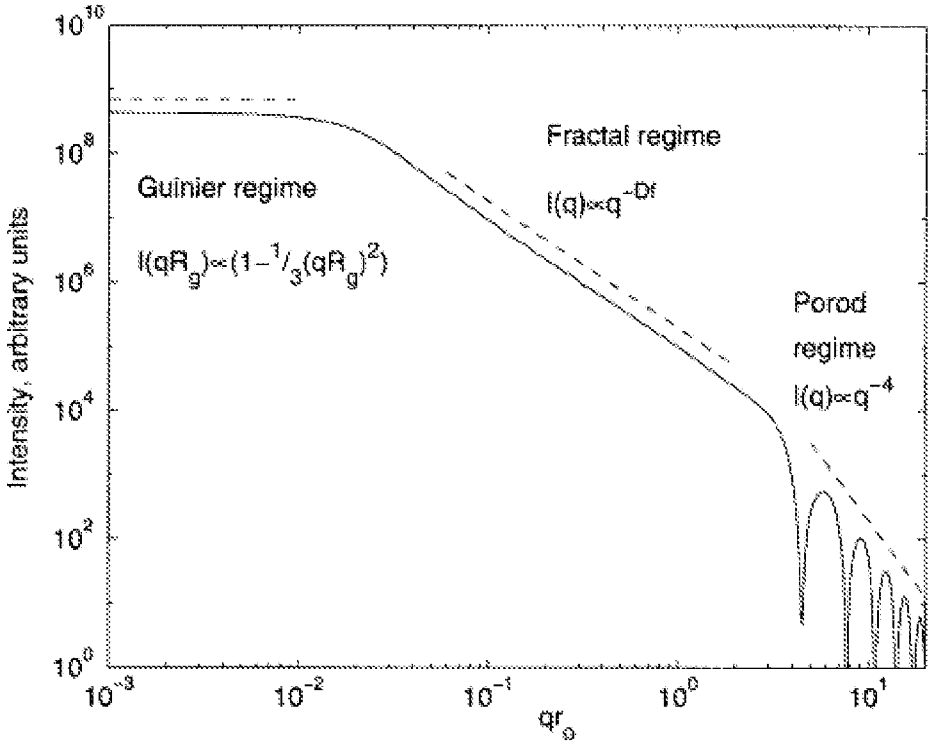


Figure 5



PRIOR ART

Figure 6

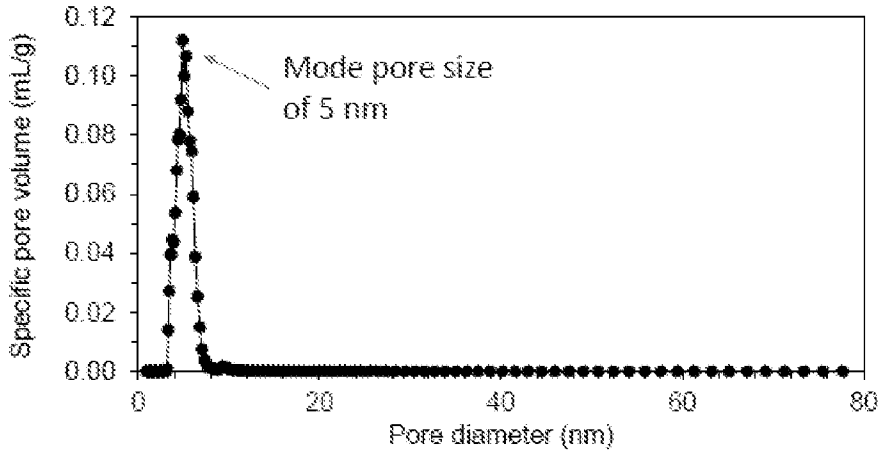


Figure 7

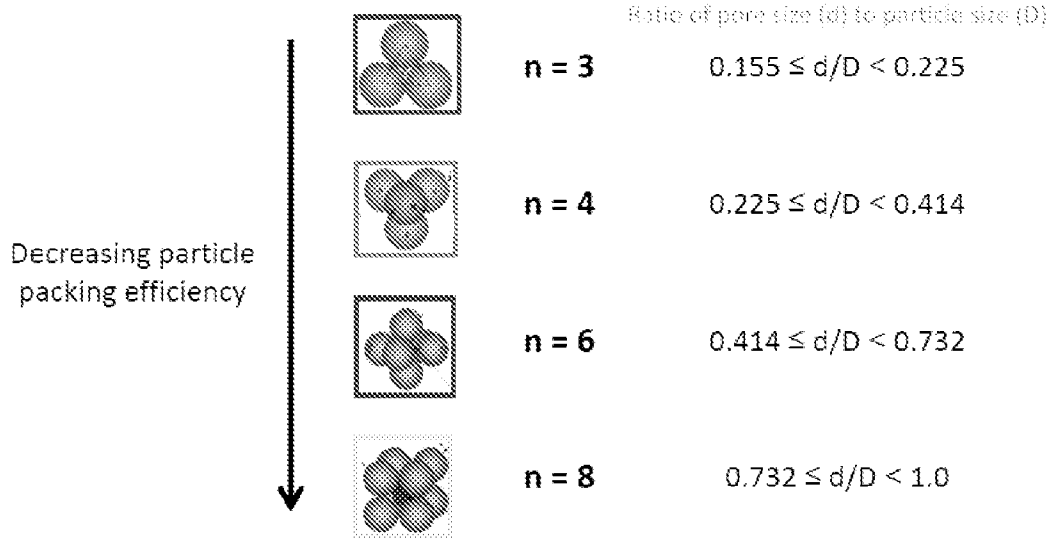


Figure 8

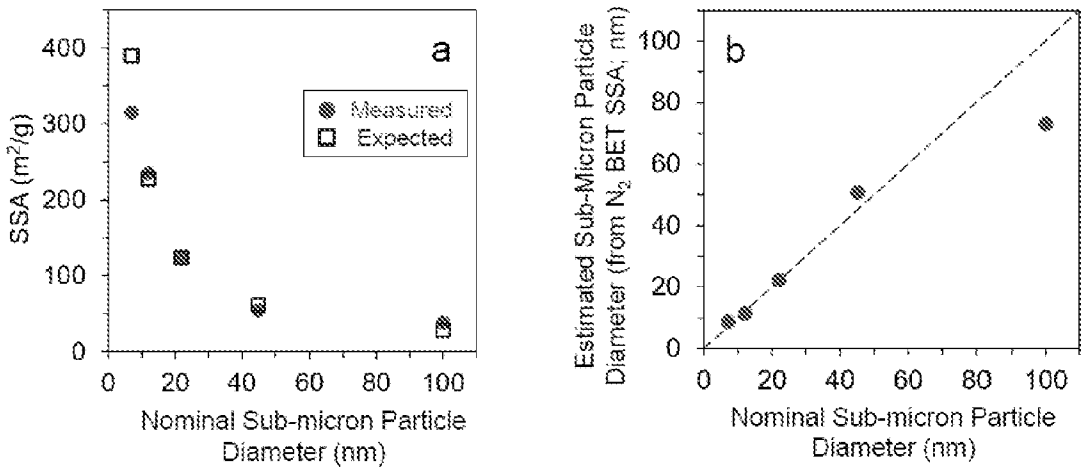


Figure 9

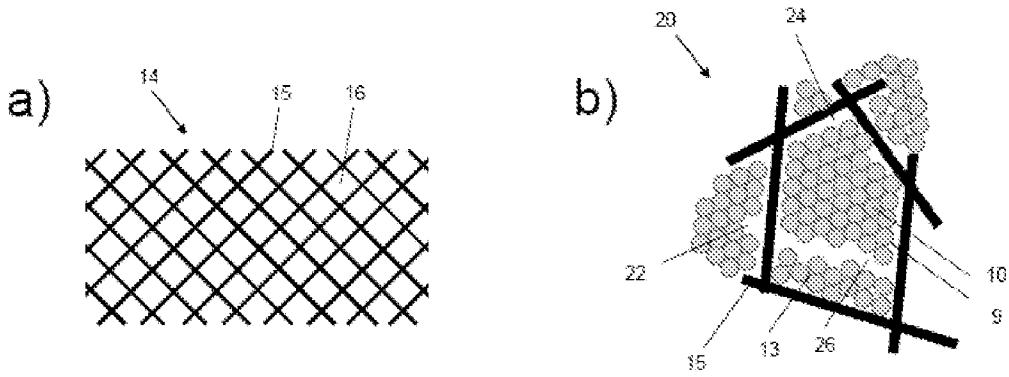


Figure 10

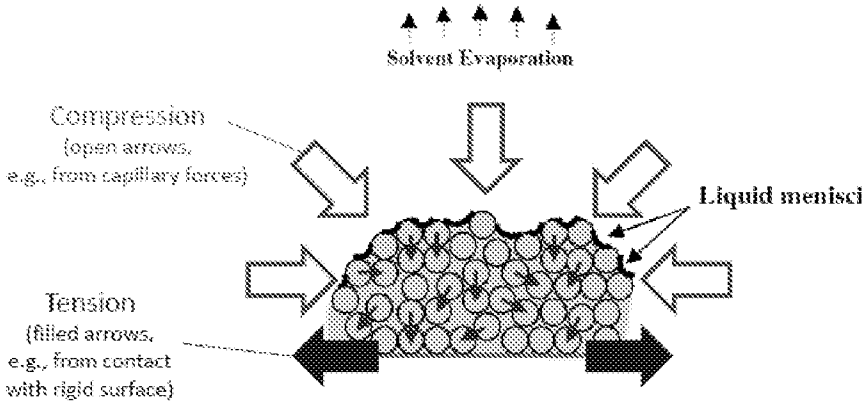


Figure 11

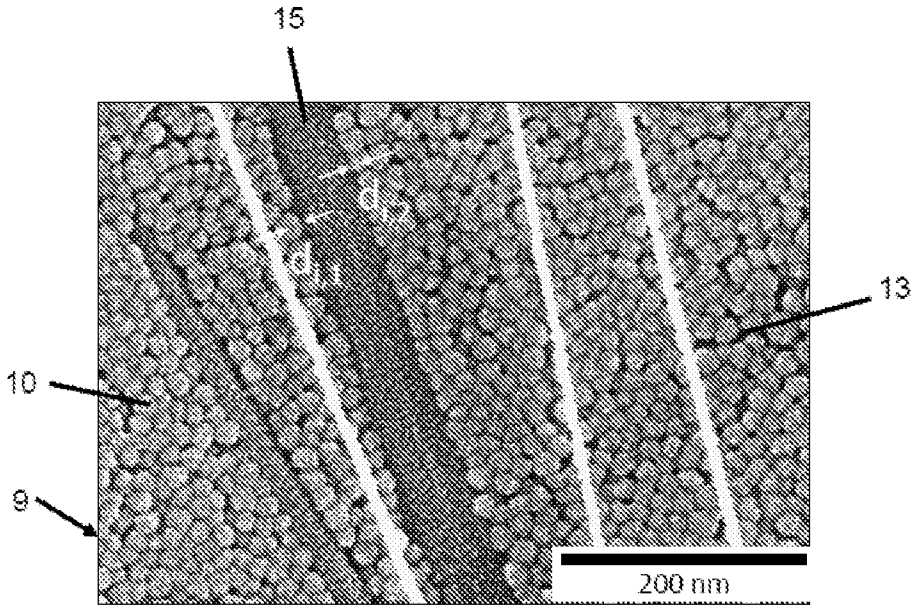


Figure 12

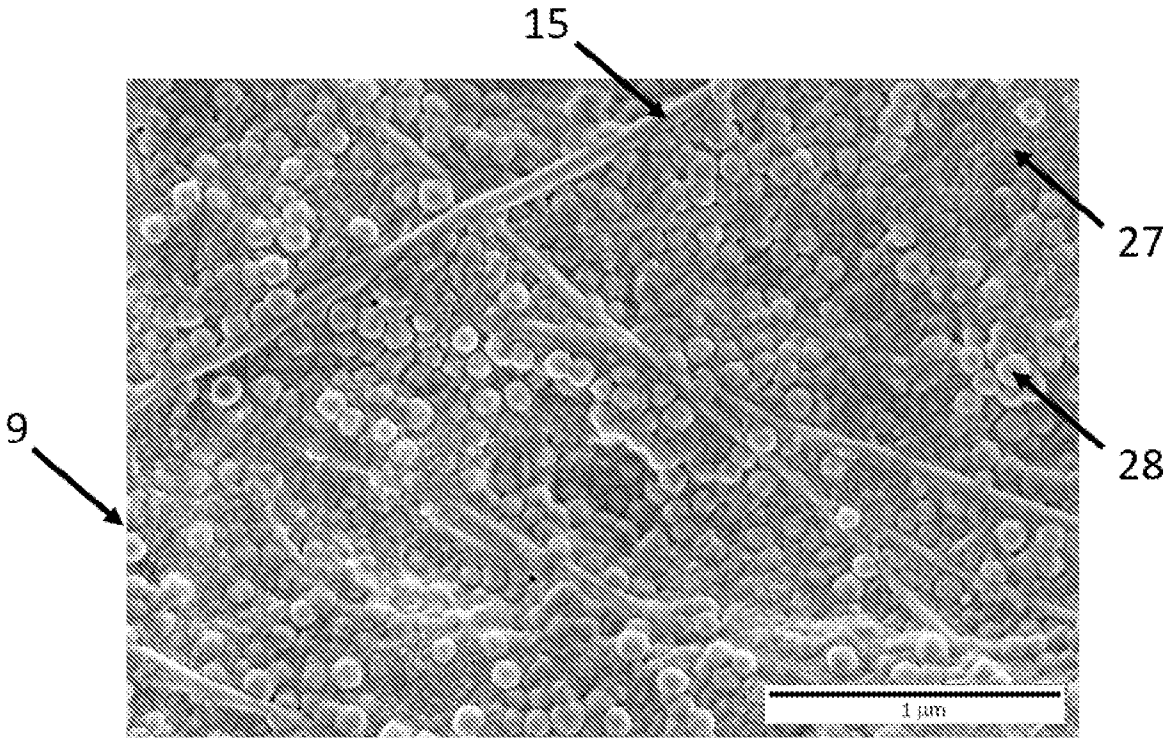


Figure 13

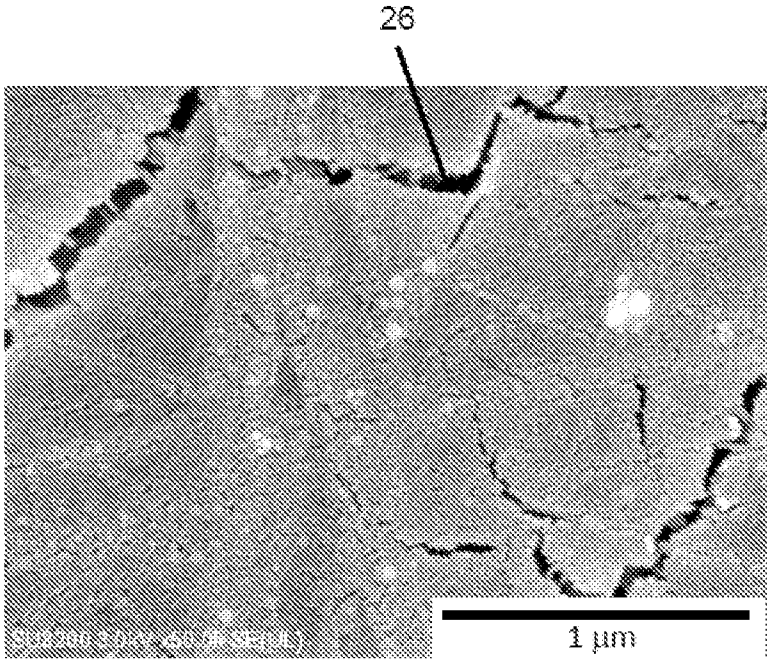


Figure 14

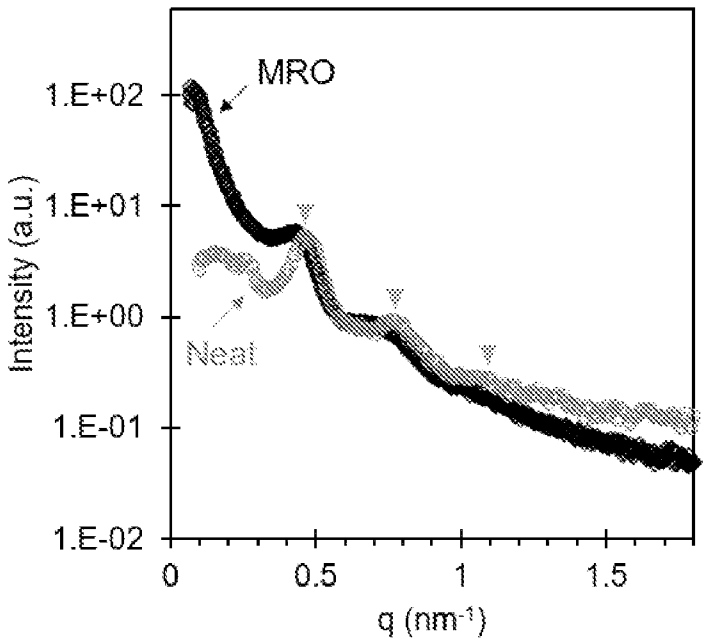


Figure 15

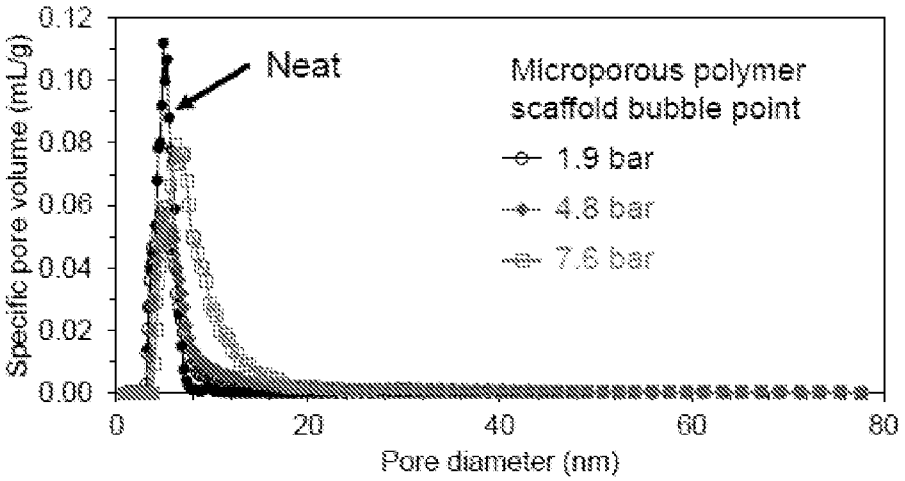


Figure 16

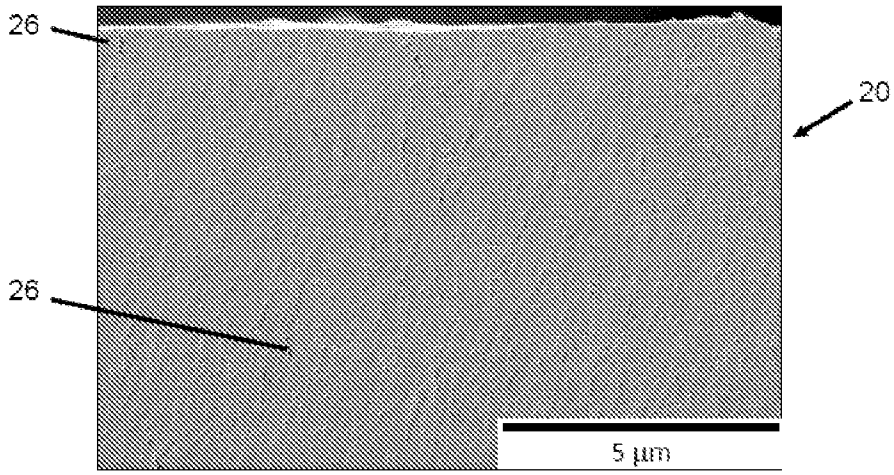
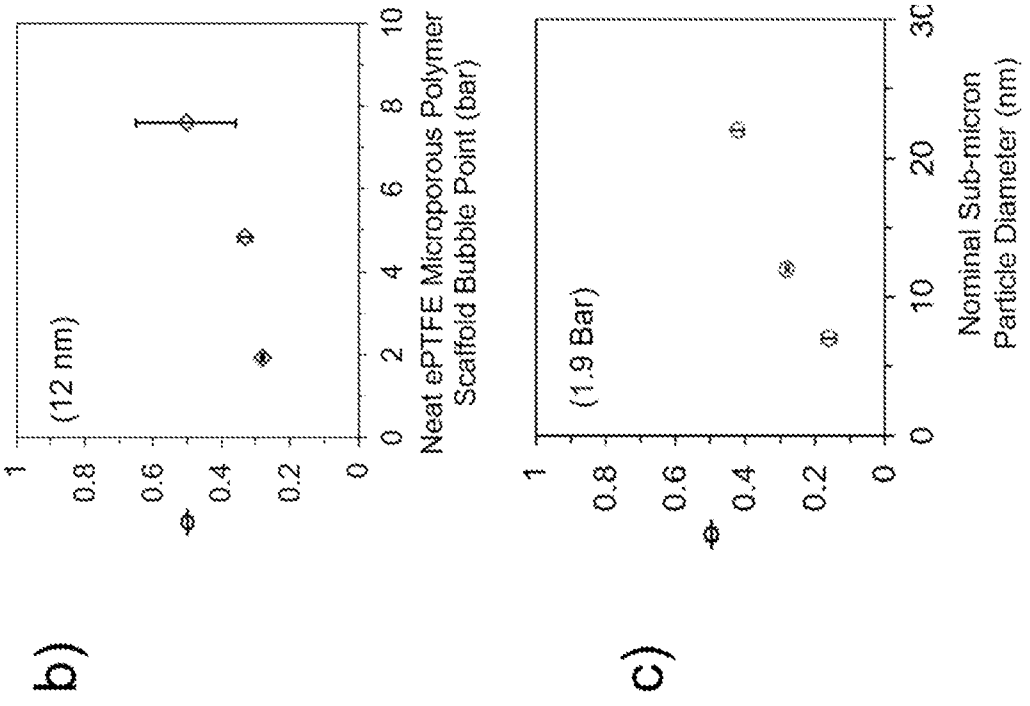


Figure 18


b)
(12 nm)
Neat ePTFE Microporous Polymer
Scaffold Bubble Point (bar)
c)
(1.9 Bar)
Nominal Sub-micron
Particle Diameter (nm)

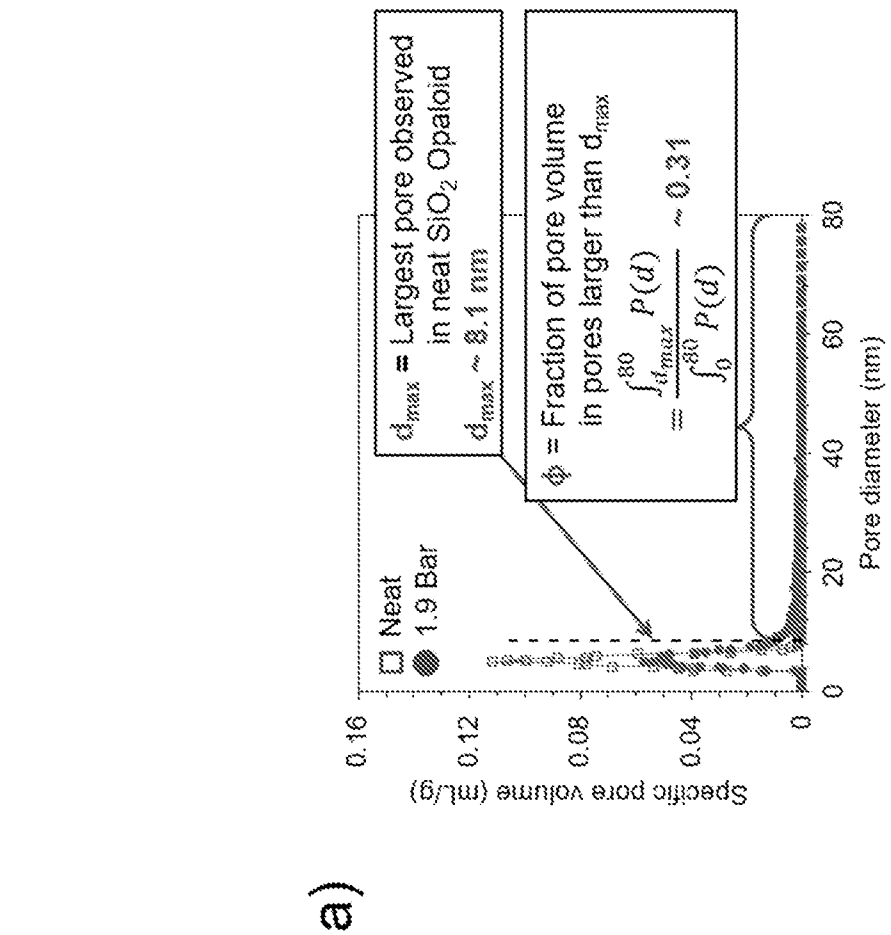

a)
Neat
1.9 Bar
d_{max} = Largest pore observed in neat SiO_2 Opaloid
d_{max} ~ 8.1 nm
Φ = Fraction of pore volume in pores larger than d_{max}
$\equiv \frac{\int_{d_{max}}^{80} P(d)}{\int_{0}^{80} P(d)} \sim 0.31$
Specific pore volume (mL/g)
Pore diameter (nm)

Figure 17

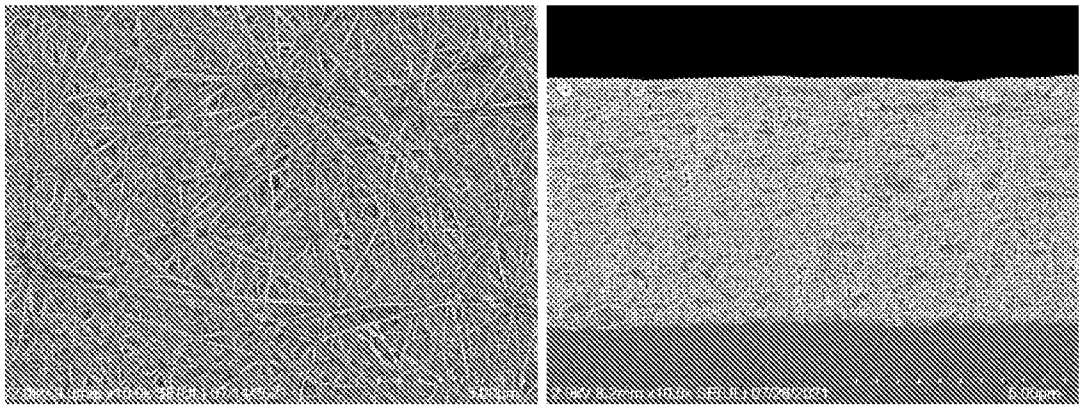


Figure 19

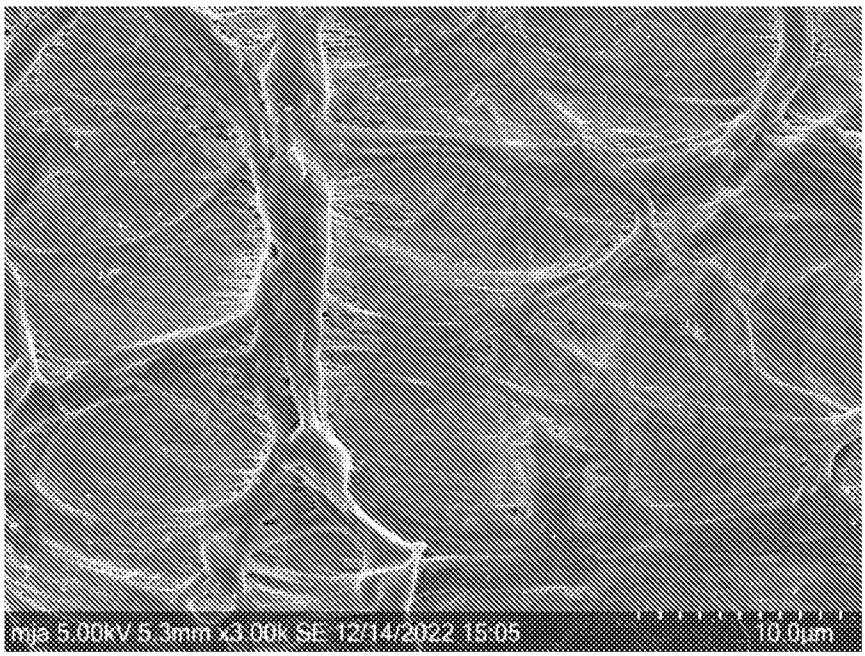


Figure 20

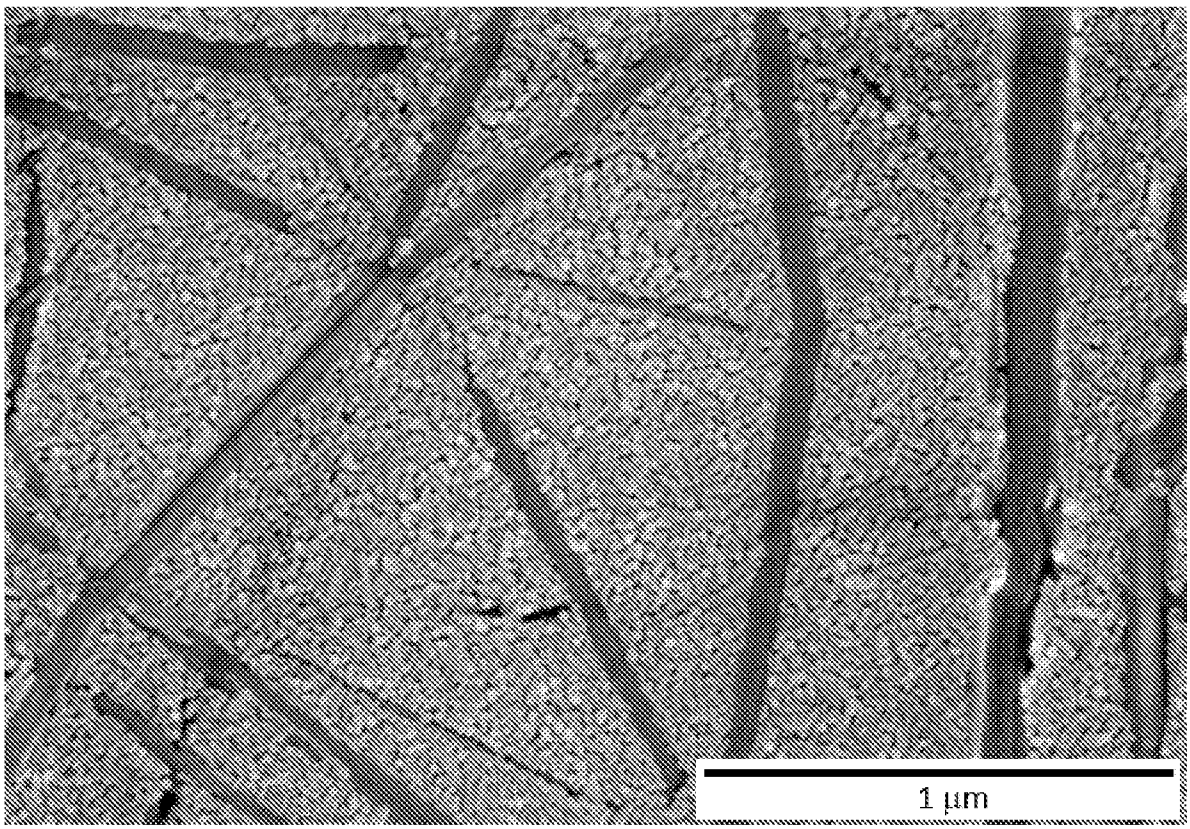


Figure 21

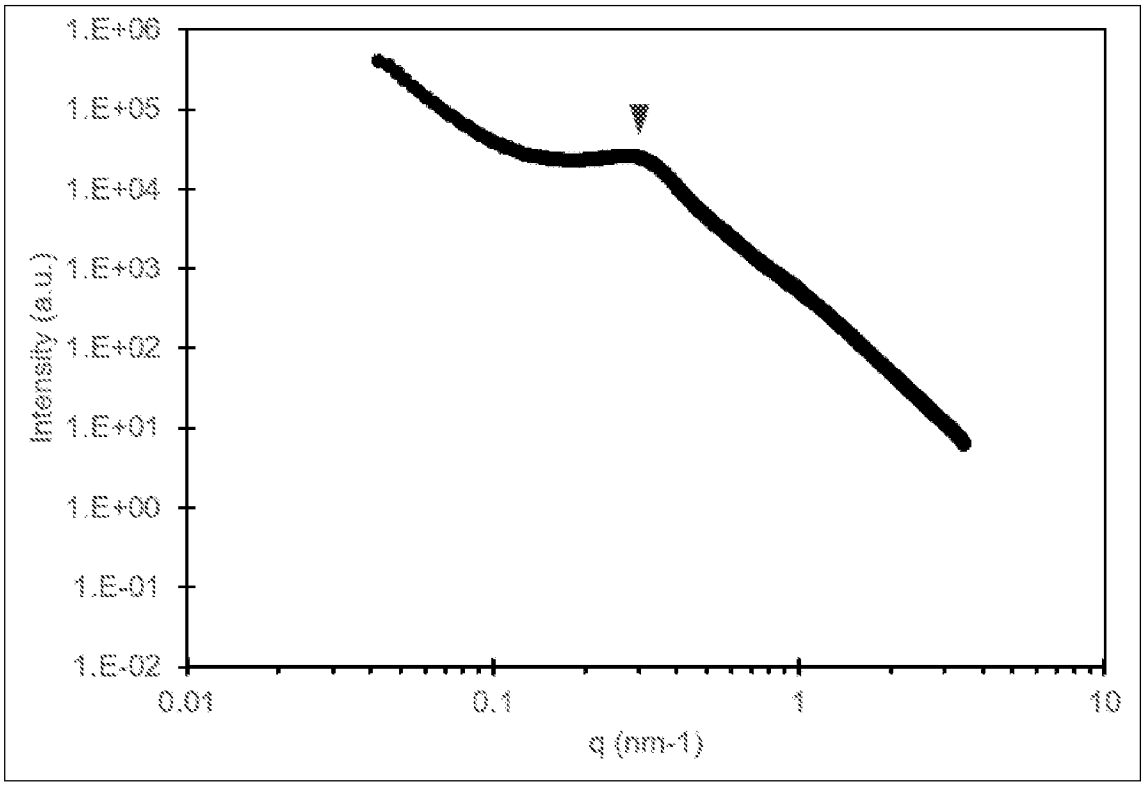


Figure 22a

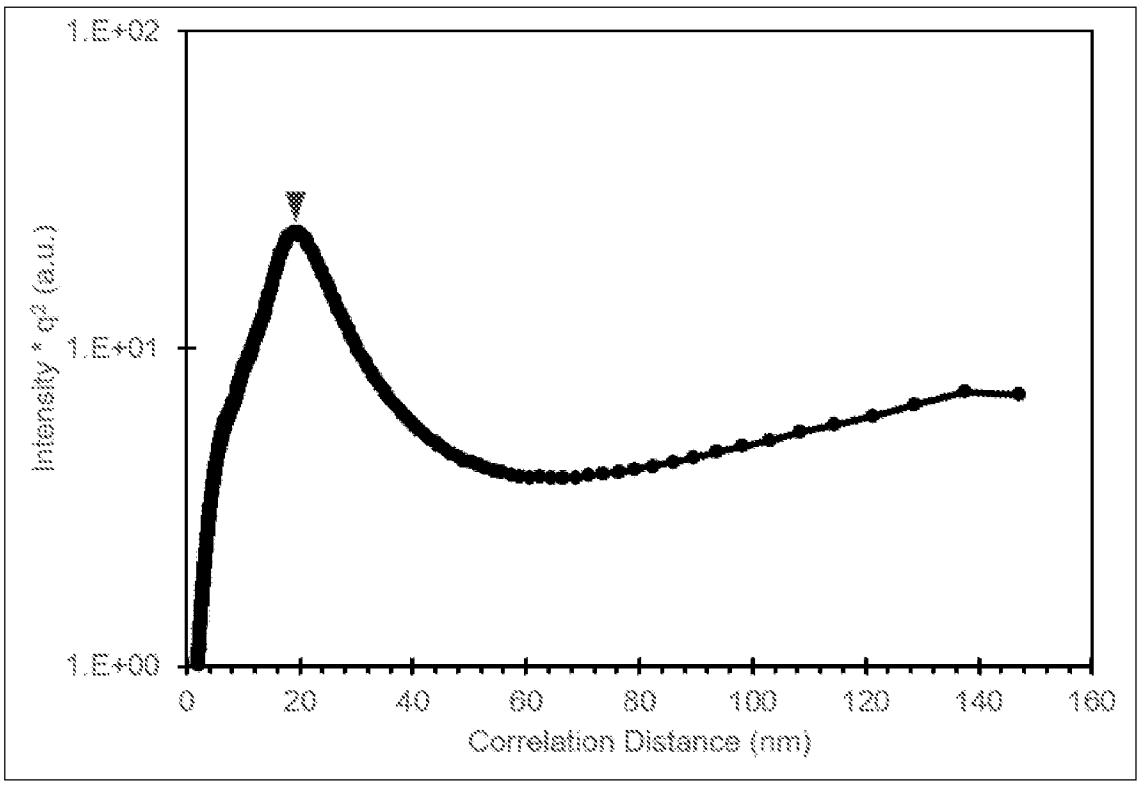


Figure 22b

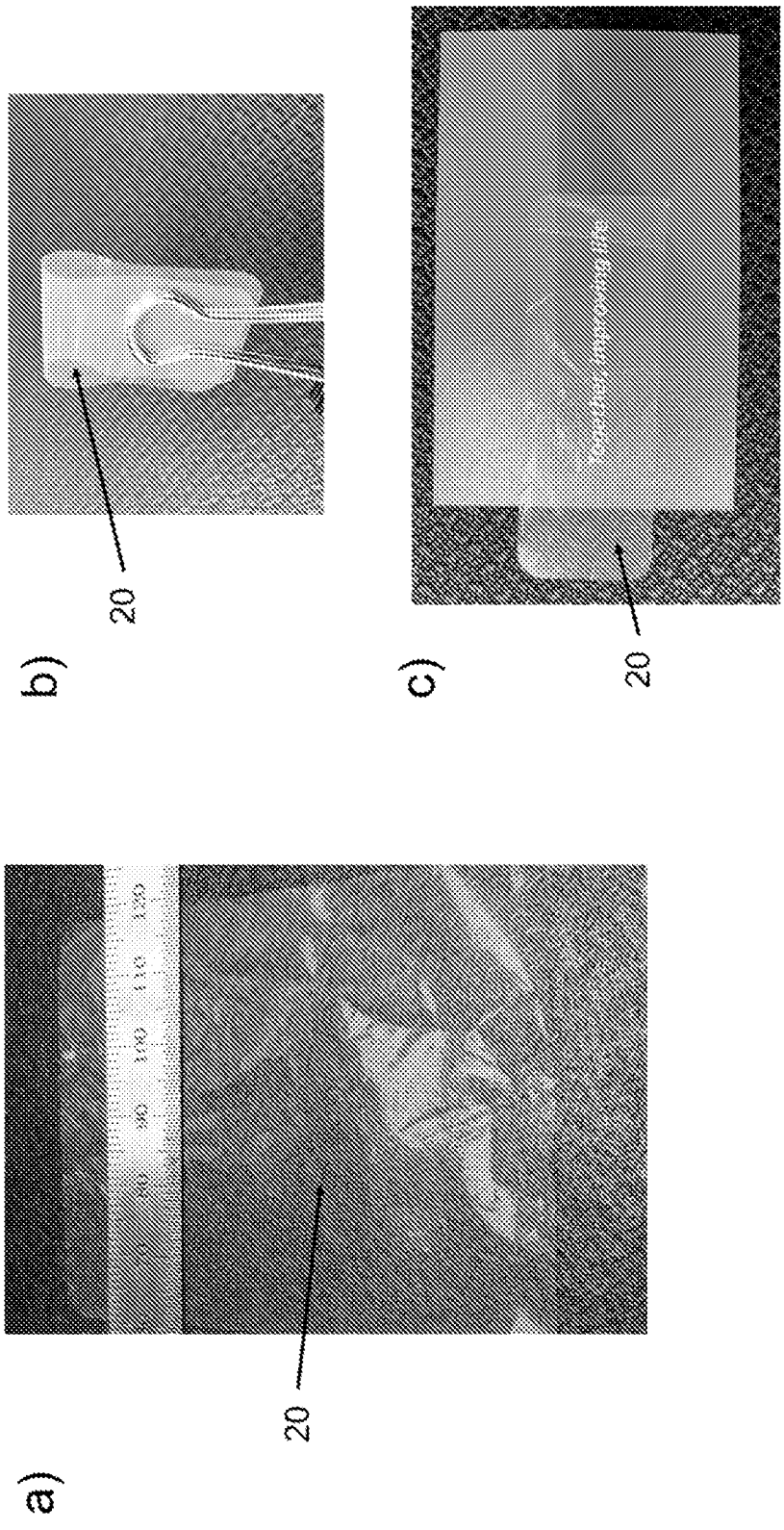


Figure 23

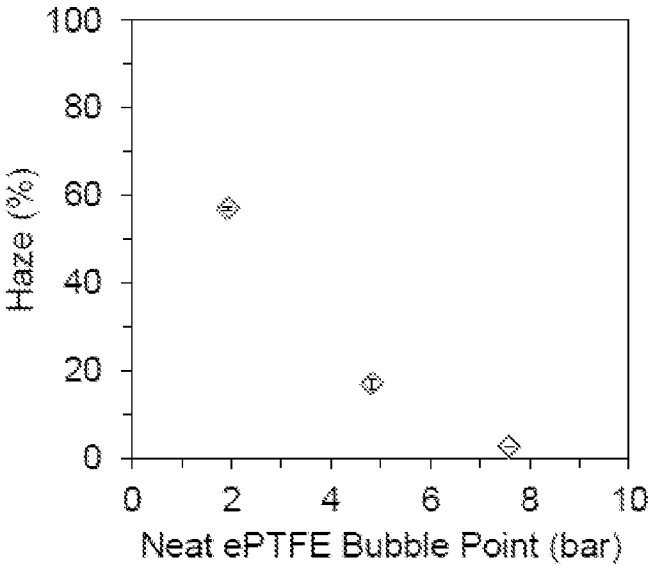


Figure 24

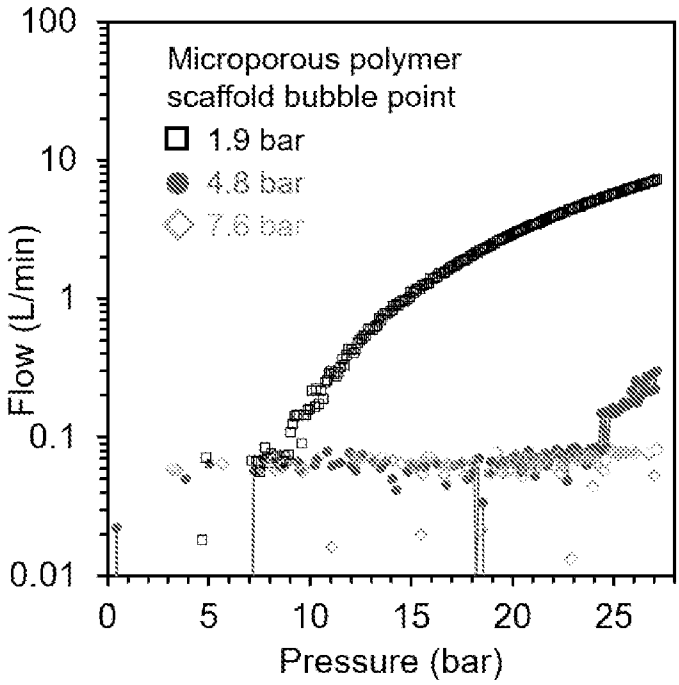


Figure 25

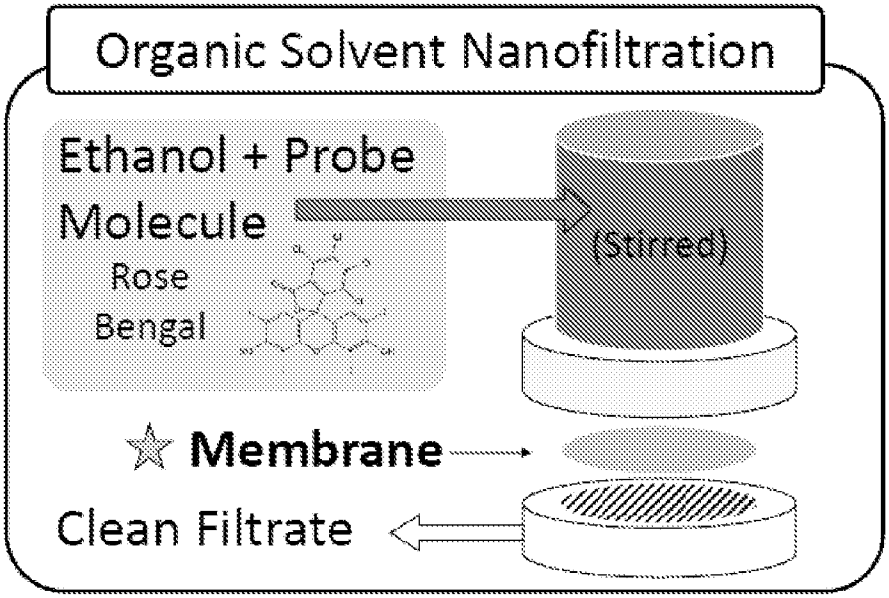


Figure 26

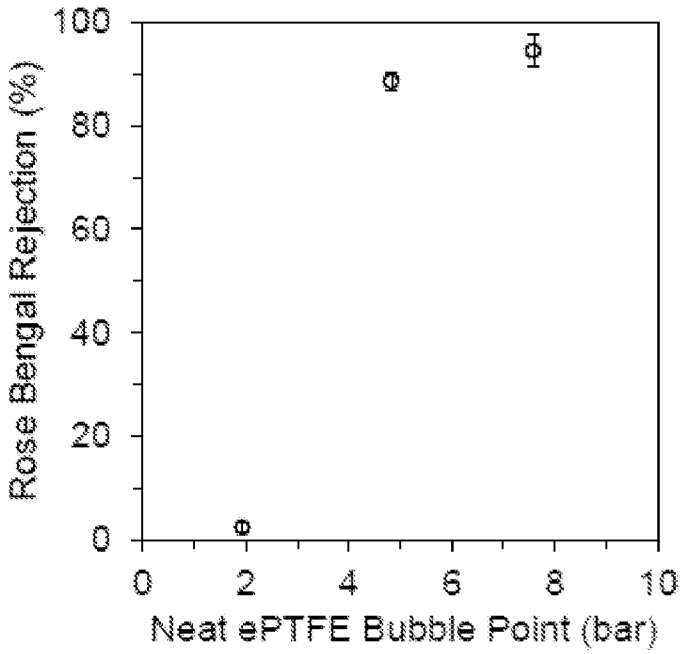


Figure 27

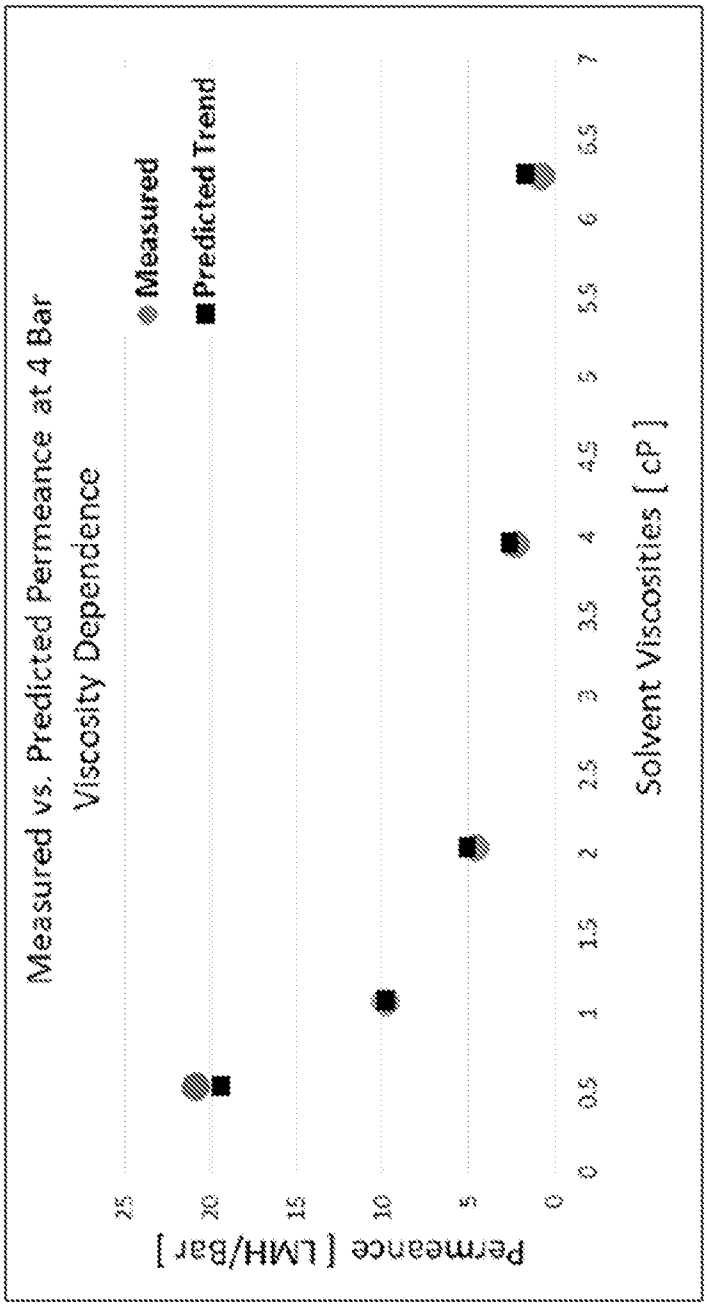
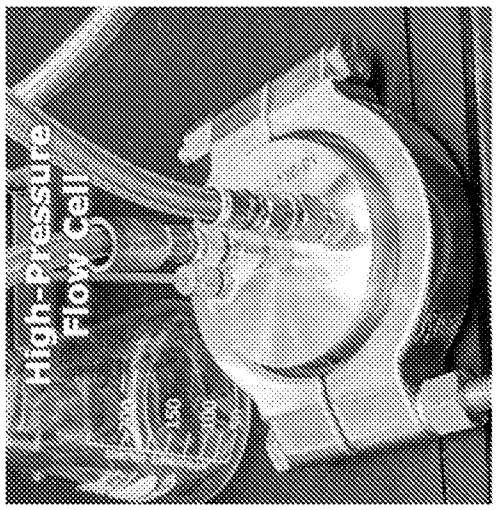

Measured vs. Predicted Permeance at 4 Bar
Viscosity Dependence
Measured
Predicted Trend
Permeance [LMH/Bar]
25
20
15
10
5
0
0
0.5
1
1.5
2
2.5
3
3.5
4
4.5
5
5.5
6
6.5
7
Solvent Viscosities [cP]

Figure 28


a)
High-Pressure
Flow Cell

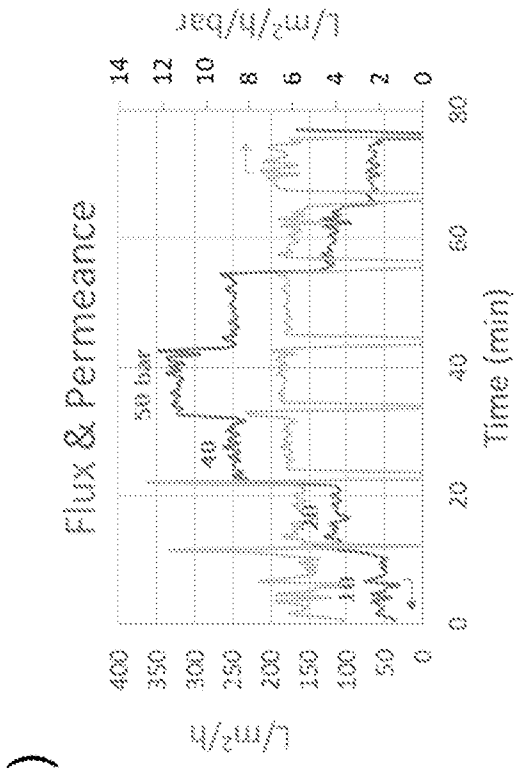

b)
Flux & Permeance
L/m²/h
L/m²/h/bar
Time (min)
50 bar
40
30
20
10

Figure 29

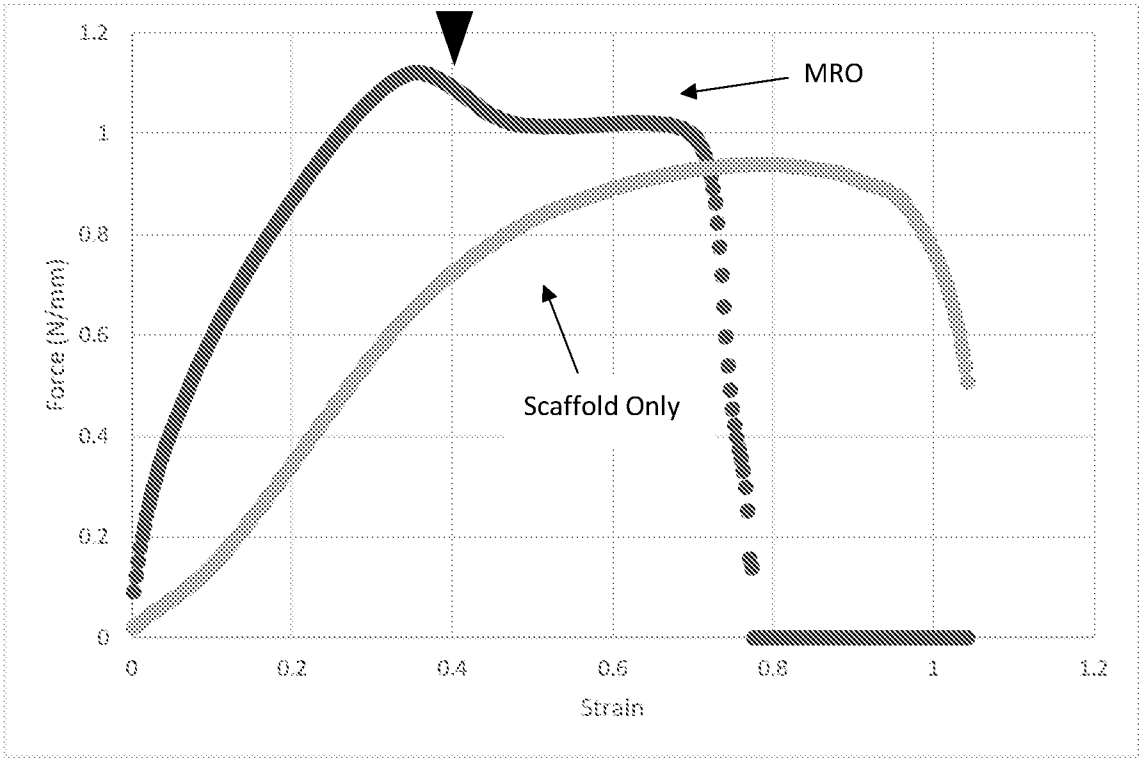

1.2
1
0.8
0.6
0.4
0.2
0
Force (N/mm)
0
0.2
0.4
0.6
0.8
1
1.2
Strain
MRO
Scaffold Only

Figure 30a

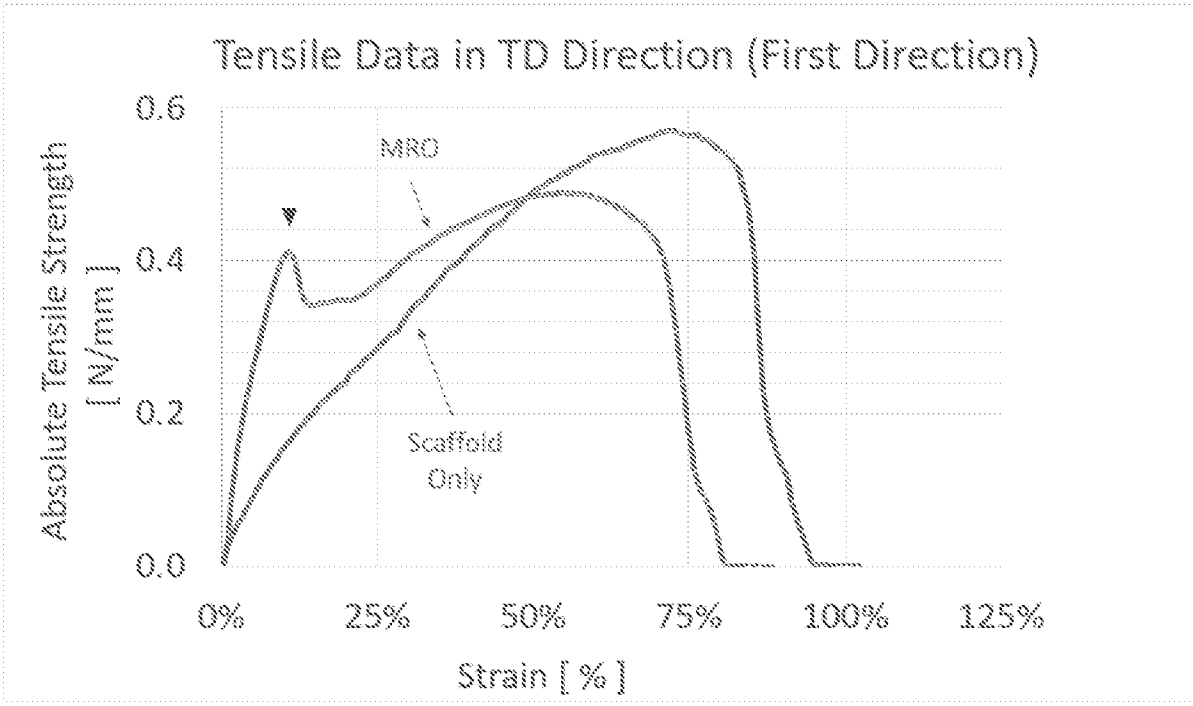


Figure 30c

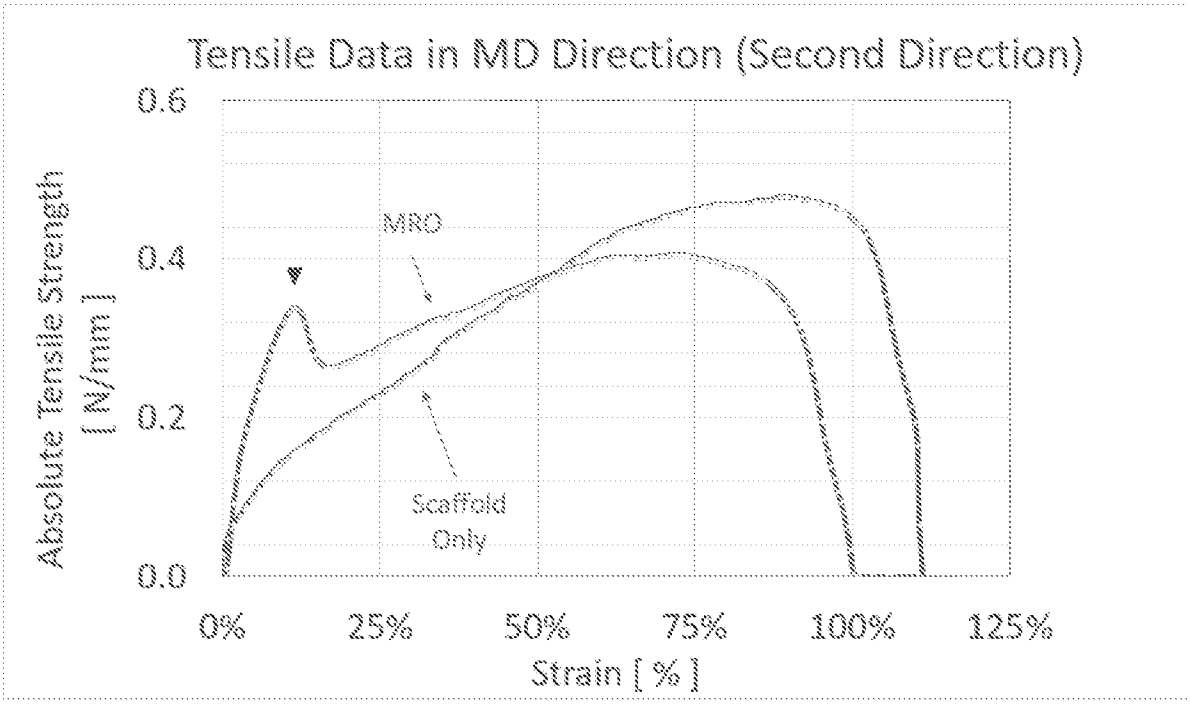


Figure 30c

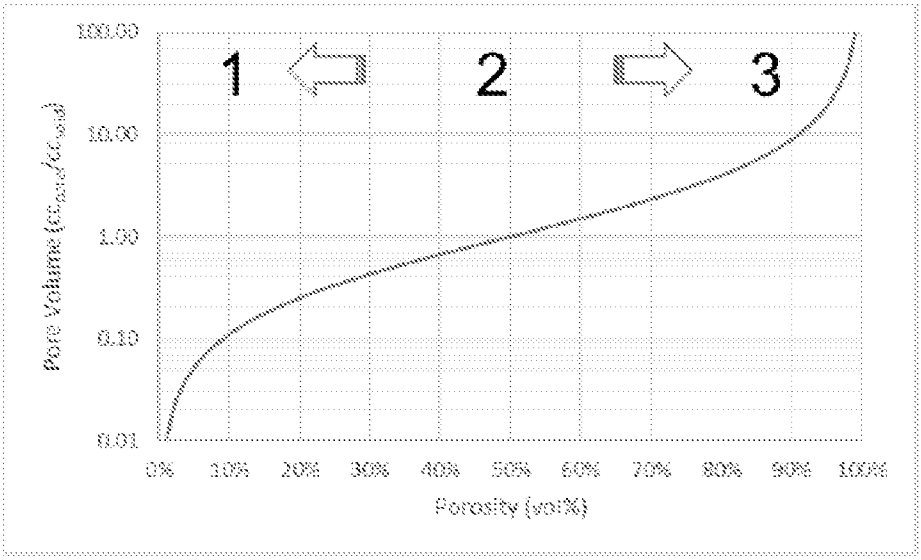


Figure 31

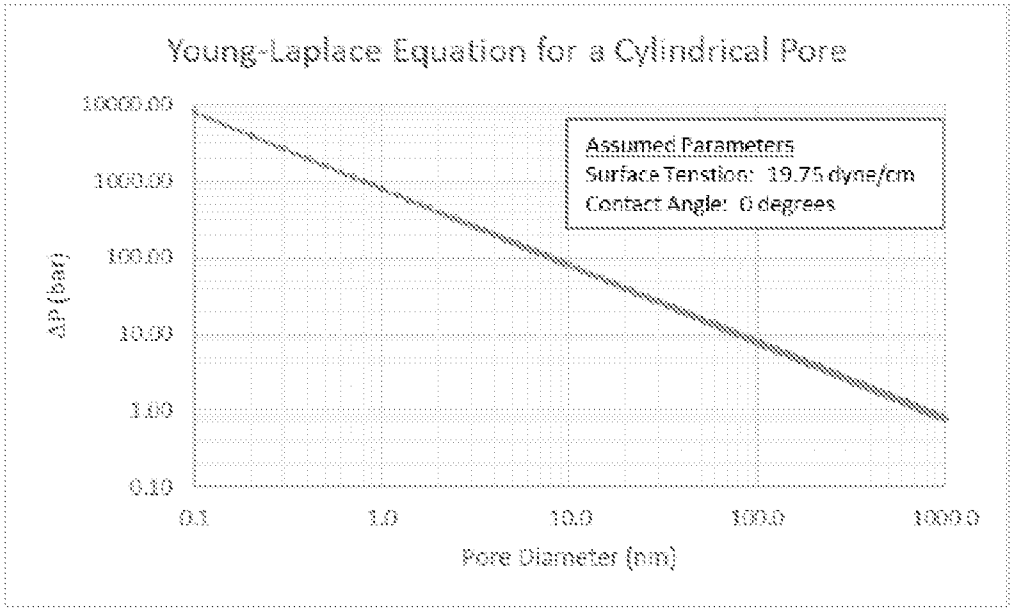


Figure 32

INTERNATIONAL SEARCH REPORT

International application No
PCT/US2024/036011

A. CLASSIFICATION OF SUBJECT MATTER

INV. B01D61/38 B01D69/14 B01D69/10 B01D69/12 B01D71/02
B01D71/26 B01D71/36 B01D67/00 B01D71/04

ADD.

According to International Patent Classification (IPC) or to both national classification and IPC

B. FIELDS SEARCHED

Minimum documentation searched (classification system followed by classification symbols)

B01D

Documentation searched other than minimum documentation to the extent that such documents are included in the fields searched

Electronic data base consulted during the international search (name of data base and, where practicable, search terms used)

EPO-Internal

C. DOCUMENTS CONSIDERED TO BE RELEVANT

Category*	Citation of document, with indication, where appropriate, of the relevant passages	Relevant to claim No.
X	US 2020/101423 A1 (NEWBLOOM GREGORY M [US] ET AL) 2 April 2020 (2020-04-02) paragraphs [0180], [0181], [0107] - [0109], [212ff]; claims 1-3,6; figures 1,2; example 3 paragraphs [0098], [0099]	1-32
X	CN 103 682 209 A (DALIAN CHEMICAL PHYSICS INST) 26 March 2014 (2014-03-26) claim 3; example 1	1-32
X	CN 105 342 755 A (BEST MEDICINE TECHNOLOGY CHANGZHOU CO LTD) 24 February 2016 (2016-02-24) claims 1,5	1-7,9, 10, 12-28,32

-/--

[x] Further documents are listed in the continuation of Box C.

[x] See patent family annex.

* Special categories of cited documents :

"A" document defining the general state of the art which is not considered to be of particular relevance

"E" earlier application or patent but published on or after the international filing date

"L" document which may throw doubts on priority claim(s) or which is cited to establish the publication date of another citation or other special reason (as specified)

"O" document referring to an oral disclosure, use, exhibition or other means

"P" document published prior to the international filing date but later than the priority date claimed

"T" later document published after the international filing date or priority date and not in conflict with the application but cited to understand the principle or theory underlying the invention

"X" document of particular relevance;; the claimed invention cannot be considered novel or cannot be considered to involve an inventive step when the document is taken alone

"Y" document of particular relevance;; the claimed invention cannot be considered to involve an inventive step when the document is combined with one or more other such documents, such combination being obvious to a person skilled in the art

"&" document member of the same patent family

Date of the actual completion of the international search	Date of mailing of the international search report
3 September 2024	13/09/2024

Name and mailing address of the ISA/	Authorized officer
European Patent Office, P.B. 5818 Patentlaan 2 NL - 2280 HV Rijswijk Tel. (+31-70) 340-2040, Fax: (+31-70) 340-3016	Hennebrüder, K

1

Form PCT/ISA/210 (second sheet) (April 2005)

INTERNATIONAL SEARCH REPORT

International application No
PCT/US2024/036011

C(Continuation). DOCUMENTS CONSIDERED TO BE RELEVANT

Category*	Citation of document, with indication, where appropriate, of the relevant passages	Relevant to claim No.
X	US 2019/255482 A1 (BALL EARL [US] ET AL) 22 August 2019 (2019-08-22) paragraph [0061] -----	1-7,9, 10, 12-28,32
X	JP H10 92444 A (JAPAN GORE TEX INC) 10 April 1998 (1998-04-10) claim 1; example 1 -----	1-32

1

INTERNATIONAL SEARCH REPORT

Information on patent family members

International application No
PCT/US2024/036011

Patent document cited in search report	Publication date	Patent family member(s)	Publication date
US 2020101423 A1	02-04-2020	AU 2019205299 A1	06-08-2020
		BR 112020013645 A2	01-12-2020
		CA 3087258 A1	11-07-2019
		CN 111867709 A	30-10-2020
		EP 3735314 A1	11-11-2020
		IL 275638 A	31-08-2020
		JP 7491842 B2	28-05-2024
		JP 2021509884 A	08-04-2021
		KR 20200127975 A	11-11-2020
		SG 11202006398R A	28-08-2020
		US 2019217252 A1	18-07-2019
		US 2020101423 A1	02-04-2020
		US 2021362095 A1	25-11-2021
		US 2024024826 A1	25-01-2024
		WO 2019136272 A1	11-07-2019
CN 103682209 A	26-03-2014	NONE	
CN 105342755 A	24-02-2016	NONE	
US 2019255482 A1	22-08-2019	CN 109843413 A	04-06-2019
		EP 3523012 A1	14-08-2019
		JP 6940599 B2	29-09-2021
		JP 2019529102 A	17-10-2019
		KR 20190053969 A	20-05-2019
		US 2019255482 A1	22-08-2019
		WO 2018067944 A1	12-04-2018
JP H1092444 A	10-04-1998	AU 4268797 A	02-04-1998
		CA 2264830 A1	19-03-1998
		CN 1230293 A	29-09-1999
		DE 69717674 T2	04-12-2003
		EP 0958624 A1	24-11-1999
		JP H1092444 A	10-04-1998
		KR 20000036071 A	26-06-2000
		US 6242135 B1	05-06-2001
		WO 9811614 A1	19-03-1998